Order Number 8914796

# New robust methods for superresolving signal recovery and bandlimited signal extrapolation

Stojancic, Mihajlo M., Ph.D.

City University of New York, 1988

U·M·I
300 N. Zeeb Rd.
Ann Arbor, MI 48106

# NEW ROBUST METHODS FOR SUPERRESOLVING SIGNAL RECOVERY AND BANDLIMITED SIGNAL EXTRAPOLATION

by

Mihajlo M. Stojancic

A dissertation submitted to the Graduate Faculty in Engineering in partial fulfillment of the requirements for the degree of Doctor of Philosophy, The City University of New York.

1988

This manuscript has been read and accepted for the Graduate Faculty in Engineering in satisfaction of the dissertation requirement for the degree of Doctor of Philosophy.

June 24, 1988
Date

Chair of Examining Committee

June 27, 1988
Date

Executive Officer

L. Roytman

F. Thau

G. Eichmann

Supervisory Committee

The City University of New York

# Abstract

NEW ROBUST METHODS FOR SUPERRESOLVING SIGNAL RECOVERY AND BANDLIMITED SIGNAL EXTRAPOLATION

by

Mihajlo M. Stojancic

Adviser: Professor George Eichmann

The reconstruction of signals and images degraded by a linear, frequency low-pass degradation operator, or obscured due to a finite space (time) observation interval, is an ill-posed problem. This thesis focuses on the developing of new robust methods to alleviate the aforementioned problem. In particular three different methods are proposed. First, based on a new constrained associative memory (CAM) method, the reconstruction (restoration) of an arbitrary binary object from an image, degraded by a linear shift-invariant (LSI) or a linear shift-variant (LSV) degradation operator, in the presence of strong noise, is achieved. Using an appropriate training set of signals, related ideally by a perfect degradation operator inverse, the CAM method yields a general one-step impulsive-type inverse filter in a form of two dimensional array of coefficients. Computer simulation results of the reconstruction of 1D and 2D signals and images, degraded by LSI and LSV systems, in the presence of strong noise, are presented. Second, a new iterative method, based on the weighted least-squares (WLS) and best linear

unbiased estimate (BLUE) algorithms, is presented. This algorithm focuses on desighning a suitable symmetric weighting matrix that will, without disturbing the system consistency, perform an implicit filtering of the system degradation operator singular values (SV). A specific SV filter performs twofold function: it compensates for the ill-conditioning of the system degradation operator by decreasing its matrix condition number and by improving the low-to-high-order SV ration it improves the convergence rate of a recursive computation of the object signal estimate. Last, a new algorithm for the extrapolation in the space domain of a partially observed low space-bandwidth product (SBP) sequence, or equivalently, the resolution of the Fourier spectra in the frequency domain, in the presence of appreciable noise, is developed. Using an approach similar to the Simulated Annealing method the extrapolated sequence samples are constructed from variable size elementary grains. The new iterative algorithm, at each iteration step, based on a random number generator, decides both the sample position to be considered, and the sign of a grain that might be added to the current sample value. A variable size sample update in each iteration step is either accepted or rejected in accordance with an appropriate decision rule. Several simulation examples, for the extrapolation of low SBP sinusoidal and other arbitrary sequences and in the presence of high level of noise, are presented.

## ACKNOWLEDGEMENTS

I wish to thank Professor George Eichmann for providing me with the opportunity to explore this topic and for his invaluable assistance in obtaining the desired results.

Special thanks to my mother Eda for her continual support and encouragement during this endeavor.

M. M. S.

# TABLE OF CONTENTS

## LIST OF FIGURES

# 1. INTRODUCTION

Signal recovery and bandlimited signal extrapolation refer to a class of problems that are among the most fundamental in signal processing. In its most general form the signal recovery problem can be stated as [63]: Given data g, determine the source f that produced g. Several questions about the properties and form of the operational equation, that relates f and g, can be posed. A common linear operator used to describe the system effect to the input signal f is a linear degradation operator derived from the system impulse response or point-spread function (PSF). The exact form of this operator depends on number of factors. For example, if in question is an imaging system, the PSF can be separable or non-separable, or in general for one-dimensional (1D) or two-dimensional (2D) systems, the PSF can be space-variant or space-invariant, or of finite or infinite support. The kinds of degradation encountered in imaging applications are those associated with the finite aperture of the imaging system and lens aberration defocusing, which in general exibit a low-pass characteristic. In spectroscopy and image processing, signal spreading and blurring are qualitative terms frequently used to describe the signal degradation process, mathematicaly usualy modeled by the convolution. In general all physical instruments limit the amount of data one can collect, especially in the frequency domain. Often the fine details of an

2D image or 1D signal are beyond the reach of the resolving power of an instrument. Therefore designing methods and algorithms that will increase the resolving power of, for instance, telescops, spectrometers, seismic and imaging systems by processing of the measured signal, is of crutial importance. These signal processing methods and algorithms yield the resolution of larger instruments that we do not have at the time when the experiment has been performed.

Resolution is the measure of the discernable distance between two points. A frequently used resolution limit is the Rayleigh distance. This is the distance between impulses such that the maximum of the first impulse response falls on the first zero of the second impulse response, when the impulses are the input to an ideal lowpass filter (ILPF). This translates as the the value of unity for the space-bandwidth product, i. e.,

$$TW_c = 1 \qquad (1.1)$$

where T is the distance between the impulses and $W_c$ is the bandwidth of the ILPF transfer function. The Reyleigh distance and the resolution are reciprocally related, which is expressed in signal analysis by well known uncertainty principle [49]. If, by processing a signal, the resolution is incresed beyond the Reyleigh limit, then the process is called superresolving. This

thesis focuses on the developing of new robust methods that are superresolving.

The problems of signal and image degradation by a linear system can be modeled by a superposition integral equation of the form

$$\int_{-b}^{b} h(s,x)f(s)ds = g(x), \quad |x| < a \tag{1.2}$$

where $g(x)$ is an observed function, $h(s,x)$ is a known kernel, and $f(s)$ is the unknown function to be determined. In an image restoration problem, for example, $g(x)$ would represent the observed image, $h(s,x)$ would be the point spread function of the imaging system, and $f(s)$ would be the object distribution. In the case of an ideal lowpass filtering of spatial frequencies, the integral kernel in Eq. (1.2) is

$$h(s,x) = \frac{\sin(w_c(x-s))}{\pi(x-s)} \tag{1.3}$$

where $w_c$ is the cutoff frequency.

Equation (1.2) is known as a Fredholm integral equation of the first kind [29]. It is well known that this equation is

generally ill-posed [28, 63, 30] in the sence that small perturbation in the observed signal g can give rise to unacceptably large changes in the solution f. In practical problems, due to contamination of the observed function g(x) by noise or other sources of error, an approximate solutions for f should be sought that achieve the proper balance between accuracy and stability. In order to illustrate the ill-posed nature of the integral equation (1.2), and point out the problems in determining the object function f(s), in the following we discuss a direct method for recovering f(s) from g(x), well known as the Prolate Spheroidal Function (PSF) method [60, 61].

To define the problem to be considered more precisely, two linear projection operators are introduced. The spatial truncation operator S is defined by

$$Sf(x) = \begin{cases} f(x), & |x| < a \\ 0, & \text{otherwise} \end{cases} \qquad (1.4)$$

and the bandlimiting operator B is defined by

$$Bf(x) = \int_{-\infty}^{\infty} f(s) \frac{\sin[w_c(x-s)]}{\pi(x-s)} ds \qquad (1.5)$$

Thus, operating on f(x) with B is equivalent to passing f(x) trough an ideal lowpass filter.

If we assume that the f(x) function is of finite extent, i. e. f(x) satisfies

$$Sf(x) = f(x) \tag{1.6}$$

and a linear system degradation operator is an ideal lowpass filter, the Fredholm integral equation (1.2) becomes

$$g(x) = Bf(x) \tag{1.7}$$

Initially, in Eq. (1.7) we ignore noise in the observed signal g(x), although the effect of noise is critical in obtaining the solution for f(x).

It is well known [60, 61] that under the conditions described above, f(x) can be expanded in a series of the form

$$f(x) = \sum_{k=0}^{\infty} c_k q_k(x) \tag{1.8}$$

where $q_k(x)$ are prolate spheroidal wave functions, and $c_k$ are constant coefficients to be determined. These functions are orthogonal eigenfunctions of the operator equation

$$SBq_k(x) = b_k q_k(x) \tag{1.9}$$

and satisfy the orthogonality property

$$\langle q_j, q_k \rangle = \int_{-\infty}^{\infty} q_j(x) q_k(x) dx = \delta_{jk} \tag{1.10}$$

where $\delta_{jk}$ is Kronecker symbol and $\langle .,. \rangle$ denotes the inner product. The eigenvalues $b_k$ in Eq. (1.9) satisfy

$$0 < \ldots < b_k < \ldots < b_1 < b_0 < 1 \tag{1.11}$$

All eigenvalues are distinct, the function $\{q_k(x)\}$ are complete in the space of functions satisfying $Sf = f$, and the functions $\{Bq_k(x)\}$ are complete in the space of functions bandlimited to $[-w_c, w_c]$. Furthermore, the $\{q_k(x)\}$, in addition to satisfying (1.10), also satisfy

$$\langle Bq_j, Bq_k \rangle = b_k \delta_{jk} \tag{1.12}$$

This expression determines the eigenvalues $b_k$, which are the portion of energy in $q_k(x)$ that lies in the frequency band $[-w_c, w_c]$.

In the absence of noise, it is possible in principle to reconstruct $f(x)$ exactly from $g(x)$. The observed signal $g(x)$ can be written as

$$g(x) = Bf(x) = \sum_{k=0}^{\infty} c_k Bq_k(x) \tag{1.13}$$

Forming the inner product of $g(x)$ an $q_m(x)$ as

$$\langle g, q_m \rangle = \sum_{k=0}^{\infty} c_k \langle Bq_k, q_m \rangle = b_m c_m \qquad (1.14)$$

we can get the coefficient $c_m$ from Eq. (1.8) as

$$c_m = (1/b_m)\langle g, q_m \rangle \qquad (1.15)$$

Substituting $c_m$ from Eq. (1.15) into Eq. (1.8) the $f(x)$ can be obtained as

$$f(x) = \sum_{m=0}^{\infty} (1/b_m)\langle g, q_m \rangle q_m(x) \qquad (1.16)$$

assuming that the eigenfunctions $q_m$ are known.

In practical applications the effect of noise must be considered. From Eq. (1.16) we can get a rather clear idea of the effect of noise by noting that the eigenvalues $b_m$ go approximately as a unit step as a function of the index, i. e. the higher order $b_m$ drop to nearly zero rather sharply. The number of the eigenvalues close to unity is a function of the space-bandwidth product (SBP). For any real measured signal there will be some high order noise components. The PSF method of Eq. (1.16) requires that the components of the measured signal be

divided by the eigenvalues $b_m$. Thus, any noise in the higher order $m^{th}$ component will be greatly amplified by dividing by a very small $b_m$, pointing out the ill-posed nature of the problem. One obvious modification to (1.16) would be to retain only those terms whose eigenvalues are near unity and to eliminate the remaining terms. However, the PSF are not easily generated, and the integrations which must be performed before the final series expansion can be evaluated, are numerically combersome. Furthermore this method cannot yield superresolving restorations since the high order components in the expansion of Eq. (1.16) correspond to the high frequency signal components. Thus, to gain stability, most of the high frequency information, that is precisely the information the superresolution seeks to recover, is eliminated.

The continuous-time Fredholm integral equation of Eq. (1.2) can be converted into a set of N algebraic equation employing some quadrature rule on the integral [4]. Thus, the discrete-time model of the degradation in the absence of noise is

$$\mathbf{g} = \mathbf{H}\mathbf{f} \tag{1.17}$$

where H is an M*N degradation system matrix, f is N-element object and g is M-element measured sampled vector. This discrete formulation is still ill-conditioned. To show this we expand the H matrix as

$$H = \sum_{k=1}^{N} \sigma_k u_k v_k^T \qquad (1.18)$$

where $u_k$ and $v_k$ are the orthogonal eigenvectors of $HH^T$ and $H^TH$ respectively. The $\sigma_k$ are the singular values (SVs) of H, defined as the positive square roots of the associated eigenvalues

$$HH^T u_k = \sigma_k^2 u_k ,$$
$$H^T H v_k = \sigma_k^2 v_k , \quad k = 1, 2, \ldots, N \qquad (1.19)$$

The decomposition of Eq. (1.18) is known as singular value decomposition (SVD) [20, 11], and the singular values are ordered so that

$$1 > \sigma_1 > \sigma_2 > \ldots > \sigma_N > 0 \qquad (1.20)$$

The Eq. (1.18) can be written as

$$H = ULV^T \qquad (1.21)$$

where U and $V^T$ are orthogonal matrices, with the left and right singular vectors $u_k$ and $v_k^T$, respectively, as the columns. The L is a diagonal matrix consisting of the SVs. The SVs of the degradation matrix H are bounded in the interval (0,1), with the sharp transition between those close to unity, and those close to zero [29]. This behavior corresponds to the behavior of the

eigenvalues in the continuous-time case. Thus, the inverse of H given by

$$H^{-1} = VL^{-1}U^T \tag{1.22}$$

is numerically very unstable due to the diagonal matrix $L^{-1}$ which containes the reciprocal SVs of H. Again, one obvious solution to this problem is to truncate the H matrix SVs in such a way that the high order SVs close to zero are descarded, reducing the rank of H. However, while this procedure stabilizes the numerical problem, it attenuates the restored signal high frequency components necessary for superresolution.

This thesis focuses on the problem of estimating the original object signal from a noisy degraded signal, either by determining directly the inverse of an ill-conditioned linear discrete-time (space) system degradation operator, that results in a one-step signal restoration procedure, or by developing new iterative methods to obtain a stable estimate. Four new methods, appropriate for various applications, that are shown to give superresolving results, are developed.

Proposed one-step methods are based on a modified linear associative memory (LAM) algorithm [32], originaly introduced by Kohonen for the least squares optimal pattern (vector) maching.

Here, it is shown that a degradation system input-output set of signals can be utilized as a "training" set of vectors to create an inverse system degradation operator in a form of a LAM matrix. By limiting the set of reconstructible signals to the class of signals belonging to the "training" set, an exceptionally robust superresolving inverse filter is obtained. However, when the "training" vectors are linearly dependent the LAM algorithm shows poor performance, producing an inadequate associative memory matrix with large dynamic range of elements. Hence, a new constrained associative memory (CAM) method, suitable for determining of the inverse of an ill-conditioned system degradation operator, is developed.

In Chapter 4, based on this new CAM method, superresolving reconstruction of an arbitrary binary object from an image, linearly degraded by a shift-invariant, or shift-variant degradation operator, in the presence of strong noise is achived. Using an appropriate training set of signals related idealy by a perfect degradation operator inverse, the CAM method yields a general one step, impulsive type (spiking) inverse filter [47], in a form of a simple two dimensional array of coefficients. The presented method is particularly suited for impulsive type of signals and images. Computer simulation results of superresolving reconstruction of 1D and 2D signals and images, linearly degraded by shift-invariant and shift-variant systems, in the presence of strong noise, are demonstrated.

In Chapter 5 a new iterative method for the discrete-space linearly degraded signal restoration in the presence of appreciable noise is proposed. This method, based on the weighted least-squares (WLS) and best linear unbiased estimate (BLUE) algorithms [1, 44], focuses on designing a suitable symmetric weighting matrix that will, without disturbing the system consistency, perform an implicit filtering of the system degradation operator singular values (SV). A specific SV filter, incorporated into the new weighting matrix, performs a twofold function; it compensates for the ill-conditioning of the system degradation operator by decreasing its matrix condition number and by improving the low-to-high-order SV ratio it affects the convergence rate of a recursive computation of the object signal estimate. Radically different from hitherto used schemes, the SV filter is a step-type function that operates on the system degradation operator low-order as well as the high-order SVs. To facilitate the imposition of a priori known object signal constraints, a recursive WLS estimate computation is used. Also, to eliminate the inconsistency of the linear system degradation model due to a measurement error or noise, a preprocessing step is introduced. When the noise statistics are known, the BLUE algorithm that minimizes the noise variance is employed. Here, the new weighting matrix, in a combination with the noise covariance matrix, is used to form a weighted BLUE (WBLUE) algorithm. The WLS and WBLUE algorithms are presented in the

uniform format so that an identical recursive estimate computation can be applied. The new recursive algorithm serves as a kernel of the proposed constrained iterative method. The effects of the imposition of different constraints on the object signal estimate are demonstrated. Several numerical examples are presented.

The estimation of spectra, or bandlimited signal extrapolation can be considered as the dual of the previous problem, i. e. exchanging the roles of time and frequency it can be solved in a similar fashion. In the dual problem an observed signal is a time truncated version of a bandlimited signal. From the given observation interval the original bandlimited signal could be infered either by extrapolating outside of the given interval using some iterative method and signal bandlimit as a constraint, or increasing the resolution of the Fourier spectra in the frequency domain. In Chapter 6 a partialy observed bandlimited sequence extrapolation in the space domain, or equivalently resolution of the Fourier spectra in the frequency domain, in the presence of considerable noise, is considered. A new method is developed that reconstructs the unknown portion of a bandlimited sequence using the grains of variable size as the elementary building blocks of each sequence sample. The unknown sequence estimate is based on a number of acquired samples on a given measurement interval and the prior knowledge of the signal frequency bandlimit. An approach similar to a Monte-Carlo method

[6, 31], using those variable size elementary grains, is adopted to develope a new iterative algorithm. This new algorithm, at each iteration step, based on a random number generator, decides both the sample position to be considered, and the sign of a grain that might be added to the current sample value of the sequence being estimated. A sample update in each iteration step is either accepted or rejected in accordance with an appropriate decision rule. While exploiting the extrapolated sequence frequency bandlimit as a constraint this decision rule is based on a nonincreasing $l_1$-norm of a cumulative error vector. As the extrapolated sequence approaches its final form, the elementary grain size is decreased to allow for subtle sample updates. A heuristic schedule for gradual change of the elementary grain size, similar to the temperature schedule of the Simulated Annealing method [33, 45], is used. A preprocessing, that compensates for the model inconsistency, due to either presence of noise, and/or lack of precision of the linear degradation operator is employed. It is also shown that an additional constraint, such as a given signal upper-bound, greatly improves the quality of reconstruction. Several simulation examples for the extrapolation of a low SBP sinusoidal and other arbitrary sequences and in the presence of high level of noise, are presented. Finally, in Chapter 7, a summary and conclusions, regarding the proposed methods, are presented.

# 2. BACKGROUND

## 2.1 INTRODUCTION

The problem of recovery or restoration of a signal or image that has been distorted by a linear degradation operator is common to different application areas such as diffraction optics, radio astronomy, seismic array of sensors, electron microscopy, sonar, radar etc. It can be stated, in general, as the problem of reconstruction of a Fourier transform pair (f,F) from partial data on either/or both domains (spatial and/or spatial frequency) [5]. The extrapolation of bandlimited signals has been addressed by several authors. A number of iterative extrapolation algorithms, for example, by Gerschberg [19], Papoulis [48] and by Youla [72], and also direct algorithms, such as by Cadzow [9] and by Sabry and Steenart [57], have been proposed. For linearly degraded signal recovery, when the measurement noise is negligible and for a moderate system degradation, direct spatial frequency domain inversion of the degradation process is possible [30, 15]. In the presence of noise, a linear method such as Wiener-type filtering [30, 15] is more appropriate. However, in many signal restoration problems, the measurement error is greatly amplified so that the error dominates the estimate. Hence, signal and image restoration methods which impose various

constraints either or both on the object signal estimate and the system degradation operator SVs (or its eigenvalues and eigenfunctions), have widely been analyzed [30, 63]. For example, in Jansson [30], Howard [26, 27], Frieden [15], Youla [72], Stark et al. [64], Sanz & Huang [58], Rushford [52], Barakat & Newsam [5], Mammone & Eichman [39, 40], Mammone & Rothacker [41] and Eichman & Stojancic [14], a number of constrained iterative and direct signal restoration methods have been proposed. An analysis and generalization of constrained iterative algorithms, either for bandlimited signal extrapolation or linearly degraded signal recovery, is given in Schafer et al. [59].

In the following sections, an overview of some conceptualy important linear and nonlinear signal and image recovery methods is presented.

## 2.2 LINEAR RESTORATION METHODS

### Linear Inverse Filter

If the system degradation operator is linear and shift (time) invariant the restoration problem is commonly known as the deconvolution problem. The convolution equation that describes the system degradation can be readily expresed using the convolution operator * as

$$g(x) = f(x)*h(x) \tag{2.1}$$

The approach of the inverse filtering is to form a linear filter function y(x) that will undo, by convolution with the g(x), the smearing of the system degradation. Using the Fourier transform, the frequency domain equivalent to Eq. (2.1) is

$$G(w) = F(w)H(w) \tag{2.2}$$

Clearly, the Fourier transform of the inverse filter is given by

$$Y(w) = \frac{1}{H(w)} \tag{2.3}$$

It is apparent that the inverse Fourier transform of Y(w) yields the desired inverse filter function y(x). However, when the high

frequency components of $f(x)$ are strongly suppresed, the $H(w)$ is very small for large $w$. If the data $g(x)$ are noisy, the estimate of $F(w)$ (see Eq. (2.2)) using the inversion of Eq. (2.3), will be dominated by the noise, thus producing very poor and unstable estimate of $f(x)$. With this method, as it was shown by Frieden [15], assuming uncorrelated object and noise statistics and uncorrelated object and noise, it is possible to carry out the inverse processing within some optimum frequency band $|w| < w_p$, where $w_p < w_c$, determined by

$$w_p = w_c[1-(p_n/p_o)^{1/2}] \qquad (2.4)$$

where $p_o$ and $p_n$ are the power spectra of the object signal and noise, respectively, and $w_c$ is the degradation system transfer function frequency band-limit.

## Wiener-Type Filters

In the presence of noise Eq. (2.1) is

$$g(x) = f(x)*h(x) + n(x) \qquad (2.5)$$

Numerical solution for $f(x)$ yields an estimate $f(x)$ that minimizes, in some sence, the error (noise). If $h(x) = \delta(x)$, where $\delta(\cdot)$ is the impulse function, $g(\cdot)$ in Eq. (2.5) is

corrupted with noise only. For this case the inverse filter function $y(x)$ is sought that minimizes the estimation error

$$e(x) = \hat{f}(x) - f(x) = y(x)*[f(x) + n(x)] - f(x) \qquad (2.6)$$

By minimizing the ensamble average of the mean-squared error

$$E[\int_{-\infty}^{\infty} |e(x)|^2 dx], \qquad (2.7)$$

where $E[...]$ denotes the expected value, well known optimum smoothing Wiener filter [30] is obtained

$$Y(w) = \frac{P_o(w)}{P_o(w) + P_n(w)} \qquad (2.8)$$

Since the system degradation function is an impulse function, this inverse filter yields only the optimum noise reduction. However, in the presence of system degradation $h(x)$, using identical approach, i. e., minimizing

$$E[\int_{-\infty}^{\infty} |y(x)*[h(x)*f(x) + n(x)] - f(x)|^2 dx], \qquad (2.9)$$

a linear inverse filter can be obtained as [24]

$$Y(w) = \frac{H^*(w)P_o}{|H(w)|^2 P_o + P_n} \qquad (2.10)$$

where * denotes complex conjugate. If the noise is additive and gaussian distributed, and the noise and object signal power spectra are known, this is an optimum linear inverse degradation filter.

In a similar approach Frieden [15] added a sharpeness criterion to the ensamble average of Eq. (2.9). Thus an inverse filter is obtained by minimizing

$$E\left[\int_{-\infty}^{\infty} |y(x)-[h(x)*f(x)+n(x)]|^2 dx\right] + rE\left[\int_{-\infty}^{\infty} \left|\frac{df(x)}{dx}\right|^2 dx\right] \qquad (2.11)$$

within the allowed processing bandwidth. In Eq. (2.11) the second term represents the sharpening criterion with a variable parameter r. The Frieden's sharpeness-constrained filter given by

$$Y(w) = \frac{H^*(w)p_o}{|H(w)|^2 p_o + p_n} \frac{1}{1+rw^2}, \qquad (2.12)$$

allows for signal or image sharpeness control by varying the r parameter. Thus the high frequency components of a signal or image, within the processing bandwidth, can be either suppressed or enhanced, depending on whether $r > 0$ or $r < 0$.

Presented Wiener-type linear inverse filters require knowledge of the object signal and noise power spectra. However, the power spectra are not always easy to obtain. On the other hand, very often, some additional a priori knowledge or information on the object signal is available that can not be exploited by the Wiener-type filters. In the case of a heavier system degradation and in the presence of noise, this a priori information plays a crucial role in obtaining a satisfactory estimate.

## Iterative Jansson-Van Cittert-type methods

This type of methods are based on classical numerical methods for solving a general system of n equations in n unknowns $f_1, f_2, \ldots, f_n$. The problem can be formulated as

$$u_i(f_1, f_2, \ldots, f_n) = 0, \quad i = 1, 2, \ldots, n \tag{2.13}$$

where $u_1, u_2, \ldots, u_n$ are functions of n variables. In vector notation Eq. (2.13) can be written as

$$u(f) = 0 \tag{2.14}$$

where u is a vector valued function of $f = (f_1, f_2, \ldots, f_n)$. A particular example of a system of Eq. (2.14) is the linear system

$$\mathbf{Hf} - \mathbf{g} = \mathbf{0} \tag{2.15}$$

where H is an n*n system degradation matrix and f and g are the system input an output vectors, respectively. We are interested here in an iterative solution of Eq. (2.14), i. e., in solving a sequence of linear systems of the same type, iteratively approaching a fixed point in the n-dimensional solution space. Of particular interest are the fixed point iteration and relaxation methods [12, 28].

The fixed point iteration methods are derived from the general system of n equations in n unknowns, Eq. (2.14), presented by an equivalent equation of the form

$$\mathbf{f} = \mathbf{z}(\mathbf{f}) \tag{2.16}$$

where z is a vector valued function. Starting from some initial guess $\mathbf{f}^{(0)}$ one forms the iteration

$$\mathbf{f}^{(k)} = \mathbf{z}(\mathbf{f}^{(k-1)}) \tag{2.17}$$

which, if the vector function z satisfies certain necessary conditions, converges to the fixed point f. Considering now the example of linear degradation system of Eq. (2.15), the z function can be formed as

$$z(f) = Cg + (I - CH)f = f + C(g - Hf) \qquad (2.18)$$

where C is a so called approximate inverse of H that satisfies

$$\|I - CH\| < 1 \qquad (2.19)$$

in some matrix norm. The condition of Eq. (2.19) is a necessary condition for z to be contractive [12, 28], i. e., because

$$[z(f) - z(h)] = (I - CH)(f - h), \qquad (2.20)$$

only if Eq. (2.19) is satisfied

$$\|z(f) - z(h)\| < \|f - h\|. \qquad (2.21)$$

Thus, starting from any initial guess $f^{(0)}$, the fixed point iteration

$$f^{(i)} = f^{(i-1)} + C(g - Hf^{(i-1)}), \qquad (2.22)$$

derived from the Eq. (2.17) and (2.18), converges to the unique solution f. The convergence of the iteration of Eq. (2.22) can also be shown by observing that the error

$$e^{(i)} = f - f^{(i)} \qquad (2.23)$$

satisfies

$$e^{(i)} = (I - CH)e^{(i-1)} \qquad (2.24$$

Clearly, if the condition of Eq. (2.19) is satisfied, the error vector norm $\|e^{(k)}\|$ approaches zero as k approaches infinity.

There is a number of methods to choose the C matrix in Eq. (2.22) [12]. One of possible choices is $C = D^{-1}$ (Jacobi method), where D is a diagonal invertible matrix obtained by the decomposition

$$H = L + D + U \tag{2.25}$$

where L and U are the lower-triangular and upper-triangular matrices, respectively. Another choice for C is $C = (L + D)^{-1}$ (Gauss-Seidel method) which usually yields a faster convergence rate [12]. In general, C in Eq. (2.22), can be considered as a relaxation, or gain, parameter that ensures or speeds up the convergence of the algorithm, providing a minimum amount of computation.

A rader naive approach was adopted by Van Cittert [69] setting the relaxation parameter in Eq. (2.22) C to an identity matrix. This method has a mere historical importance opening up the reach area of the methods of numerical analysis to the optical applications. For example, Jansson [30] applied it using

a relaxation parameter that is a function of the object estimate as

$$C = r(f^{(k)}) = r_0(1 - 2|f^{(k)} - 1/2|) \qquad (2.26)$$

where $r_0$ is a constant, thus neutralizing the nonphysical components of the estimate. Frieden [15, 30] used

$$r(f^{(k)}) = r_0[1 - 2(a - b)^{-1}|f^{(k)} - (a - b)/2|] \qquad (2.27)$$

as the relaxation parameter that treats the case of a priori known upper-object-signal-bound $b$ and lower-object-signal-bound $a$. As it will be pointed out in the next section, several other nonlinear iterative image restoration methods can be treated by the general iterative Eq. (2.22). Due to the fact that only the size of the error generated in a single iteration step is important, in general, iterative methods are less vulnerable to the growth of the numerical round-off error. On the other hand, iterative methods do not always converge, or they require a large number of iteration steps that is unacceptable in many applications.

## 2.3 CONSTRAINED ITERATIVE RESTORATION METHODS

Many signal and image restoration problems can be presented by an operational equation of the form

$$\mathbf{g} = \mathbf{H}\mathbf{f}. \tag{2.28}$$

where H can take on various forms depending on the properties of the system degradation or transformation. The f and g are, as usual, the system input and output vectors, respectively. An iterative equation, similar to the Eq. (2.17), but in operator form, can be written as

$$\mathbf{f}^{(k)} = \mathbf{A}\mathbf{f}^{(k-1)} \tag{2.29}$$

where A is an operator obtained from Eq. (2.28). The following analysis and generalization of some classical signal restoration algorithms using iterative Eq. (2.29) parallels in part the derivation given by Schafer et al. [59]. The A operator, in general, depends on H and it may also incorporate constraints based upon known properties of the desired solution. The flexibility which is available for mixing constraints and distortion using iteration like Eq. (2.29) causes a great practical advantage in estimating the object signal function, especially in the presence of measurement error or noise. There is a number of properties of the object signal we may know a

priori. A convenient way of expressing such a priori knowledge is by introducing a constraining operator D, such that if f satisfies the constraint then

$$f = Df. \tag{2.30}$$

Thus the signal positivity constraint operator P is defined by

$$D[f_n] = P[f_n] = \begin{cases} f_n, & \text{if } f_n > 0 \\ 0, & \text{otherwise} \end{cases} \tag{2.31}$$

where $f_n$, $-\infty < n < \infty$, are the elements of infinite vector f. Also, if f is known to be bandlimited to frequencies below $w_c$, then the bandlimiting constraint operator B, for the case of discrete-time signals, is defined by

$$D[f_n] = B[f_n] = \sum_{m=-\infty}^{\infty} f_m \frac{\sin[w_c(n-m)]}{\pi(n-m)} \tag{2.32}$$

Using this representation of a priori constraints, Eq. (2.28) can be written as

$$g = HDf \tag{2.33}$$

where HD is concatenation of D folowed by H. A constrained iteration of Eq. (2.22) can now be written as

$$f^{(k)} = Df^{(k-1)} + C(g - HDf^{(k-1)}). \tag{2.34}$$

Clearly, the constrained operator A (see Eq. (2.29)) is defined by

$$Af^{(k-1)} = Df^{(k-1)} + C(g - HDf^{(k-1)}). \qquad (2.35)$$

A signal f that satisfies Eq. (2.29), i. e.,

$$f = Af \qquad (2.36)$$

is called the fixed point of the operator A [28].

A number of existing signal restoration algorithms can be represented by the general constrained iteration of Eq. (2.34) [59]. In the following a brief review of these algorithms is presented.

## Landau and Miranker method

The problem of recovering a bandlimited signal degraded by a non-linear frequency bandlimiting system operator has ben considered by Landau [35] and Landau & Miranker [36]. Here the constraint operator is the bandlimiting operator B ( see Eq. (2.32)) and the distortion operator F is a memoryless non-

linearity, proposed as a model for transmission of companded signals trough a telephone channel, such that

$$g = BFf \tag{2.37}$$

The non-linear operation of companding finds also applications in image quantization [50]. Landau and Miranker showed that the original signal can be recovered by the iteration

$$\begin{aligned} f^{(0)} &= Cg \\ f^{(k)} &= Cg + f^{(k-1)} - CBFf^{(k-1)} \end{aligned} \tag{2.38}$$

It is easy to show that by substituting into the Eq.(2.34) the constraint operator D for B and the distortion H for BF, the iteration of Eq. (2.38) is obtained. Note that, because all the approximations $f^{(k)}$, k =1, 2, ..., in Eq. (2.38) are bandlimited, $Bf^{(k-1)}$ for any k can be replaced by $f^{(k-1)}$. Therefore, the general iteration of Eq. (2.34) can be directly applied to this problem with an appropriate choice of the constraint and degradation operators. For the condition for convergence of this algorithm see Ref. [36].

### Papoulis-Gerchberg and other bandlimited signal extrapolation methods

Iterative extrapolation of a bandlimited function from a finite duration segment has been considered by several authors.

Gerchberg [19] and Papoulis [48] employed a fast Fourier transform (FFT) algorithm to realize a frequency band-limiting constraint in the iterative Eq. (2.34). In this case of band-limited signal extarpolation, the distortion operator is a time-limiting operator S such that

$$D[f_k] = S[f_k] = \begin{cases} f_k, & -\infty < a \leqslant k \leqslant b < \infty \\ 0, & \text{otherwise} \end{cases} \qquad (2.39)$$

and the frequency band-limiting operator B is defined by Eq. (2.32). In the case that the discrete-time signal is obtained by sampling of a continuous-time band-limited signal with the frequency band-limit $w_c$, the sampling period must satisfy $\pi/T > w_c$, i. e., the signal must be sampled with the frequency higher then twice the Nyquist rate in order to talk about a frequency band-limited sequence. In Eq. (2.32) the sampling period T is normalized to unity and therefore omited.

Using Eq. (2.30) and the S and B operators as defined above, the Papoulis-Gerchberg iteration can be written as

$$f^{(k)} = Bf^{(k-1)} + (g - SBf^{(k-1)}) \qquad (2.40)$$

or

$$f^{(k)} = g + (I - S)Bf^{(k-1)} \qquad (2.41)$$

where I is an identity operator. In Eq. (2.40) the relaxation C is set to an identity and the iteration starts with $f^{(0)} = g$. It

is easy to show that the operator (I - S)B in Eq. (2.41) is a nonexpansive operator [59], thus insuring the convergence of the algorithm, although not to a unique fixed point in the case of a discrete-time signals. Nonuniqueness of the solution in the discrete case is due to the fact that the knowledge of a finite segment of a band-limited sequence does not uniquely specifies the sequence everywhere [59]. This leads to a serious noise sensitivity of the iteration of Eq. (2.40).

Considering the Papoulis-Gerchberg algorithm, Sabri & Steenart [57] proposed a one-step solution, i. e., a matrix formulation of the extrapolation problem. This matrix formulation follows from the Eq. (2.40) introducing a linear operator G = (I - S)B so that

$$f^{(k)} = g + Gf^{(k-1)} \tag{2.42}$$

The iteration Eq. (2.42) can be written as

$$f^{(k)} = gG^{0} + Gg + G^{2}g + \ldots + G^{k}g \tag{2.43}$$

where $G^{0}$ is an identity operator and $G^{1}$ is understood as multiple application of the same operator G. Since G is a linear operator Eq. (2.43) can be written as

$$f^{(k)} = \sum_{i=0}^{k} G^{i}g. \tag{2.44}$$

Since G is a non-expansive operator, i. e., $\|Gf\| \leq r\|f\|$ where $0 < r < 1$, the sum in Eq. (2.44) can be written in a closed form, so that

$$f^{(k)} = (I - G)^{-1}(I - G^{k+1})g. \qquad (2.45)$$

Clearly, since $\|G^{k+1}\| \leq r^{k+1}\|f\|$, $\|G^{k+1}\|$ approaches zero as k approaches infinity, and the Eq. (2.45), for large k, reduces to

$$f = (I - G)^{-1}g \qquad (2.46)$$

Eq. (2.46) presents a one-step solution to the band-limited signal extrapolation problem. Although the one-step solution of Eq. (2.46) is appealing, the $(I - G)^{-1}$ is an ill-conditioned operator, hence the determination of its inverse is a difficult task. An approach to the determination of the inverse $(I - G)^{-1}$ using a singular value decomposition method is presented in Ref. [29, 67].

Another approach to bandlimited discrete-time signal extrapolation, similar to Papoulis-Gerchberg iteration of Eq. (2.40), was presented by Cadzow [9]. Here the iterative equation is

$$f^{(0)} = Bg$$

$$f^{(k)} = Bg + (I - BS)f^{(k-1)} \qquad (2.47)$$

At the first glance this equation is different then Eq. (2.40), but applaying the band-limiting operator B to both sides of Eq. (2.40) we obtaine

$$Bf^{(k)} = Bg + (I - BS)Bf^{(k-1)} \qquad (2.48)$$

that reduces to Eq. (2.47) if the iteration starts with a band-limited **g**, i. e., B**g**, since every estimate $f^{(k)}$ is already band-limited. However, this algorithm applies different order of the band-limiting and truncation operations that may be advantageous for discrete-time signal extrapolation [9].

## Youla's alternating orthogonal projections method

Youla [72] developed an algorithm similar to the iteration of Eq. (2.22), but adopting a radically different point of view. In a Hilbert space [28] setting, linearly degraded signal restoration problem was considered as a sequence of geometrical orthogonal projections of a degraded signal vector onto two convex sets.

If L and ortL are a closed linear vector subspace and its orthogonal complement, respectively, in Hilbert space $H^s$, then the projection theorem [1, 28] states that for every $f \in H^s$ there is an unique decomposition

$$f = g + h \tag{2.49}$$

where $g \in L$ and $h \in ortL$, and the vector inner product $(g, h) = 0$. Since the vectors g and h are orthogonal we can introduce the orthogonal projection operators [1, 28] P and Q such that

$$g = Pf \tag{2.50}$$

and

$$h = Qf. \tag{2.51}$$

Let introduce two known vector subspaces $L_a$ and $L_b$ with their orthogonal complements $ortL_a$ and $ortL_b$, respectively, and their respective orthogonal projection operators $P_a$, $P_b$, $Q_a$ and $Q_b$. If, in the Hilbert space $H^s$, an object $f \in L_b$ is known only by its orthogonal projection $g = P_a f$ onto the $L_a$, then

$$g = P_a f = P_a P_b f = (I - Q_a) P_b f = P_b f - Q_a P_b f = f - Q_a P_b f \tag{2.52}$$

where I is an identity operator and $f = P_b f$, since $f \in L_b$. Based on Eq. (2.52) Youla introduced the iteration

$$f^{(i)} = g + Q_a P_b f^{(i-1)} \tag{2.53}$$

with $f^{(0)} = g$. Eq. (2.53) closely ressembles Eq. (2.17) or Eq. (2.29). As the matter of fact, with an appropriate choice of the two linear vector spaces $L_a$ and $L_b$, i. e., the signal spaces corresponding to a degradation system input and output f and g, respectively, the iteration of the Eq. (2.22) or the Eq. (2.34) can be obtained. The geometric meaning of the Eq. (2.53) is as follows; using the orthogonal projection operator $P_b$, $f^{(k-1)}$ is projected onto $L_b$, the result is then projected onto orthogonal complement of $L_a$, i. e., $ortL_a$, using the orthogonal projection $Q_a$, and this result is added to g to obtain $f^{(k)}$.

As it was proved by Youla, f is uniquely determined by its projection $g = P_a f$ onto $L_a$ if and only if

$$L_b \cap ortL_a = \{0\} \tag{2.54}$$

where $\{0\}$ denotes an empty set and $\cap$ denotes the set intersection; problem of reconstructing f from $P_a f$ is completely posed [72] if and only if

$$angle(L_b, ortL_a) > 0 \tag{2.55}$$

that is, if and only if

$$\|Q_a P_b\| < 1 \tag{2.56}$$

is satisfied. In both cases the sequence $\{f^{(k)}\}$, $k = 1, 2 \ldots$, generated by the iterative Eq. (2.53) converges to $f$ in norm.

For example, the discrete-time band-limited signal extrapolation from a finite duration segment can be performed using Youla's method with appropriate definitions of the vector subspaces $L_a$ and $L_b$ and the corresponding projection operators $P_a$, $P_b$, $Q_a$ and $Q_b$ in a given Hilbert space $H^s$. Let $L_a$ be the subspace of all the finite extent discrete-time signals in $H^s$ that vanish on the index $|n| > a$, and $L_b$ be the subspace of all the band-limited sequences with the band-limit $w_c$. Clearly $ortL_a$ denotes all the sequences in $H^s$ that vanish on the idex $|n| < a$, and $ortL_b$ denotes all the sequences in $H^s$ whose frequency components vanish in the frequency range $|w| < w_c$. The orthogonal projection $P_a$ is now a time-truncation operator of Eq. (2.39), i. e., $P_a = S$. The orthogonal projection $P_b$ is the bandlimiting operator of Eq. (2.32), i. e., $P_b = B$. Obviously $Q_a = I - P_a = I - S$. Substituting $P_b = B$ and $Q_a = I - S$ into the Eq. (2.53) the Eq. (2.41) is obtained, i. e., the original Papoulis-Gerchberg equation.

The Youla's method provides some additional theoretical insight into the problem of signal recovery, generalizing it from a geometric point of view. Formaly, in practical applications,

the algorithm reduces always to a functional equation described in the previous section and requires some additional interventions to neutralize the effect of noise and ill-posed nature of a particular problem. Some recently proposed new signal and image recovery methods are based on Eq. (2.53), used in conjunction with various object signal constraints (see Ref. [62, 64]).

## 2.4 AUTOREGRESSIVE AND MAXIMUM ENTROPY METHODS

The discrete-time signal power spectral density (PSD) estimation, a problem simmilar to the discrete-time band-limited signal extrapolation, received recently much attention. Conventional FFT spectral estimation is based on a Fourier series model of the data. This method, while computationally efficient has several inherent performance limitations [34, 42]. The most important one is poor frequency resolution, i. e., inabiliti to distinguish between two or more signal frequency components, especially when the observed sampled signal is of short duration. Several other approaches, developed initially in nonengineering areas, showed better performances. Among them the most prominent position has been taken by autoregressive (AR) [71, 70] and maximum entropy (MEM) [8] methods that will be briefly reviewed in this section.

Much of the current research in the area of PSD estimation deals with the autoregressive moving average (ARMA) models, that are a generalization of the AR model. In ARMA model the input $g = (g_0, g_1, \ldots, g_n, \ldots)$ and the output $f = (f_0, f_1, \ldots, f_n, \ldots)$ vector (or sequence) elements of a linear system are related by a difference equation of the form [42]

$$f_n = \sum_{m=0}^{q} b_m g_{n-m} - \sum_{k=1}^{p} a_k f_{n-k} \qquad (2.57)$$

where $b_m$, $a_k$ are constant coefficients. Using the z-transform method [46], the system transfer function H(z) can be written as

$$H(z) = \frac{B(z)}{A(z)} \qquad (2.58)$$

where

$$A(z) = \sum_{m=0}^{p} a_m z^{-m} \qquad (2.59)$$

and

$$B(z) = \sum_{m=0}^{q} b_m z^{-m}. \qquad (2.60)$$

If the input stochastic signal power spectrum is $P_g(z)$, the power spectrum, $P_f(z)$, at the output of the linear system, represented by its transfer function z-transform H(z), is [46]

$$P_f(z) = H(z)H^*(1/z^*)P_g(z). \qquad (2.61)$$

This expression can be evaluated on the unite circle, i. e., at the points $z = \exp(jwT)$, to obtain

$$P_f(w) = |H(w)|^2 P_g(w) \qquad (2.62)$$

where the independent variable exp(jwT) is replace by w in order to simplify the notation. If the system input process is a zero-mean white noise sequence with the variance v, then

$$P_f(w) = v|B(w)/A(w)|^2 \qquad (2.63)$$

where

$$B(w) = \sum_{m=0}^{q} b_m \exp(-jwmT) \qquad (2.64)$$

and

$$A(w) = \sum_{m=0}^{p} a_m \exp(-jwmT). \qquad (2.65)$$

By specifying the coefficients $b_m$ and $a_m$ in Eq. (2.64) and (2.65), respectively, and the input white noise variance v, the power spectrum $P_f(w)$ in Eq. (2.63) is determined.

In general, there are three ways to tackle the problem of PSD estimation using the approach presented above. The most general one is by using a linear system which represents a causal infinite impulse respone (IIR) filter with the system transfer function as in Eq. (2.58). The system model of this kind is usualy termed the ARMA model and consequently the PSD estimate, denoted by $P_{fARMA}(w)$, is termed the ARMA PSD estimate. If all the

coefficients $\{a_m\}$ except $a_0 = 1$ vanish, then the system difference equation becomes

$$f_n = \sum_{m=0}^{q} b_m g_{n-m} \tag{2.66}$$

In signal processing literature this system model is called an all-zero model, or moving average (MA) model of order q. The MA PSD estimate is now

$$P_{fMA}(\omega) = v|B(\omega)|^2. \tag{2.67}$$

The third possibility is that all $\{b_m\}$ coefficients except $b_0 = 1$ in Eq. (2.57) vanish. The system model, termed the all-pole, or autoregressive model, is now

$$f_n = -\sum_{m=1}^{p} a_m f_{n-m} + g_n. \tag{2.68}$$

The AR PSD estimate is

$$P_{fAR}(\omega) = v[1/|A(\omega)|^2]. \tag{2.69}$$

In the following, as an example, the AR PSD estimation is considered in more detail. It can be shown [34, 42], that the ARMA, MA and AR models are closely related, i. e., any stationnary ARMA or MA process of finite variance can be

represented as a unique AR model of possibly infinite order. The converse of this statement is also valid. Since the procedure to determine the coefficients for an AR model results in a system of linear equations, this method is very popular.

AR Model

Based on the Eq. (2.69), the AR PSD estimate can be written as

$$P_{fAR}(w) = \frac{v}{\left| 1 + \sum_{m=1}^{p} a_m \exp(-jwmT) \right|^2} \qquad (2.70)$$

From Eq. (2.70), it is clear that to estimate $P_{fAR}(w)$ it is necessary to estimate the set of papameters $\{a_1, a_2, \ldots, a_p, v\}$. Assuming a finite number N samples of the sequence $f = (f_0, f_1, f_2, \ldots)$ are known, the $M < N$ lags of the autocorrelation function $R_{ff}(m)$ can be estimated as

$$R_{ff}(m) = [1/(N-m)] \sum_{k=0}^{N-k-1} f_{k+m} f_k^* \qquad (2.71)$$

for $m = 0, 1, \ldots, M$. Having a known or estimated autocorrelation function $R_{ff}(m)$, the relationship between the AR parameters $\{a_m\}$

and this autocorrelation function can be established using the Yule-Walker [71, 70, 7] equations

$$R_{ff}(m) = \begin{cases} -\sum_{k=1}^{p} a_k R_{ff}(m-k), & \text{for } m > 0 \\ -\sum_{k=1}^{p} a_k R_{ff}(-k) + v, & \text{for } m = 0 \end{cases} \tag{2.72}$$

for $m = 1, 2, \ldots, p$. The Eq. (2.72) represents a linear system of $p + 1$ equations in $p + 1$ unknowns $\{a_1, a_2, \ldots, a_p\}$ and $v$. The values of the autocorrelation function at negative lags are obtained using its symmetry property, i. e., $R_{ff}(-m) = R_{ff}^{*}(m)$. An efficient algorithm, known as Levinson-Durbin [38, 13] algorithm, exploits Hermitian and Toeplitz properties of the autocorrelation matrix to solve the linear system of Eq. (2.72).

For the PSD estimation, in practical situations, usually a finite data set is available rather then a set of autocorrelation lags. Although it could be used to approximate the autocorrelation function, frequently a standard estimation theory is used to extrapolate the AR parameters. The estimation method usually used for the set of non-random parameters is the maximum likelihood method (MLM) [34, 42]. However, for shord data set, i. e., when the order of the AR model is close to the number of available data samples, the MLM produces poor results. To yield a better AR parameter estimate, an improvement can be achieved

using the least squares techniques [42] that operate directly on the data, utilizing forward or combination of forward and backward linear prediction (LP) techniques. However, in general, given a data set, the difficulties in determination of the order of the AR model are considerable. On the other hand, spectral estimation using the AR method is significantly noise sensitive. If the order of the AR model is not appropriate, and in the presence of noise, the results of estimation of spectra can be quite deteriorated. By increasing the system order this difficulties can be overcome, but at the expence of the increase in the processing requirements.

## Maximum Entropy Spectral Estimation (MESE)

Although the MESE and the AR spectral estimation are based on different approaches, they produce an identical result for Gaussian random processes and a known autoccorelation sequence of uniform spacing. The MESE is based on extrapolating of a known first p lags of the autocorrelation sequence with the constraint that the entire autocorrelation sequence is positive semi-definite. Burg [8] proposed a method that maximizes the randomnes of an unknown time series knowing its first p autocorrelation lags $\{R_{ff}(0), R_{ff}(1), \ldots, R_{ff}(p-1)\}$. Consequently, the estimated time series will have the flattest spectrum of all the spectra

with the given sequence of autocorrelation lags. To realize this goal Burg maximized the entropy of the PSD $P_f(w)$, i. e.,

$$\int_{-\pi/T}^{\pi/T} \ln P_f(w)\,dw \tag{2.73}$$

subject to the constraint that the p known autocorrelation lags sutisfy

$$\int_{-\pi/T}^{\pi/T} P_f(w)\exp(-jwmT)\,dw = R_{ff}(m) \tag{2.74}$$

for m = 0, 1, ..., p. Using the Lagrange multiplier method, the solution for the $P_f(w)$ is identical to Eq. (2.70) with $\{a_{p1}, a_{p2}, \ldots, a_{pp}\}$ as the $p^{th}$ order predictor parameters and v as the prediction error power.

This method, as the AR method, will provide high resolution for low noise level, although a spectral line spliting can occure. However, the determination of the order of the prediction model to be used remains a critical issue.

# 3. SUPERRESOLVING SIGNAL AND IMAGE RESTORATION USING A LINEAR ASSOCIATIVE MEMORY

## 3.1. INTRODUCTION

Direct discrete solution of the integral Eq. (1.1) can be obtained employing some numerical quadrature rule [24]. Assuming that the number of samples of a measured (degraded) sampled object vector g is equal to the number of samples of the sampled object vector f, we have

$$\mathbf{g} = \mathbf{H}\mathbf{f} \tag{3.1}$$

where H is an N*N degradation matrix operator obtained from the quadrature rule. The solution for f of Eq. (3.1) requires a matrix inversion. As in the continuous case, because the higher order eigenvalues of H tend rapidly to zero, H is a nearly singular matrix. Thus, the inverse of H does not exist, or if it exists, during the inversion process, the higher spatial frequency components of the signal are greatly amplified, causing numerical instability. If the degraded image g is noisy, even if $H^{-1}$ (where the superscript stands for the inverse) can be

properly approximated, the result of restoration may differ radically from the true solution.

To determine an approximate superresolving inverse $H^{-1}$, we employ here a set $\{(\mathbf{f}_k, \mathbf{g}_k)\}$, $k = 1, 2, \ldots, N$ of known degradation system input/output training sampled vectors and the LAM technique. The LAM relates the two given vectors $\mathbf{f}_k$ and $\mathbf{g}_k$ by the matrix equation [32]

$$\mathbf{f}_k = M\mathbf{g}_k \tag{3.2}$$

where M is an unknown matrix. In this terminology, the vectors $(\mathbf{f}_k, \mathbf{g}_k)$ are identified as the data and key vectors, respectively. The LAM matrix M represents a content addressable memory that allows, by specifying the proper key, the data recall. If the key and the data are identical, the recall is termed autoassociative, otherwise it is a heteroassociative recall [32]. To identify, or to restore superresolving linearly degraded signals or images, in the presence of appreciable noise, heteroassociative recall operation is proposed. In this model of associative memory, the k-th item to be stored consists of two parts, the key vector $\mathbf{g}_k$ and the data vector $\mathbf{f}_k$. The key and the data vectors are encoded as column vectors in the key X and the data Y matrix, respectively. The number of elements in the key g and the data f vectors need not be the same. The recall LAM matrix is in general $M = YX^{+}$, where + denotes the Moore-Penrose pseudo (generalised)

inverse [1]. The recall operation is performed by multiplying an input key vector $\mathbf{g}'$ (which can be a noisy or corrupted vector) by M to yield the desired data vector $\mathbf{f}'$. This result is the minimum norm least squares approximation to data vector $\mathbf{f}$, paired to the key vector $\mathbf{g}$, that is closest, in the sense of least squares, to the input vector $\mathbf{g}'$. However, in the case of heteroassociative recall it has been found [65] that, for certain structures of the key, or input matrix X, while the conditions for noiseless recall may be satisfied, the LAM can be sensitive to input noise. As the determinant of $(X^TX)$ approaches zero, in spite of even linear independence of the columns of X, the elements of the LAM matrix M may become unacceptably large. Very similar problem arises in the application of LAM to superresolving signal restoration, when, due to small SBP, the key matrix X containes a large number of similar columns. Hence, to achieve superresolution a constrained optimization of the dynamic range of the LAM matrix M elements with respect to the particular data-key set is proposed. The LAM matrix M is determined by a new constrained recursive training algorithm with a set of known degradation system input/output sampled vector pairs $\{(\mathbf{f}_k, \mathbf{g}_k)\}$, $k = 1, 2, \ldots, N$. The training set represents a known data-key set. Using this constrained LAM matrix M, it is shown that a superresolution far below the Rayleigh limit, even in the presence of large measurement noise, is attainable.

In section 3.2 the new constrained recursive training algorithm for the determination of a constrained LAM matrix and its application to the superresolving restoration is described. In section 3.3, the superresolution results are presented. Both 1D signal and 2D image superresolution, for different level of noise and space-bandwidth products, are demonstrated. Also, the results of restoration of particular test images, such as a triangle, a trapezoid and a gaussian pulse of different width and slope edges, are considered. Restoration in the presence of considerable additive noise and different space-bandwidth products, is demonstrated. Section 3.4 presents the summary and conclusions regarding the proposed method.

## 3.2. RECURSIVE CONSTRAINED VECTOR ASSOCIATIVE MAPPING ALGORITHM

In the linearly degraded image restoration problem, Eq. (3.1) relates the object f to the degraded image g by a linear degradation operator H. However, in the presence of noise, Eq. (3.1) is amended

$$g = Hf + n \tag{3.3}$$

where n is assumed to be uncorrelated, zero-mean, noise vector. It can be shown [1] that a minimum least squares norm estimate of f is

$$f = H^{+}g \tag{3.4}$$

where $H^{+}$ is the Moore-Penrose pseudo inverse [1]. $H^{+}$ can, in general, be determined by a singular-value decomposition (SVD) method [20]. The SVD method clearly indicates that the singular values of H, where H is an approximation to a discrete ILPF, as a function of the space-bandwidth product (SBP), change abruptly from approximately unity to nearly zero. This fact introduces numerical instability in the determination of the inverse of H. To deal with this problem, a number of direct or iterative regularized algorithms were proposed [15, 30, 63]. In general,

these regularization algorithms tend to attenuate those signal components that correspond to the high order singular values of H at the expense of superresolution, where precisely these high order eigenvalues are needed [2]. In this Chapter, to obtain an approximation to the system inverse degradation operator, we propose a new constrained LAM method. The unconstrained LAM algorithm is considered first, and then the new constraining procedure, that provides a stable system inverse degradation operator, is introduced.

Let a degradation system input-output set of vectors be $\{f_r\}$ and $\{g_r\}$, $r = 1, 2, \ldots, N$, respectively. Each pair of vectors $(f_r, g_r)$ can be related by a matrix M (see Eq. (3.2)). We form the key X and the data Y matrices with the column-vectors $\{g_r\}$ and $\{f_r\}$, respectively, as

$$\begin{aligned} X &= [g_1, g_2, \ldots, g_N] \\ Y &= [f_1, f_2, \ldots, f_N] \end{aligned} \tag{3.5}$$

From Eq. (3.4), a matrix equation is obtained

$$Y = H^t X. \tag{3.6}$$

If we identify $H^t = M$ then

$$Y = MX, \tag{3.7}$$

where the least squares sense optimum solution for M is again

$$M = YX^{+}. \tag{3.8}$$

To determine an approximation to the inverse degradation M, the pseudo-inverse $X^{+}$ is required. A number of methods for the determination of $X^{+}$ [1,21,22,51,56] could be employed. However, all those pseudo-inversion methods, because of ill-conditioning of the X matrix for small SBP, show a numerical instability, producing an inadequate inverse. Here, to evaluate the M matrix, a recursive gradient projection algorithm, that is based on a theorem of Greville [21,22] on pseudo-inverses of partitioned matrices (see Kohonen [32]), is used. This algorithm is a trade-off between numerical complexity and computational speed, but it provides a mechanism for adding constraints to the M matrix. A brief outline of the unconstrained recursive algorithm is as follows.

Let $M_r = Y_r X_r^{+}$ be the r vector pair LAM matrix (by r vector pair we mean that both the Y and X matrices contain r columns). The $Y_r$ matrix can be partitioned as $[Y_{r-1}, f_r]$. Applying Greville's theorem [21,22], the $X_r^{+}$ can be determined as

$$X_r^{+} = \begin{bmatrix} X_{r-1}^{+}(I - g_r c_r^{T}) \\ \hline c_r^{T} \end{bmatrix} \tag{3.9}$$

where I is the N*N identity matrix, T stands for transpose, and

$$c_r = \begin{cases} \dfrac{(I - X_{r-1}X_{r-1}^{+})g_r}{\|(I - X_{r-1}X_{r-1}^{+})g_r\|^2} & \text{if denumerator is} \neq 0 \qquad (3.10a) \\ \dfrac{(X_{r-1}^{+})^T X_{r-1}^{+} g_r}{1 + \|X_{r-1}^{+} g_r\|^2} & \text{otherwise} \qquad (3.10b) \end{cases}$$

where $\|.\|$ represents a quadratic vector norm. Multiplying the partitioned matrix $Y_r$ by $X_r^{+}$ (see Eq. (3.9)) yields

$$M_r = Y_{r-1}X_{r-1}^{+} + (f_r - Y_{r-1}X_{r-1}^{+}g_r)c_r^T \qquad (3.11)$$

or, equivalently,

$$M_r = M_{r-1} + (f_r - M_{r-1}g_r)c_r^T \qquad (3.12)$$

In the case where $g_r$ is linearly independent of the previous columns of X, for $c_r^T$ Eq. (3.10a) applies, otherwise Eq. (3.10b) implies $M_r = M_{r-1}$ [32]. Therefore, the recursive algorithm for $M_r$ given $M_{r-1}$ is

$$M_r = \begin{cases} M_{r-1} + (f_r - M_{r-1}g_r)\dfrac{p_r^T}{\|p_r\|^2} & \text{for } \|p_r\| \neq 0 \\ M_{r-1} & \text{otherwise} \end{cases} \qquad (3.13)$$

where $p_r$ is the orthogonal projection of $g_r$ to the vector subspace spanned by the column vectors of the key matrix X, i.e., $(g_1, g_2, \ldots, g_{r-1})$. The orthogonal projection vector $p_r$ can be obtained either from a Gram-Schmidt orthogonalization (GSO), or a modified GSO (MGSO) procedure [20]. The GSO algorithm for the orthogonal projection vectors is

$$p_r = g_r - \sum_{i=1}^{r-1} \frac{(g_r, p_i)}{\|p_i\|^2} p_i \qquad (3.14)$$

where the bracket $(.,.)$ denotes the vector inner product. Similar mechanism is also available for the MGSO procedure. In Eq. (3.14), the sum over "i" is taken for the nonzero $\|g_i\|$ only. The initial LAM matrix $M_0$ can be choosen to be either a zero, or the identity matrix, or the covariance matrix obtained from the deterministic set of degraded training vectors $\{g_k\}$ as

$$C_{gg} = (1/N) \sum_{i=1}^{N} g_i g_i^T \qquad (3.15)$$

When the SBP is small (especially when SBP $< 1$), the key matrix X, composed of the similar column vectors $(g_r)$ (degraded images of the original object vectors $\{f_r\}$), is also ill-conditioned. For example, for an impulsive type of object vectors $\{f_r\}$ with closely spaced impulses, the SVD of X clearly shows that the high-order singular values, as a function of the SBP,

drop abruptly to almost zero. Thus, the recursive algorithm of Eq. (3.13), for small SBP, shows numerical instability by producing a solution for M with a very large quadratic matrix norm $\|M\|$. This is due to the large number of nearly zero vectors in the orthogonalized set $\{p_r\}$, calculated by either a GSO or MGSO (see Eq. (3.14)), so that the number of algorithmic recursion steps (see Eq. (3.13)) is small. This fact suggests a search for a new set of projection directions $\{p_1, p_2, \ldots, p_N\}$, which may not correspond to the orthogonal directions, but could provide a large number of recursion steps. In order to realize this objective, the GSO process is reconsidered. GSO performs well when the vectors $\{q_r\}$, $r = 1, \ldots, N$, are linearly independent. However, when X is rank-deficient or ill-conditioned with a large number of nearly linearly dependent vectors $q_r$, the resulting set of orthogonalized gain vectors $\{p_r\}$ contains a large number of zero, or nearly zero, vectors rendering the algorithm of Eq. (3.13) useless. For such an X matrix, in order to carry on a procedure for searching for a new set of 'pseudo-orthogonal' gain vectors $\{p_r\}$, the GSO process is modified by introducing a variable threshold parameter P. The role of the threshold parameter P is to point out the terms in the sum of Eq. (3.14) where $\|p_i\| < P$. Those terms that satisfy this condition are discarded and a search for more appropriate set of the gain vectors $\{p_i\}$ with respect to the quadratic matrix norm of M is initiated. The value of P is determined to minimizes the quadratic matrix norm of an approximate solution for M (i. e., its first singular value). The new set of the 'pseudo-orthogonal'

vectors $\{p_r\}$, if available, provides a large number of the recursion steps of the algorithm of Eq. (3.13). The recursive LAM algorithm of Eq. (3.13) and (3.14), together with this constraining procedure, is termed the constrained associative memory (CAM) method.

The new set of "pseudo-orthogonal" vectors $\{p_r\}$ is obtained as follows. Using the P parameter, the norm $\|p_i\|$ in Eq. (3.14) is tested before it is added to the previous set of terms. The following decision rule is used: the $\|p_i\|$ is compared to P, if $\|p_i\| < P$ then the related term in the sum of Eq. (3.14) is discarded, otherwise a division by $\|p_i\|$ is performed and it is accepted. Thus, for a given value of P, a new set of 'pseudo-orthogonal' $\{p_r\}$ vectors is formed as the result of constrained Gram-Schmidth orthogonalization process. To determine the set $\{p_r\}$ that minimizes $\|M\|$, one starts with a small initial threshold parameter $P_0$. Next, in an iterative loop, for increasing values of P, new LAM matrices are generated and their quadratic matrix norms are calculated until a minimum is reached. The LAM matrix M with the smallest quadratic matrix norm is used for signal reconstruction (associative recall). It is performed by a simple matrix-vector multiplication of the inverse-degradation CAM matrix M and a noisy degraded signal g. Thus, for an N recursion step inverse-degradation matrix $M_N$, the vector-matrix product

$$f = M_N g, \tag{3.16}$$

where g is a degraded noisy signal, yields an estimate for the object signal f.

As an example of the constrained GSO process, and to illustrate the role of the threshold parameter P, a number of plots are next presented.

Let the elements of an ill-conditioned 128*128 matrix X be constructed using the 'sinc' functions of Eq. (1.3) with the cutoff frequency of $w_c = \pi/8$. The columns of this matrix are the vectors $\{\mathbf{g}_r\}$, r = 1, 2, ..., 128. For this example, let Y be an identity matrix. Next on the column vectors $\{\mathbf{g}_r\}$, with a threshold parameter P, the GSO process is performed. This yields the set of 'pseudo-orthogonal' vectors $\{\mathbf{p}_r\}$. To determine the M matrix, the recursive CAM algorithm is used. Next the quadratic matrix norm of M is computed. With several different threshold P values, this procedure is repeated until the quadratic matrix norm of M reaches its minimum. Figs. 3.1 through 3.4 present the result of the constrained GSO process as 3D plots of a 128*128 matrix, constructed from the set of pseudo-orthogonal column vectors $\{\mathbf{p}_r\}$, for four different values of the threshold parameter P. Fig. 3.1 presents the set of $\{\mathbf{p}_r\}$ vectors for P = 0.001, equivalent to an unconstrained orthogonalization. It is clear that most vectors are practically of zero norm. Fig. 3.2a)

presents the 3D plot of a matrix with the 'pseudo-orthogonal' vectors $\{p_r\}$ as its columns, obtained with the threshold parameter P = 0.5, while Fig. 3.2b) presents the plot of both the quadratic vector norms of $\{p_r\}$ (circles) and, as a reference, the quadratic vector norms of column vectors $\{g_r\}$ (squares). As it can be observed, now the $\{p_r\}$ set contains a considerable number of nonzero norm vectors. In Figs. 3.3a) and b) the threshold parameter P = 2 is used. For this value of P, the set $\{p_r\}$ contains an even larger number of nonzero norm vectors. Figs. 3.4a) and b) present the results for the optimal threshold parameter P = 3 (the minimum quadratic matrix norm of M). For this case (see Fig. 3. 4b)) a regular distribution of the quadratic norms of the vectors $\{p_r\}$ is observed.

In Figs. 3.5a) and b), two plots that illustrate the effect of the constraining procedure and the threshold parameter P on the resulting M matrix elements, are presented. In Fig. 3.5a), the elements of the M matrix obtained using the $\{p_r\}$ vectors of Fig. 3.3, are shown. It is clear that the dynamic range of the M matrix elements is still quite large. In Fig. 3.5b), a 3D plot of the M matrix elements, obtained using the optimum $\{p_r\}$ vectors of Fig. 3.4, is presented. For the low values of P, the elements of M are very large.

While M is usually trained with known and desired signals, however, it can also be trained to reject known, sometimes only statistically, undesirable signals. For example if we wish to reject pure noise signals, the training procedure is modified so as to include also a set of known noise $\{n_n\}$ and desired zero vectors $\{z_n\}$ (these are vectors with zero as their elements). The new training set becomes $\{(f_k, n_n; g_k, z_n)\}$, $k = 1, \ldots, M$; $n = M+1, \ldots, N$, where the pairs $(f_k, g_k)$ are ILPF inputs and outputs, and $(n_n, z_n)$ are noise and zero vectors, respectively. In this way, the M matrix can be trained to reject noise by producing a null output response. If we wish to reject either impulse noise, or sinusoidal interferences, or some other signal sets superimposed on the set of desired and known signals, a similar procedure could be used.

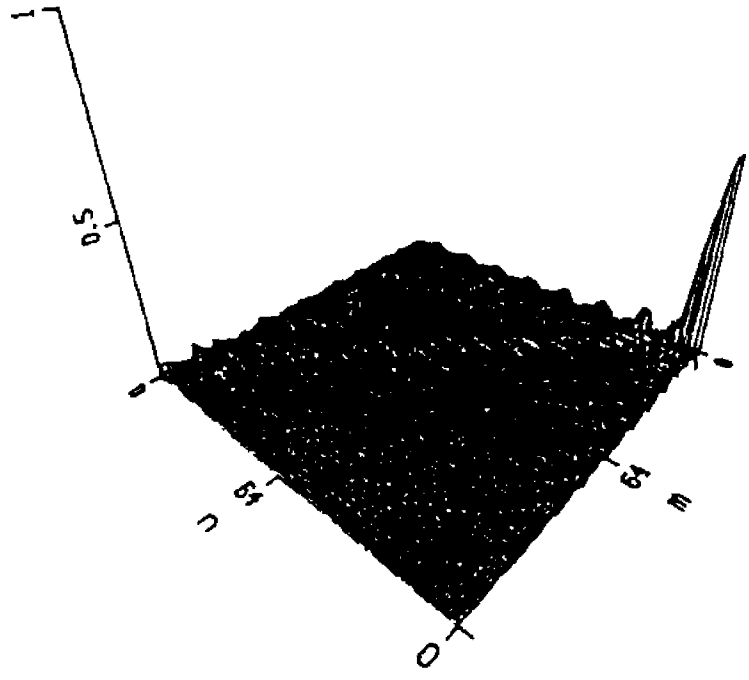


Fig. 3.1 A 3D plot of the G matrix orthogonalized column vectors ($p_r$), for the threshold parameter P = 0.001 (majority of G matrix column vectors are linearly dependent, hence most of the ($p_r$) vectors are null vectors).

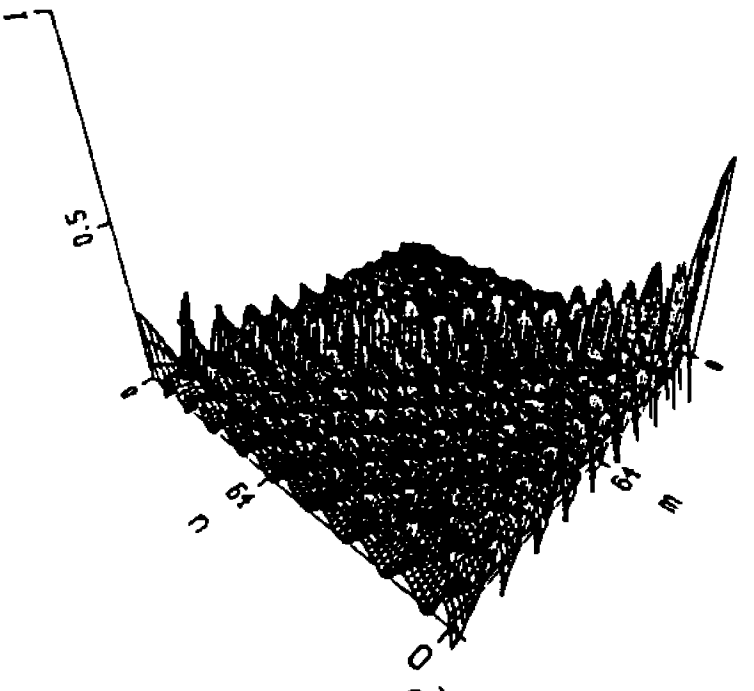


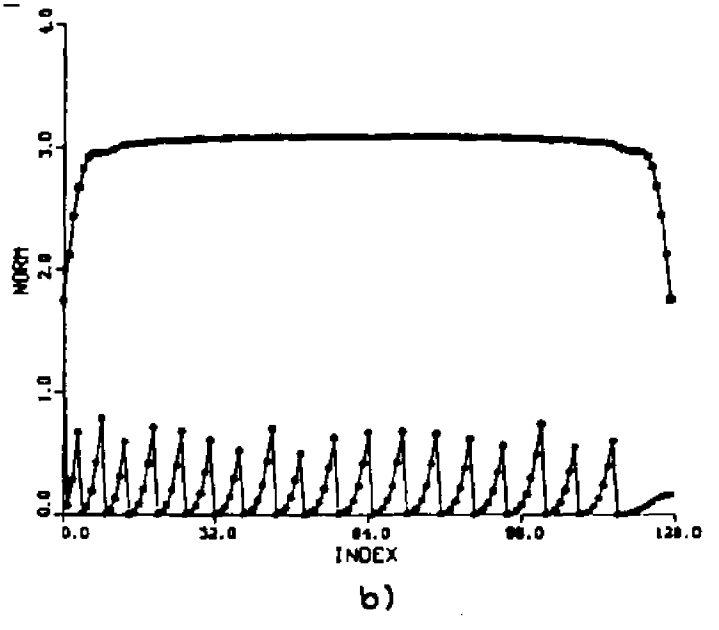


Fig. 3.2a) A 3D plot of $(p_r)$ as in Fig. 3.1, but for P = 0.5. b) The quadratic vector norms of $(p_r)$ (circles) and the original matrix B column vectors $(g_r)$ (squares).

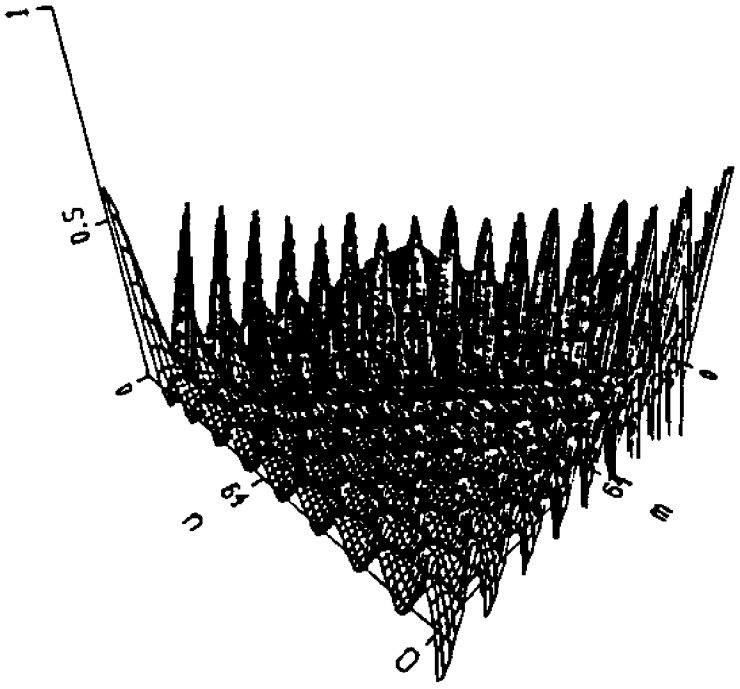


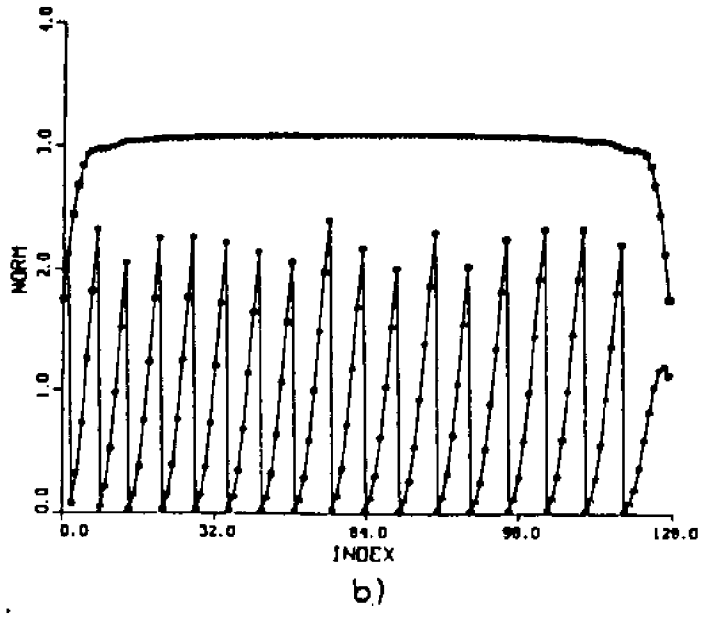


Fig. 3.3a) and b) The same plots as in Fig. 3.2a) & b), but for P = 2.0 (a large number of nonzero ($p_r$) vectors can be observed).

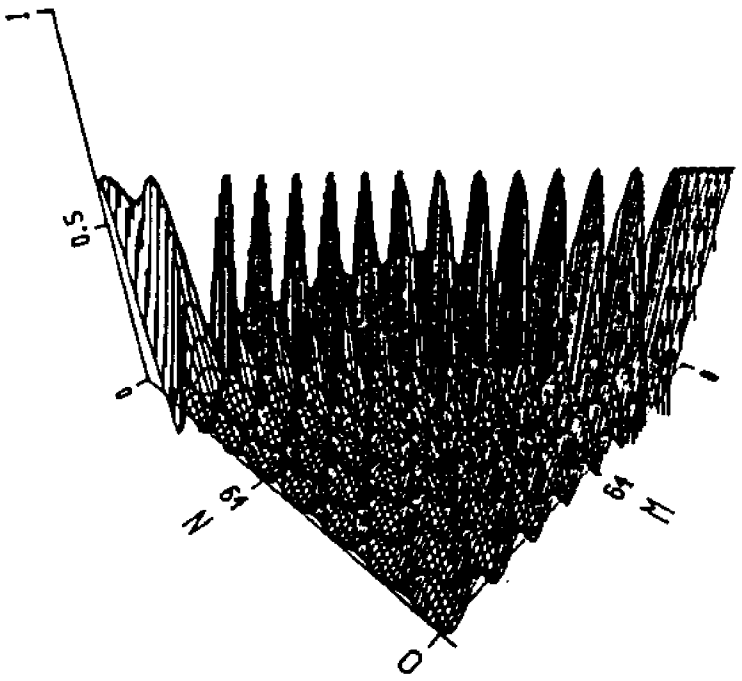


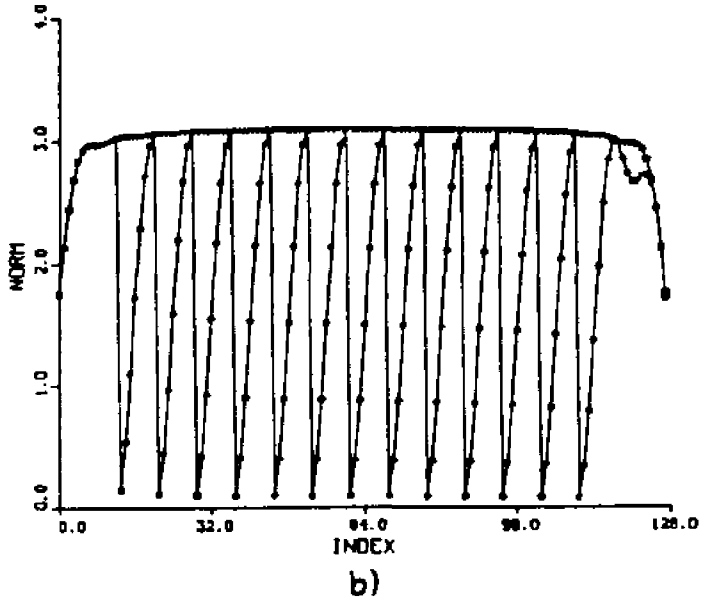


Fig. 3.4a) and b) The same plot as in Fig. 3.2 & 3.3, but for the optimal threshold parameter P = 3.0 (minimum quadratic matrix norm of M).

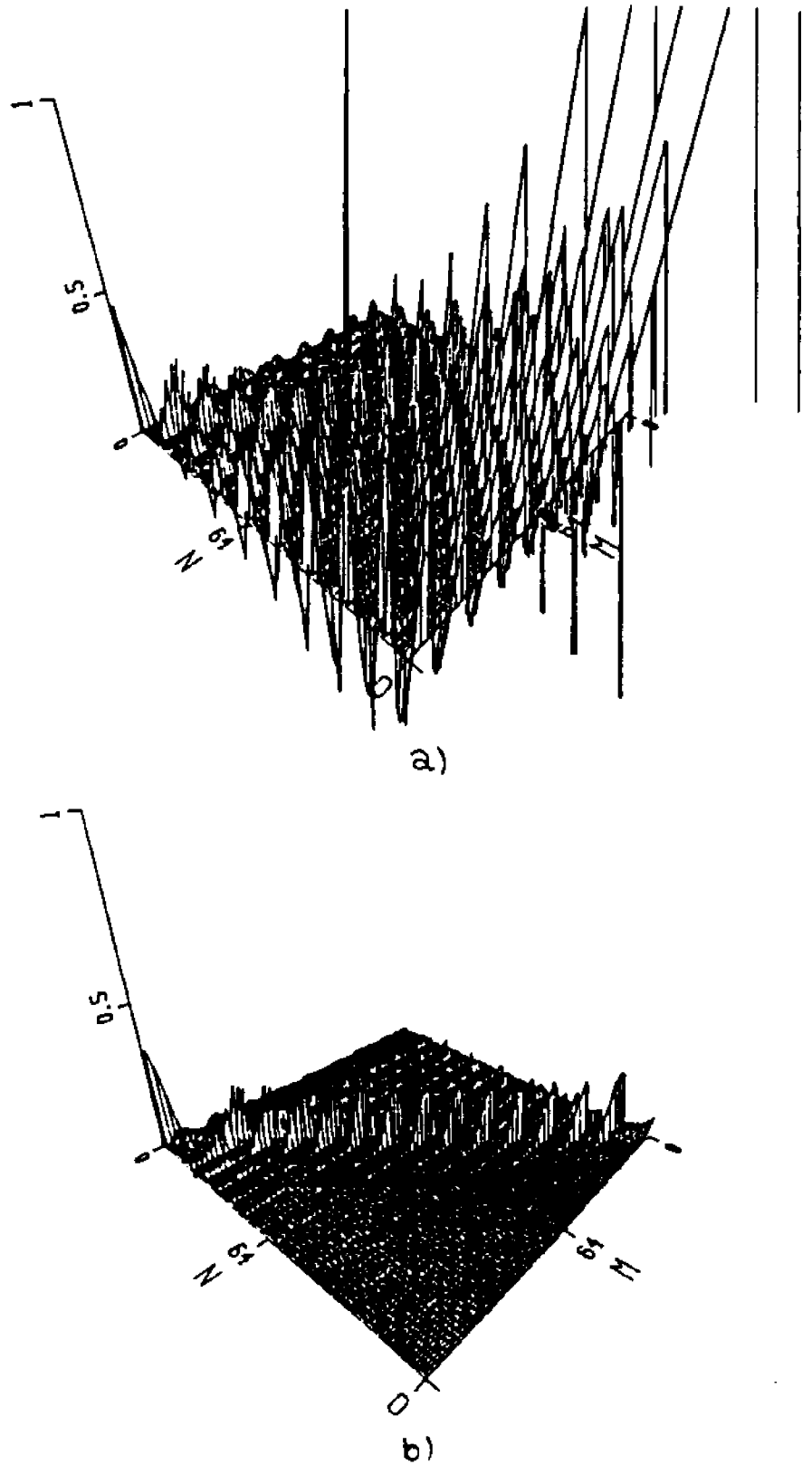


Fig. 3.5a) A 3D plot of an M matrix obtained using Gram-Smidt orthogonalization process for the threshold parameter P = 2.0. b) A 3-D plot of the M matrix for optimal P = 3.0.

### 3.3. EXPERIMENTAL RESULTS

In this section, computer simulation results for the problem of resolving two impulses, as well as to reconstruct superresolving signal waveforms, from a measured noisy output of ILPF, are presented. With different values for their SBP, the measured sampled vectors are contaminated by various levels of uniform additive noise.

First, the results for the superresolution of two-point objects, simulated by two ideal impulses are presented. To obtain the training set, a set of two-point object sampled vectors $\{f_k\}$, $k = 1,2,\ldots,100$, such that every sequence contains two ideal impulses, is formed. The impulses are arranged in such a way so that k-th sampled vector is $f_k = (1,0,\ldots,0,1,0,\ldots,0)^T$. Note, as a reference, the first impulse is always at the first slot while the second impulse shifts. The impulse strength is arbitrarily set to be unity. The data matrix Y, with its column sampled vectors $\{f_k\}$, is

$$Y = [f_1, f_2, \ldots, f_{100}] \tag{3.17}$$

To obtain the set of the training vectors $\{g_k\}$, every two-point object sampled vector $f_i$ is passed through an ILPF. From the

ILPF responses, a set of one hundred training vectors $\{\mathbf{q}_k\}$ is formed. For convenience, the number of vectors in the training set $\{\mathbf{q}_k\}$ is taken to be equal to the number of elements of the training vectors. Using this set, the columns $\mathbf{q}_k$ form the key matrix X

$$X = [\mathbf{q}_1, \mathbf{q}_2, \ldots, \mathbf{q}_{100}] \tag{3.18}$$

The order of the columns of the matrix X corresponds to the order of the columns of the matrix Y. The input and the output vectors are related by Eq. (3.7). As described in Section 3.2 (see Eq. (3.13)) next the constrained LAM matrix $M_N$ is formed. The initial matrix $M_0$ is the noise free covariance matrix (see Eq. (3.17)).

As an example, in Fig. 3.6a), the first twenty singular values of the matrix $M_N$, after the first iteration step with P = 0.2, are presented. The rest of singular values are nearly zero. It is clear that the quadratic matrix norm of $M_N$ (i. e., the first singular value $6_1$) is a large number. Fig. 3.6b) presents the first twenty singular values of the CAM matrix $M_N$. Comparing Fig. 3.6a) to Fig. 3.6b), since $6_1(M_N)$ has decreased, the dynamic range of the constrained CAM matrix $M_N$ elements must also decrease. Fig. 3.7 presents the plot of $\|M_N\|$ as a function of the threshold parameter P. It is clear that, for this particular key matrix structure, the quadratic matrix norm $\|M_N\|$ shows a minimum for P about two. The search for the optimum threshold parameter P has been initiated at $P_0 = 0.2$ and then it has been

increasing with the increments of P = 0.2 until the minimum of $\|M_N\|$ is reached. In order to ensure that a minimum has been found, because the quadratic norm of $M_N$ is mostly a monotonically decreasing function of P (see Fig. 3.7), it was sufficient to proceed with only two iteration steps past the minimum. Fig. 3.8. presents the result of a signal restoration using the CAM matrix $M_N$ whose singular values are shown in Fig. 3.6b).

In Fig. 3.9a) and b), the results of superresolving of two impulses from noisy measured sampled vectors, with SBP of 0.15 and two different levels of additive noise, SNR of 19db and 13db, respectively, are presented. While there is some discrepancy in the strength of the impulses, they clearly illustrate the noise resistant behavior of the CAM inverse filter. In Fig. 3.9c), the result of superresolving restoration of two impulses with SBP of 0.3 and SNR of 7db is presented. This result demonstrates the exceptional robustness of the CAM inverse filter.

Two dimensional images (2D) can be reduced to a long 1D signal by concatenating the rows of a 2D image [2]. As an example, a 16*16 two-point object image is formed. The two ideal impulses are distributed in such a way that the first impulse is kept at a fixed while the second one assumes all possible 256 positions. These 256 different images represent the training set of the two-point 2D object functions $(f_l)$. To obtain a set of

degraded images $\{g_k\}$, the $f_k$'s are passed through a 2D ILPF. In Fig. 3.10, some samples of the training, degraded, images $\{g_k\}$ are presented. To form the 2D constrained LAM matrix, the previous 1D analysis is followed. In Fig. 3.11, the result of superresolving restoration of a noisy degraded image with SNR of -6db and SBP of 0.5 is presented. As it can be observed, the result of superresolving resolution of a 2D image, even in the presence of high level of additive noise, is very good.

In addition to restoring impulses, the constrained LAM matrix technique can be used to reconstruct superresolving signal waveforms. In the next examples, a set of three different types of sampled waveforms, a triangle with different slope edges, a trapezoid, and a gaussian pulse of different width (see Fig. 3.12) is used. The input training set $(\{f_a\},\{f_z\},\{f_g\},\{f_n\})$ now consists of triangles $Y_1 = \{f_a\}$, trapezoids $Y_2 = \{f_z\}$, gaussian pulses $Y_3 = \{f_g\}$, with different slope edges and different width, and a set of zero vectors $Y_4 = \{z_n\}$, with 32 sampled vectors each subset. Corresponding to the set of zero vectors $\{z_n\}$, the $\{n_n\}$ is a set of pure noise vectors. Noise sampled vectors $\{n_n\}$ and their counterparts, the zero vectors $\{z_n\}$, are introduced into the training set to provide the noise rejection property for the LAM matrix by forcing to produce a null as its output response to noise. Each data sampled vector consists of 128 elements. This set is used to form the data matrix Y

$$Y = [Y_1, Y_2, Y_3, Y_4] \tag{3.19}$$

The set of output training vectors $\{(g_a),(g_z),(g_g),(g_n)\}$ $(X_1 = (g_a), X_2 = (g_z), X_3 = (g_g), X_4 = (g_n))$ is obtained from the response of ILPF to the input training set $\{(f_a),(f_z),(f_g)\}$ (see Fig. 3.12). The output training vectors form the key matrix X

$$X = [X_1, X_2, X_3, X_4] \tag{3.20}$$

The input and the output training sampled vectors are related by the matrix Eq. (3.7) which, in this case, is a 128*128 square matrix.

The restoration of the original sampled waveform is performed multiplying a noisy degraded sampled waveform, as in Fig. 3.13a) c) and e), by $M_{128}$. The results of restoration are presented in Fig. 3.13b) d) and f). In the presented examples, the restoration has been performed in the presence of the same level of additive noise and different SBP for every particular type of waveforms. In Fig. 3.13b) the result of superresolving restoration of a degraded, noisy, triangle, with SBP of 0.03 and SNR of -3db is presented. The Fig. 3.13b) shows, that for heavy degradation (SBP of 0.03) and SNR of -3db, the result of restoration is very good. In Fig. 3.13d) the result of restoration of a noisy, degraded trapezoid, for SBP of 0.15 and SNR of 9db is presented. It can be observed that the edges and

the corners of the trapezoid are well reconstructed. Finally, in Fig. 3.13f), the results of superresolving restoration of a gaussian pulse, for SBP of 0.08 and SNR of 2db is presented.

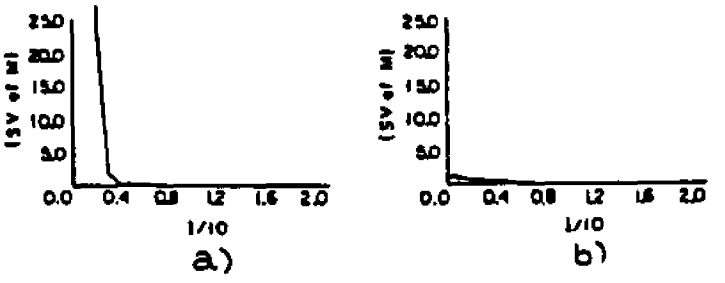


Fig. 3.6a) The first twenty singular values of an unconstrained LAM matrix M; b) as in a) for the constrained M (P = 2).

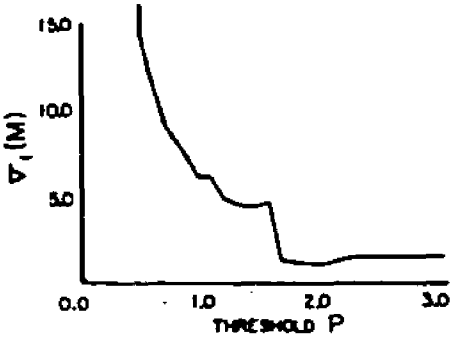


Fig. 3.7 Quadratic matrix norm of a superresolving matrix ||M|| as a function of the threshold parameter P.

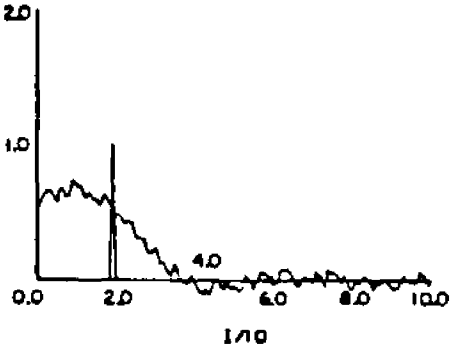


Fig. 3.8 Resolution of a degraded noisy two-point object with SNR of 19db and SBP of 1, obtained with the constrained M, with singular values as in fig. 1b). This constrained matrix M will be used in the next examples for two-point object superresolution.

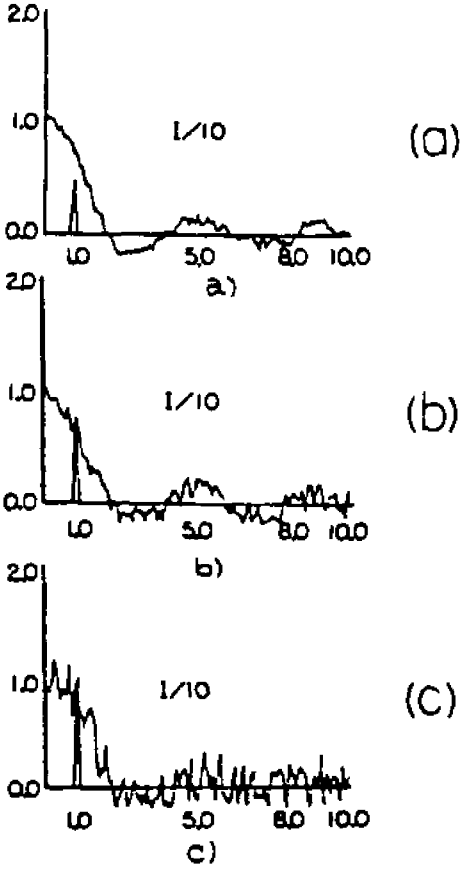


Fig. 3.9a) Superresolution of two-point objects with SBP = 0.15 and SNR of 19db; b) with SNR of 13db; c) with SNR of 7db and SBP of 0.3.

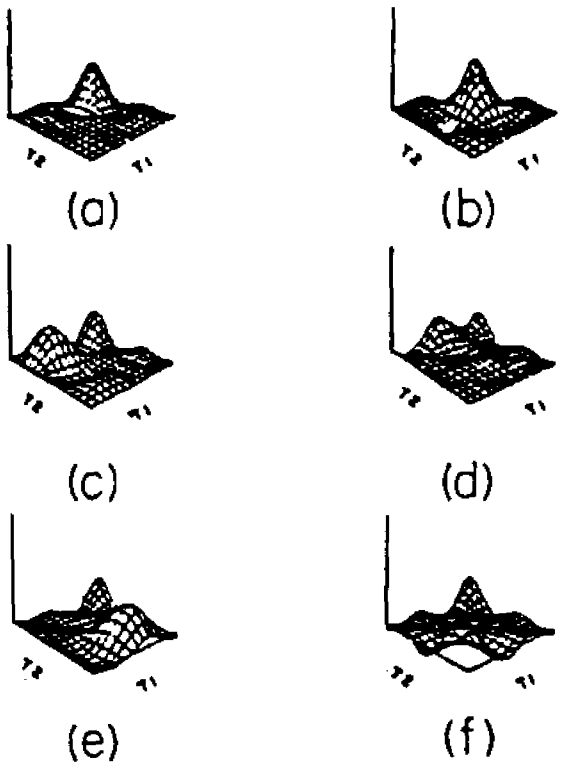


Fig. 3.10 Sample of the noise-free degraded training patterns used in constructing the 2D constrained M matrix.

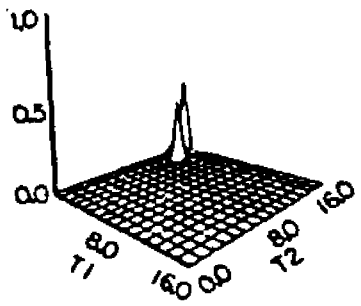


Fig. 3.11 The result of restoration of 2D two-point object with SNR of -6db and SBP of 0.5.

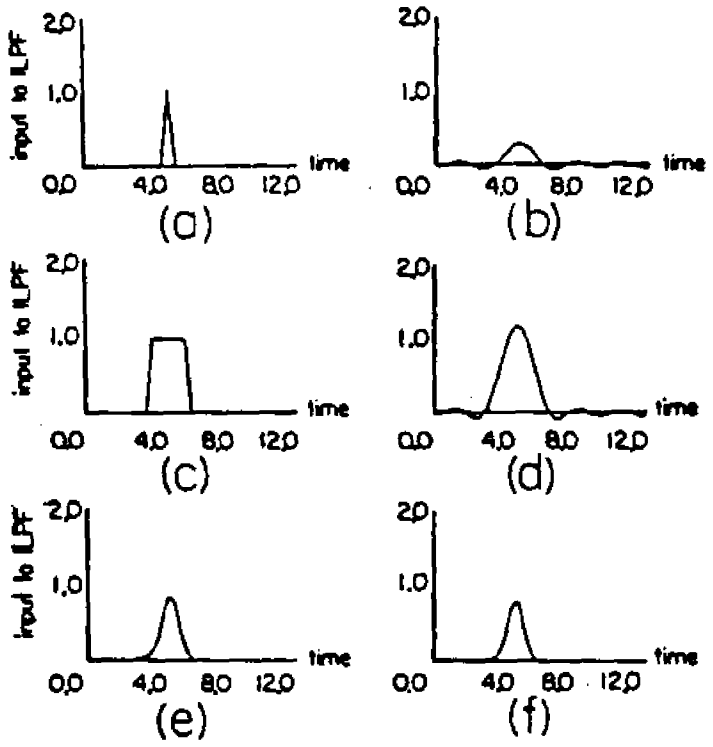


Fig. 3.12 Samples of the input-output noise-free training patterns (input-output of ILPF) used to form a LAM matrix M: a) and b) a triangle; c) and d) a trapezoid; e) and f) a gaussian pulse.

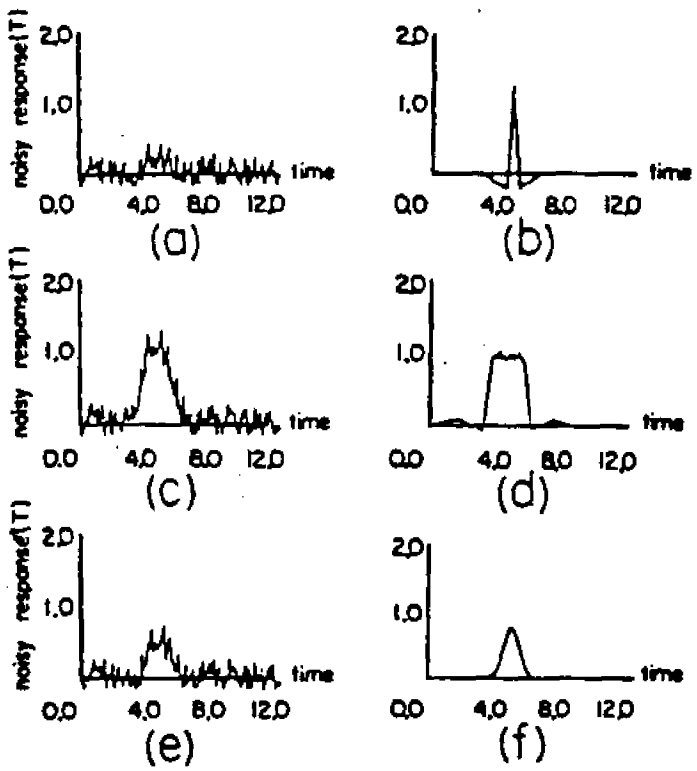


Fig. 3.13a) Noisy degraded triangle from Fig. 7a), SNR = -3 db, SBP = 0.3; b) the result of restoration of signal in a); c) noisy degraded trapezoid from Fig. 7c), SNR = 9db, SBP = 0.15; d) the result of restoration of signal in c); e) noisy degraded gaussian pulse from Fig. 7e), SNR = 2db, SBP = 0.08; f) the result of restoration of signal in e).

## 3.4. SUMMARY AND CONCLUSION

In this Chapter, a new approach for superresolving signal and image restoration has been proposed. At the expense of limiting the set of reconstructable signals, an exceptionaly robust inverse filter has been obtained. The filter is based on the principle of the content-addressable memory. A practical realisation of this memory was performed by employing the LAM technique. To determine a superresolving system degradation inverse, a new constrained, CAM, training algorithm has been introduced. The inverse filter was tested on different sets of 1D and 2D degraded signals with different levels of degradation and in the presense of very significant noise. The 1D and 2D noisy degraded two-point sources have been resolved for SBP far below unity. It has been shown that the proposed inverse filter restores equaly well both impulsive and edge-type images. The presented method limits the set of applicable signals to a known training set. However, the set of desirable signals can be extended by introducing several CAM parallel inverse filters, trained to a particular set of signals. Once calculated, for a given set of training signals, the entries of the LAM matrix M could be stored into a set of high-density read-only memory (ROM) chips for further use. With a fast optical and/or electronics vector processor (it is necessary to perform only one matrix-vector multiplication), the CAM inverse filter is easily

hardware-realizable. This suggests its use in a real-time environment.

# 4. A GENERAL ONE STEP INVERSE FILTER FOR LINEARLY DEGRADED SIGNAL RESTORATION USING THE CAM METHOD

## 4.1. INTRODUCTION

A linear degradation, blurring or smoothing, is an operator that is modeled, in the case of a linear shift invariant (LSI) system, by a convolution process. Thus, the problem of recovering a signal from its degraded image is usually referred to as a deconvolution problem. Some examples of the LSI convolution operators are the point-spread function of an optical system [30], the reflection impulse response of the layered earth in seismic applications [47], or the impulse response of a channel, or a magnetic recording medium [47], which broadens and blurs the desired message (the intersymbol interference). A linear shift variant (LSV) system is modeled by the superposition process. An example of a LSV blurring is recording of gamma-ray spectra where the amount of blurring depends on the energy [59].

An appropriate general linear discrete model of the problem considered here is the superposition sum

$$g(n) = \sum_{k=-\infty}^{\infty} f(k)h(n,k), \quad n = 0, \pm 1, \pm 2, \ldots \qquad (4.1)$$

where f(k) is the object sequence, h(n,k) is the degradation kernel, and g(n) is the degraded image sequence. The Eq. (4.1) can be written in matrix form as

$$g_{inf} = H_{inf} f_{inf} \tag{4.2}$$

where $H_{inf}$ is an infinite dimensional matrix degradation operator, and $f_{inf}$, $g_{inf}$ are infinite object and degraded vectors respectively. The exact form of the degradation operator $H_{inf}$ depends on a number of factors. For example, in the case of an LSI ideal low-pass degradation, the elements of $H_{inf}$ are [29]

$$\{h_{n,k}\} = \frac{\sin(w_c(n-k))}{\pi(n-k)}, \quad n,k = 0, \pm 1, \pm 2, \tag{4.3}$$

where $w_c$ is the filter cutoff frequency.

In the case of a LSV system, the degradation matrix operator $H_{inf}$ in Eq. (4.2) corresponds to the two-dimensional array with the elements {h(n,k)} from Eq.(4.1).

If the discrete signal f(n) corresponding to the vector $f_{inf}$ of Eq. (4.2) is of compact support, with less then N nonzero samples, the infinite dimensional discrete model of Eq. (4.2) can

be converted into a tractable finite dimensional model by a spatial truncation so as to obtain

$$g = Hf \tag{4.4}$$

The H is now in general an M*N degradation matrix, and the infinite object vectors $f_{inf}$ and $g_{inf}$ are reduced to the appropriate sizes so that the discrete finite model of Eq. (4.4) is satisfied.

If the matrix degradation operator H has a stable inverse it is possible to recover the desired signal f from the observed signal g. However, in practice, the degradation operator H is usually either rank deficient or ill-conditioned. The ill-conditioned nature of H is determined by the condition number, i. e., the ratio of the maximum to the minimum singular value of H. A large condition number, which is the measure of the relative normed distance from H to the set of singular matrices [25], indicates an ill-conditioned H. Therefore, if the linear system of Eq. (4.4) is inconsistent, due to either the presence of slight measurement noise, or to the imprecise model of the ill-conditioned degradation operator H, during the inversion proces this inconsistency is greatly emphasized, producing an unsatisfactory solution for f.

In the previous Chapter (see also Ref. [66, 14]), with the CAM method, and a known training set of the degradation input/output signals, an inverse filter has been produced applicable to a degraded signal from the same training set with some additional distortion, measurement error or noise. It has been shown that this kind of inverse filter performs well on both impulsive or edge type of signals, depending on the training set. In this Chapter, using the CAM method and a special set of training input/output signals a new robust inverse filter, particularly suited for impulsive type of signals and images, is obtained. This general inverse impulsive type filter does not depend on a particular training set of signals. Thus the inherent limit in the application of the CAM method, as to the number and the position of the impulses to be recovered, is removed. The new technique permits the recovery, even in the presence of strong noise, of arbitrary number of impulses degraded by a linear degradation operator. In order to produce such a general inverse filter, in the next section, a method is presented to determine the necessary degradation operator input/output training set of signals appropriate to the CAM method.

This Chapter is organised as follows: In section 4.2., the concept of an ideal LSI and LSV discrete inverse degradation operators as a CAM matrix, is presented. A general degradation H input/output training signal set is determined. Also, a method for 2D image reconstruction using 1D inverse degradation

operator, is described. In section 4.3., the results for the recovery of some noisy, degraded, impulsive-type signals, are presented. Both 1D signal and 2D image superresolving restoration, for different level of noise, space-bandwidth products, and degradation operators are demonstrated. In section 4.4. the summary and conclusions are presented.

## 4.2. A DIRECT CAM SUPERRESOLVING INVERSE FILTER

In general, a linear associative memory [32] relates in optimal way, in the sence of least squares, two vectors $f_r$ and $g_r$ from the set of vector pairs $\{(f_r,g_r)\}$, $r = 1, 2, \ldots, N$, by a matrix equation

$$F = MG \tag{4.5}$$

where F and G are the matrices with the column vectors $\{f_r\}$ and $\{g_r\}$, respectively. The task of the CAM method is to solve the matrix Eq. (4.5) for M, in the case when the G matrix is either rank-deficient or ill-conditioned. In this section, the problem of determining the inverse degradation operator H (see Eq. (4.4)) is formulated in a form of Eq. (4.5) appropriate to apply next the CAM method. The LSI and LSV, 1D, as well as the 2D separable [50], linear degradation systems are considered.

### a. Linear shift-invariant system

For a compact support object sequence f(n)

$$f(n) = \begin{cases} f(n), & n = 1, \ldots, N \\ 0, & \text{otherwise} \end{cases} \tag{4.6}$$

the discrete model of a LSI system is

$$g(n) = \sum_{k=1}^{N} f(k)h(n-k). \qquad (4.7)$$

The estimate $\hat{f}(n)$ sequence can be approximated as

$$\hat{f}(n) = \sum_{m=1}^{N} y(m)g(n-m) \qquad (4.8)$$

where $y(m)$ represents an unknown inverse filter impulse response sequence. Substituting $g(n)$ of Eq. (4.7) into Eq. (4.8) and interchanging the order of summation, we have

$$\hat{f}(n) = \sum_{k=1}^{N} f(k) \sum_{m=1}^{N} y(m)h(n-k-m). \qquad (4.9)$$

Let

$$a(n-k) = \sum_{m=1}^{N} y(m)h(n-k-m), \qquad (4.10)$$

Eq. (4.9) becomes

$$\hat{f}(n) = \sum_{k=1}^{N} f(k)a(n-k). \qquad (4.12)$$

It is clear that if $a(n) = \delta(n)$, where $\delta(n)$ is the unit-sample sequence, then $\hat{f}(n) = f(n)$, i. e. $\hat{f}(n)$ perfectly approximates $f(n)$. Therefore, the desirable form of Eq. (4.10) is

$$\delta(n) = \sum_{m=1}^{N} h(m)y(n-m) \qquad (4.13)$$

or, in matrix form,

$$\delta_1 = H^I h_1 \tag{4.14}$$

where $H^I$ is the ideal inverse-degradation matrix operator with the elements $\{y(n-k)\}$, $n,k = 1, \ldots, N$, $\delta_1$ is the unit-sample column vector with the unity as the first element and $h_1$ is the degradation system unit-sample response (point-spread) column vector. Introducing now a matrix shift operator S, $H^I$ and S commute [25] assuming $H^I$ is an LSI operator, we have

$$\begin{aligned}
S\delta_1 &= \delta_2 = SH^I h_1 = H^I S h_1 = H^I h_2 \\
&\vdots \\
S^{k-1}\delta_1 &= \delta_k = S^{k-1}H^I h_1 = H^I S^{k-1} h_1 = H^I h_k \\
&\vdots \\
S^{N-1}\delta_1 &= \delta_N = S^{N-1}H^I h_1 = H^I S^{N-1} h_1 = H^I h_N
\end{aligned} \tag{4.15}$$

where $S^k$, i. e., $S^k = SS...SS$ k-times, denotes the $k^{th}$ order shift. In matrix form, Eq. (4.15) is

$$[\delta_1, \delta_2, \ldots, \delta_N] = H^I[h_1, h_2, \ldots, h_N]. \tag{4.16}$$

If F and H are

$$F = [\delta_1, \delta_2, \ldots, \delta_N], \tag{4.17a}$$

$$H = [h_1, h_2, \ldots, h_N] \tag{4.17b}$$

where H corresponds to the version of a LSI degradation operator of Eq. (4.4), then Eq. (4.16) becomes

$$F = H^I H. \qquad (4.18)$$

For a rank-defficient or ill-conditioned H, the inverse-degradation $H^I$ is the pseudo-inverse, i. e. $H^I = H^+$ [1]. In that case, the product $H^+H$ will approximate, in a least squares sense, the identity matrix [1]. However, Eq. (4.18) is general in the sense that to approximate the inverse $H^I$ it is possible to relax the identity matrix requirement on F. It is clear that if a(n) is a 'sinc' sequence (see Eq. (4.3)) whose cutoff frequency $w_c$ is greater then the cutoff frequency of H, the estimate f(n) will well approximate f(n) with arbitrary resolution. As $w_c$ approaches $\pi$, the a(n) will approach a unit-sample sequence, and F becomes an identity matrix. For example, if the H approximates an ILPF, i. e. the columns of H are shifted version of a 'sinc' sequence with cutoff frequency $w_c$, while the F matrix is an approximation to another ILPF with the cutoff frequency $w_c' > w_c$, the resulting inverse operator $H^I$ is expected to recover the high frequency components of an object signal f approximately up to the frequency $w_c'$. Eq. (4.18) is in the same form as Eq. (4.5), appropriate for the application of the CAM method for the determination of the approximate solution for $H^I$.

**b. Linear shift-variant system**

For a LSV system, the linear degradation is the sampled superposition sum given in Eq. (4.1). Here, the matri-

degradation operator H is a truncated 2D array $\{h(n,m)\}$, where $n,m = 1, 2, \ldots, N$. The object sequence estimate is

$$\hat{f}(n) = \sum_{k=1}^{N} y(n,k)g(k) \tag{4.19}$$

where the 2D array $\{y(n,k)\}$, where $n,k = 1, 2, \ldots, N$, reprents the inverse LSV filter coefficients. Substituting the truncated g(n) from Eq. (4.1) into Eq. (4.19) and interchanging the order of summation yields

$$\hat{f}(n) = \sum_{m=1}^{N} f(m) \sum_{k=1}^{N} y(n,k)h(k,m), \tag{4.20}$$

Letting

$$a(n,m) = \sum_{k=1}^{N} y(n,k)h(k,m), \tag{4.21}$$

it is clear that if $a(n,m) = \delta(n-m)$, $n,m = 1, 2, \ldots, N$, $\hat{f}(n)$ will perfectly approximate the original sequence f(n).

Next, we form the matrices F, $H^I$, and H as

$$F = \{a(n,m)\}, \quad n,m = 1, 2, \ldots, N \tag{4.22}$$

$$H^I = \{y(n,m)\}, \quad n,m = 1, 2, \ldots, N \tag{4.23}$$

$$H = \{h(k,m)\}, \quad k,m = 1, 2, \ldots, N \tag{4.24}$$

Eq. (4.21) now in matrix form is

$$F = H^I H. \tag{4.25}$$

Again, if $a(n,m) = \delta(n-m)$ then F is an identity matrix and $H^I$ is an ideal inverse-degradation matrix. Since Eq. (25) is of the same form as Eq. (4.18), to determine the LSV system inverse-degradation matrix $H^I$, the same procedure as for an LSI system applies.

c. <u>Two-dimensional separable linear system</u>

In the 2-D case, a separable LSI degradation operator is considered. Hence, the degraded image matrix G, object image matrix F, and the separable LSI degradation operator matrix H, are related as [50]

$$G = HFH^T. \tag{4.26}$$

If the $H^I$ is an inverse-degradation operator, multiplying both sides of Eq. (4.26) from the left and right by $H^I$ and $(H^I)^T$, respectively, we have

$$H^I G(H^I)^T = (H^I H)F(H^I H)^T. \tag{4.27}$$

The right-hand side of Eq. (4.27) represents the object image F estimate.

The form of matrix equations (4.18) and (4.25) are now appropriate for the application of the CAM method to determine $H^I$. In the next section, some specific examples of LSI and LSV degradation operators are considered.

## 4.3. EXPERIMENTAL RESULTS

In this section, firstly computer simulation results for the problem of deconvolving (reconstructing) of 1D (2D) signals (images) from noisy outputs of an LSI low-pass degradation operator, are considered. Secondly, computer simulation results for the problem of eliminating LSV blur, caused by a gaussian pulse of space-dependent width (standard deviation), are presented.

Using a truncated ILPF (see Eq. (4.2) through (4.4)) with the cutoff frequency of $w_c = \pi/16$, an LSI low-pass degradation operator H is obtained. The columns of the H matrix form the vectors $\{h_r\}$ that correspond to the vectors $\{g_r\}$ in Eq. (3.13). The $\{f_r\}$ column vectors are formed in two different ways resulting in two experiments. The first experiment is with $\{f_r\}$ formed exactly as the columns of the above degradation operator matrix H, but with a much higher cutoff frequency $w_c = \pi/4$. For this example, the CAM algorithm is expected to produce an inverse-degradation matrix operator $M_1$ (see Eq. (3.13)), that will recover a degraded sequence lost radian frequency components of up to $\pi/4$. In Fig. 4.1a), an object sequence with five impulses and the result of degradation by the LSI degradation operator H with $w_c = \pi/16$, is presented. Fig. 4.1b) presents the same degradation operator H output with an additive noise with a signal-to-noise ratio (SNR) of 8.72 db (decibels). This noisy

signal is multiplied by the inverse-degradation matrix $M_1$ to produce the object signal estimate shown in Fig. 4.1c). It is obvious that all five spikes are resolved, with the missing frequency components recovered approximately up to $\pi/4$. In the second example while using the same LSI matrix degradation operator H, F is an identity matrix (see Eq. (4.5)). Using the CAM method a new inverse-degradation matrix $M_2$ is obtained. $M_2$ is expected to completely recover the missing high frequency components. In Fig. 4.1d), the result of multiplication of this $M_2$ by the noisy signal (vector) of Fig. 4.1b) is presented. It is clear that in spite of the presence of large noise all the impulses are recovered. In Figs. 4.2a) to d), the result of restoration of four degraded impulses using the previously calculated two inverse degradation operators $M_1$ and $M_2$ are shown. This example indicates that both $M_1$ and $M_2$ are general inverse-degradation filters.

In Figs. 4.3 and 4.4, the results of restoration of a 2D impulsive image are presented. The object F matrix (see Eq. (4.26)) is formed as an 128*128 array with three impulses, at the space sample coordinates (80,64), (64,64), (64,48). In Fig. 4.3a), the 128*128 image G, degraded using the H degradation operator (separable and symmetric) as in 1D examples with the cutoff frequency $w_c = \pi/16$, is presented. The inverse-degradation M matrix is formed using the usual procedure of the CAM method as with 1D examples. Fig. 4.3b) presents the result of

restoration of noise-free G of Fig. 4.3a). Fig. 4.4a) presents the degraded image G of Fig. 4.3a) with the additive noise with the SNR of -2.58db. Fig. 4.4b) presents the result of restoration of noisy G of Fig. 4.4a) with the same inverse-degradation matrix M. It is clear that in spite of a large noise the result of restoration is very good.

In many applications the linear degradation operator H is not shift invariant one, i. e. the full, two-dimensional array in Eq. (4.1) must be known. Of course, the two-dimensional array in Eq. (4.1) must be truncated to obtain a tractable LSV operator approximation. As a test for the newly proposed signal reconstruction method, we use here the model of LSV degradation operator appropriate for gamma-ray spectra blurring [59]

$$h(n,m) = \exp[-((n-m)/\delta(m))^2] \tag{4.28}$$

with

$$\delta(m) = 4. + (m-25)/30. \tag{4.29}$$

The LSV degradation operator H is formed using Eq. (4.28) and (4.29). With this H and an identity matrix as the F matrix in Eq. (4.25), using the CAM method of Chapter 3., with P = 2.5, the inverse-degradation matrix M has been obtained. This matrix M is used next for 1D signal deblurring.

In Fig. 5.5a) a sequence with uniformly spaced seven impulses (positioned at 32, 42, 52, ...,92), as well as noise-free result of its blurring by LSV degradation operator H, are presented. In Fig. 5.5b) the blurred output signal of Fig 5.5a) with additive noise, such that the SNR is of 19.49db, is presented. In Fig. 5.5c) the result of restoration (multiplication of the signal in Fig. 5.5b) by the M matrix) is presented. It can be observed that the impulse are not exactly of the same hight, and some artifact positive and negative spikes appeare in the entire region of support. However, considering the high level of noise, the result of reconstruction is quite satisfactory.

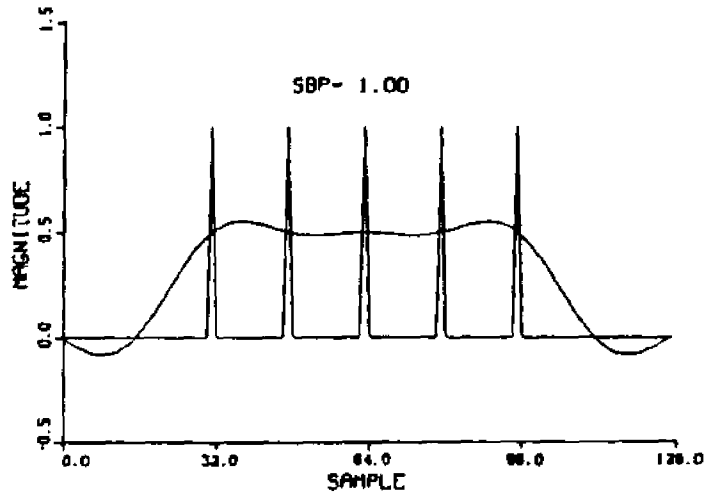


a)

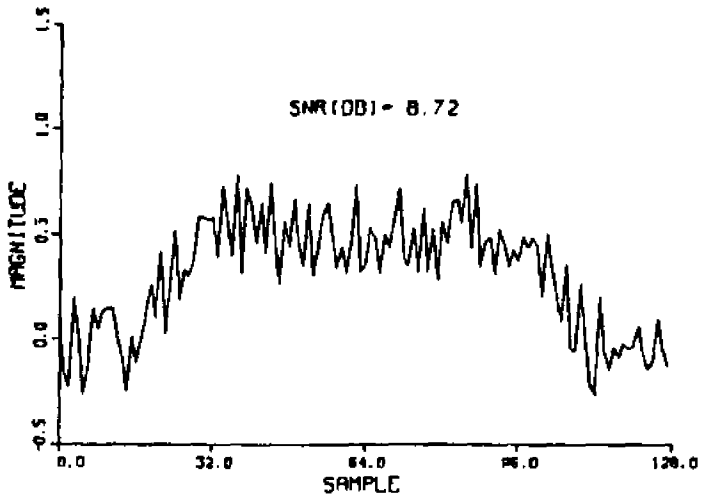


b)

Fig. 4.1a) An input sequence containing five impulses and the filtered output (H cutoff frequency $\omega_c = \pi/16$). b) Filtered output with additive noise (SNR = 8.72db). c) Resolution of the five impulses using an $M_1$ matrix obtained by Eq. (4.6) where F and H (see Eq. (4.19)) are low-pass filters with cutoff frequencies $\omega_c = \pi/4$ and $\omega_c = \pi/16$, respectively. d) Resolution of the five impulses using an $M_2$ matrix obtained as in c) but with the f matrix as an identity matrix.

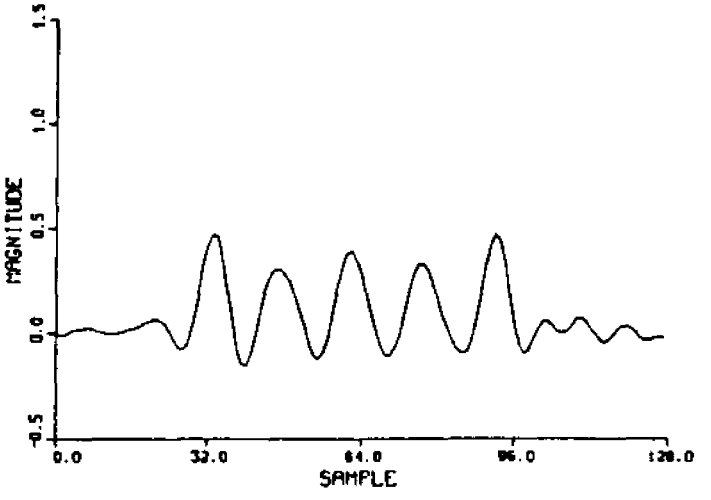


c)

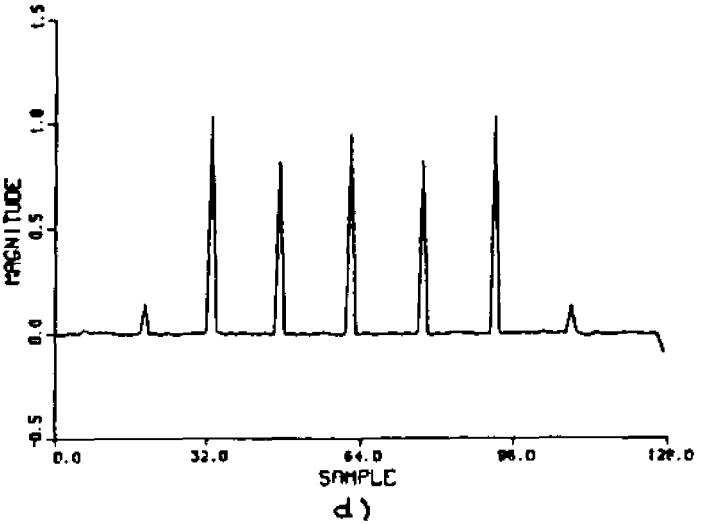


d)

Fig. 4.1 Continued.

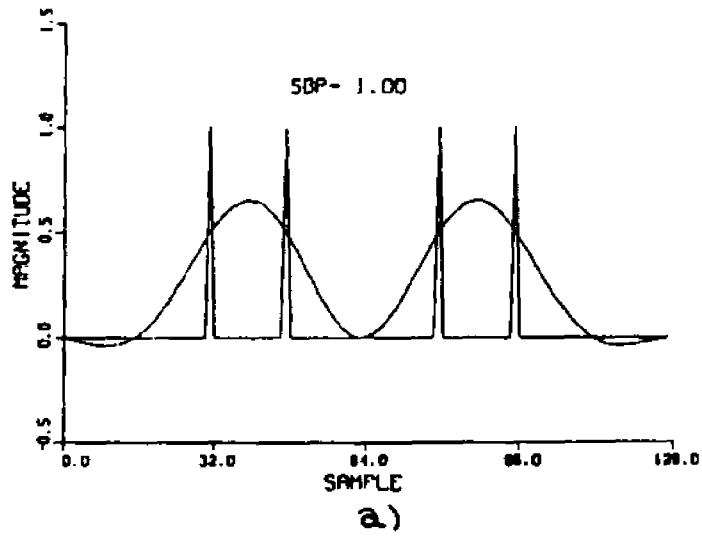


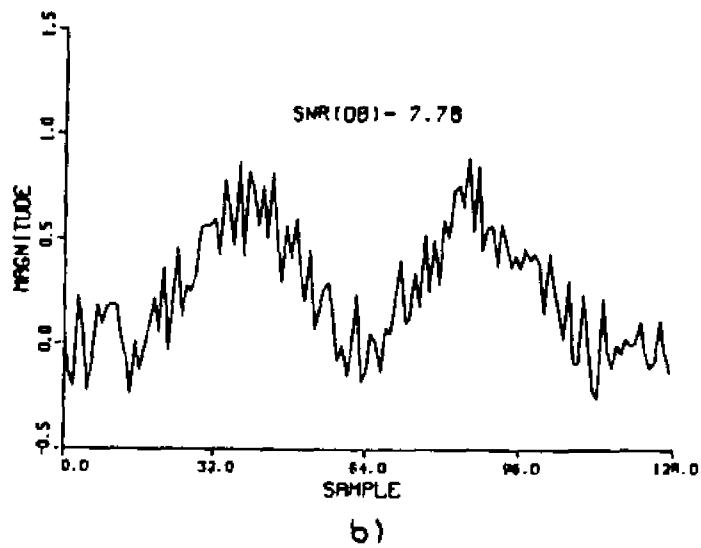


Fig. 4.2a)-d) The same experiment as in Fig. 4.1a)-d) using an input sequence with four impulses (the midle impulse of the input sequence in Fig. 4.1a) has been omitted).

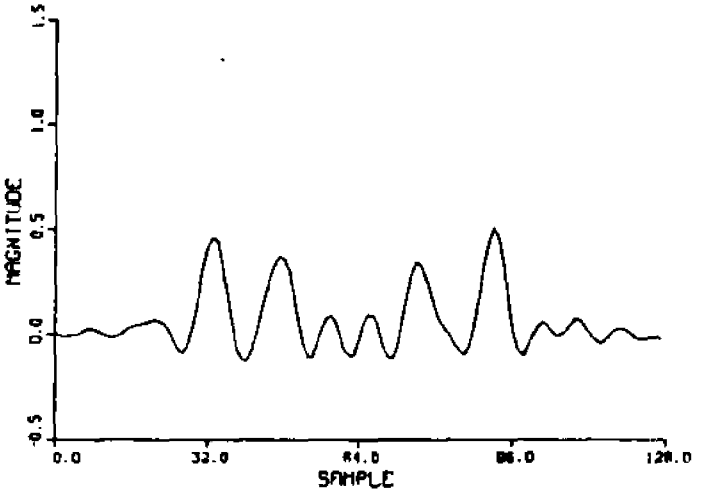


c)

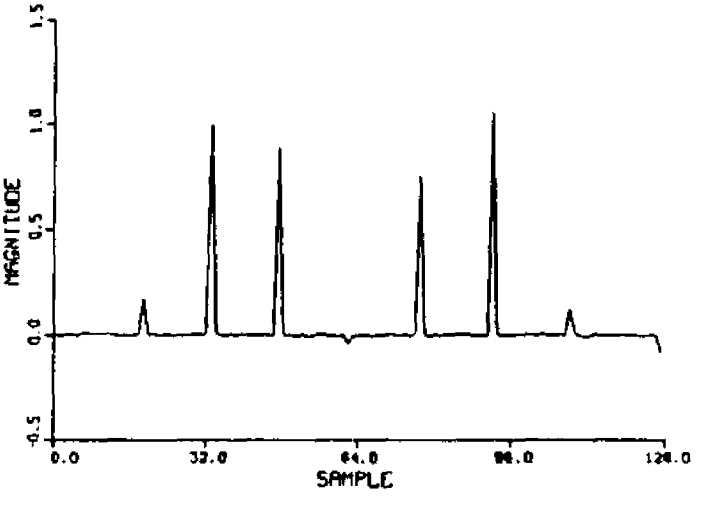


d)

Fig. 4.2 Continued.

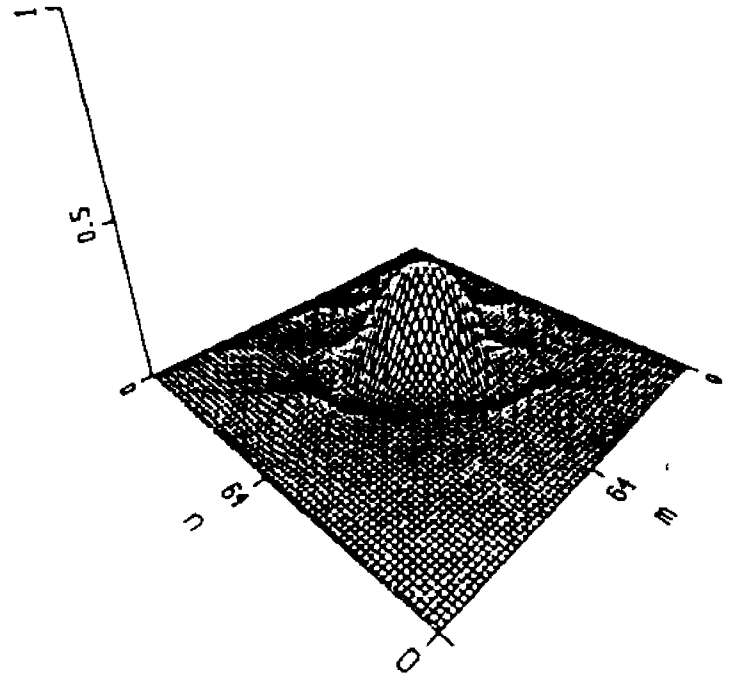


a)

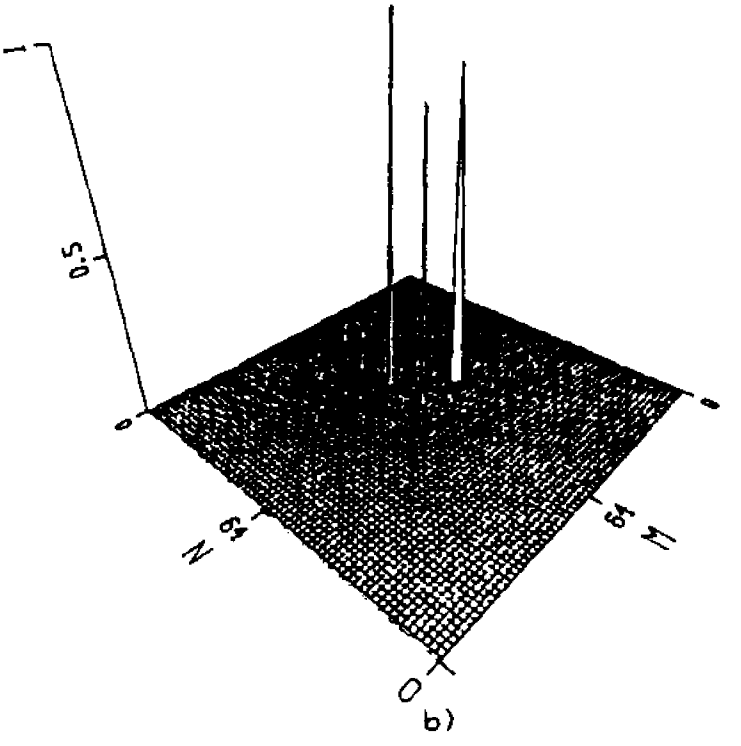


b)

Fig. 4.3a) Noise-free filtered 2-D image obtained by low-pass filtering of the image F with three impulses at the coordinates (80,64), (64,64), (64, 48) (the low-pass filter cutoff frequency is $w_c = \pi/16$). b) The restored image F.

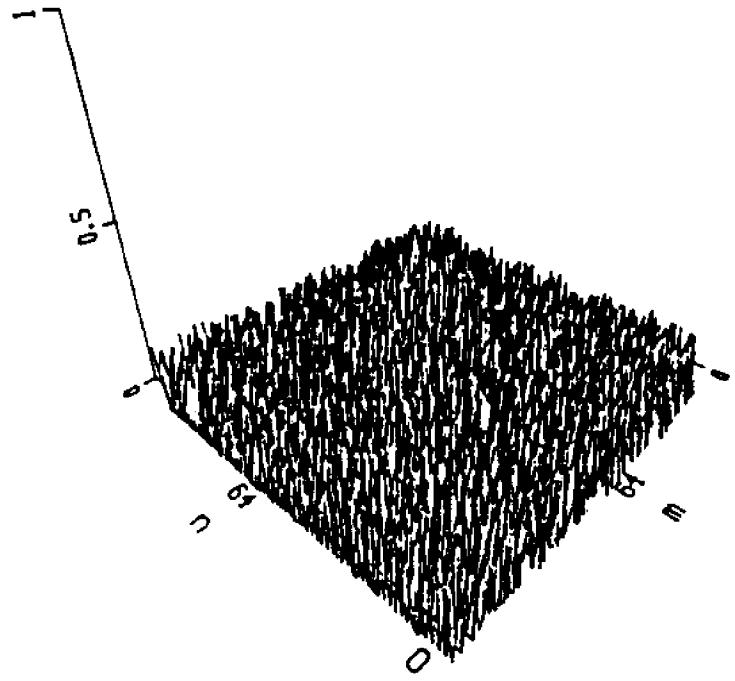


a)

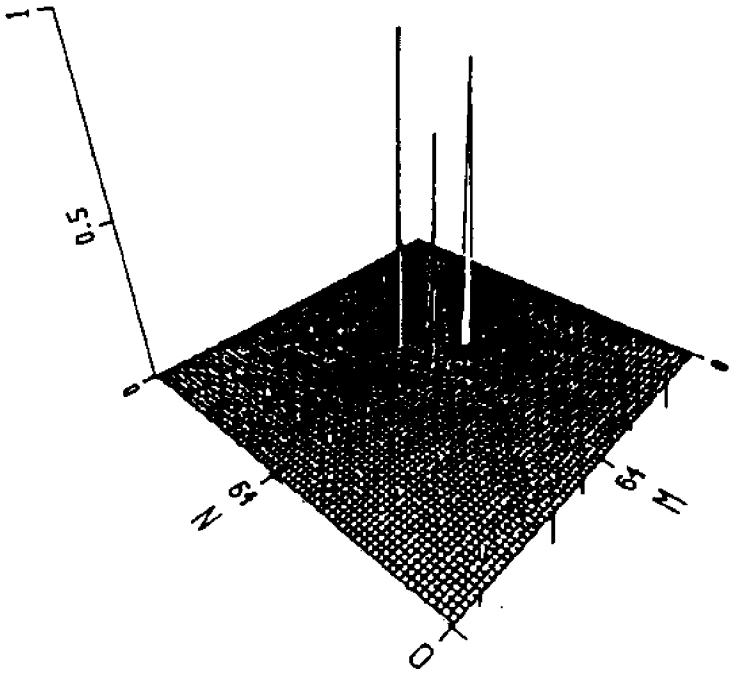


b)

Fig. 4.4a) Filtered image G of Fig. 4.3 a) with additive noise (SNR = -2.58db). b) The restored image F.

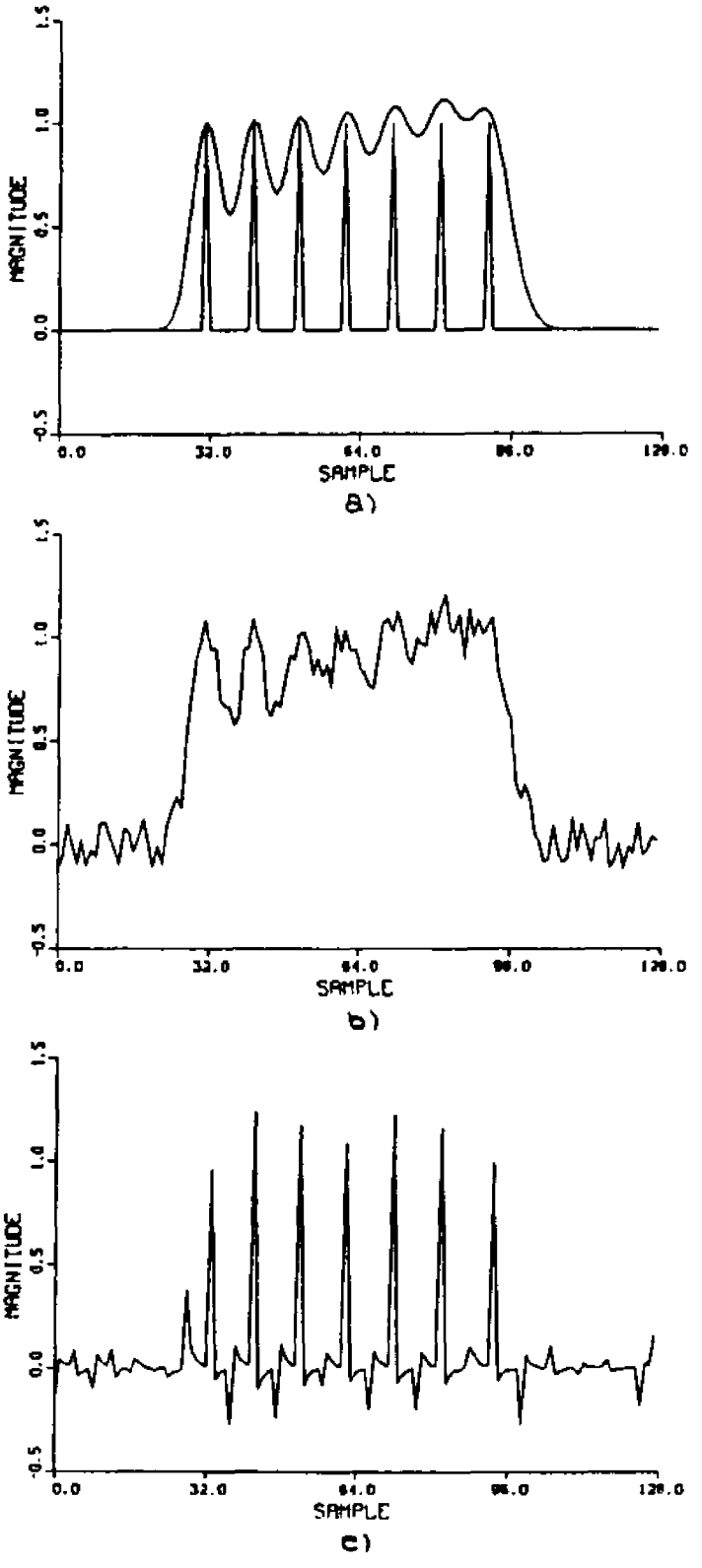


Fig. 4.5a) R sequence containing uniformly spaced seven impulses with separation of 10 samples and noise-free result of blurring by LSV H (see Eq. (4.31) and (4.32)). b) Blured output sequence in a) with additive noise (SNR = 19.49db). c) The restored sequence.

## 4.4. SUMMARY AND CONCLUSIONS

In the previous Chapter (see also Ref. (14)) it was shown that a degradation system input-output set of signals can be utilized as a "training" set of vectors to create an inverse system degradation operator in a form of a CAM matrix. By limiting the set of reconstructible signals to the class of signals belonging to the "training" set, an exceptionally robust superresolving inverse filter was obtained. In this Chapter, based on the CAM method, the problem of determination of pure inverse of a discrete linear degradation system is addressed. Using an appropriate training set of signals related idealy by a perfect system degradation inverse, the design of a general, one step, impulsive type inverse filter, in a form of a simple two dimensional array of coefficients, has been performed. Three different linear discrete-time (space) degradation system models have been considered: an LSI 1D system, modeled by the convolution process; an LSI separable 2D model, appropriate for restoration of 2D images; and an LSV 1D model. For both LSI and LSV discrete degradation systems an inverse degradation system matrix has ben computed using the CAM method. The performances and superresolving properties of these inverse degradation matrices have been tested on several 1D and 2D numerical examples. Since, using the approach adopted here, the linearly degraded signal recovery requires only a single matrix-vector multiplication, this method is suitable for an optical or electronics real-time hardware implementation.

# 5. LINEARLY DEGRADED SIGNAL RECONSTRUCTION USING A CONSTRAINED WEIGHTED LEAST-SQUARES ESTIMATE

## 5.1. INTRODUCTION

In many optical applications, the finite aperture of an optical system and measurement error, or noise, lead to a signal degradation. A non-ideal optical system, generally exhibiting low-pass filter characteristics, is usually modeled by a linear shift-invariant (LSI) frequency band-limiting operator. To recover an original signal from its filtered image a system degradation operator inversion is required. However, because of ill-conditioning of this operator, the smallest measurement error or noise in the system output may cause large fluctuations in the input signal estimate. Hence, the recovery of a linearly degraded signal is a nontrivial signal processing task.

It is well known that for a finite support, continuous space-dependent function $f(x)$, its Fourier spectrum is an entire function, and therefore, it can be analytically continued (using a Taylor series expansion) beyond its cutoff frequency. In practice, however, because of the noise-sensitive evaluation of derivatives, this method is not very useful. An alternative method, that is based on a series expansion of a Prolate Spheroidal Wave [60, 61] set of basis functions, is also noise-

sensitive. To cope with this problem, several other linear deconvolution methods have been developed. Thus, when the measurement noise is negligible and for a moderate degradation, a direct spatial frequency domain degradation inversion is possible [15, 30]. However, recently developed iterative procedures allow the control of spurious fluctuations by interacting with the evolving solution. The improved performance, and a degree of noise immunity of these new techniques have revived the interest in this problem. Both Rushforth [54] and Gerschberg [19] considered the restoration of optical image details degraded by the diffraction effects of a finite aperture optical system. Papoulis [48] described the extrapolation and spectral estimation problem from a Fourier analysis point of view while Youla [72] described it as alternating orthogonal projections onto a convex set. Stark et al. [62] employed Youla's theoretical results to generate image restoration procedures based on two orthogonal projections. While the above iterative methods yield an exact noiseless estimate, when noisy sampled data are used, the inversion of the degradation process is highly unstable. On the other hand, for the algorithms that employ a discrete Fourier transform (DFT), implicit windowing of the data and limited number of samples degrade the frequency resolution.

To cope with both the noise and the ill-conditioned nature of the degradation operator, constrained iterative restoration methods were proposed. Frequently applied constraints are object

signal smoothness, positivity, and finite spatial extent. For example, Howard [27] developed a method of continuing the Fourier spectra by minimizing the sum of the square of the negative values of the estimate. In Ref. [73], a least-squares reconstruction of spatially limited noiseless object signals, using both smoothness and non-negativity constraints, was presented. Stark et al. [64], in the absence of measurement error or noise, described a nonlinear alternating projections onto closed convex set method (see Ref. [72]), that also uses a non-negativity constraint. Schafer et al. [59] showed that a frequency-limiting distortion can be modeled by a general functional equation that is applicable to many signal reconstruction problems. Sanz & Huang [58] presented a unified Hilbert space approach to a number of iterative least-squares signal restoration algorithms, using a general functional equation and different regularizing operators that substantially improve, in the absence of noise, the performance of some of the classical algorithms.

In addition to object signal constraints, discrete constrained iterative methods also employ regularization techniques that impose constraints on either the singular values (SVs) of the system degradation operator or the object signal eigenfunctions. For example, Rushforth & Frost [52] considered an eigenvalue-smoothing procedure that retrieves only those estimated signal eigenfunctions that are significant for signal

restoration, i. e., it eliminates those higher-order eigenfunctions that are substantially contaminated by noise. In addition to that, at each iteration step, the range of the bandlimiting operator was extended by a frequency increment. Although it improves the Gerchberg algorithm [19], the proper choice of the iteration step frequency increment remains an open question. In Rushforth et al. [53], in a similar approach, a regularizing parameter that operates on the SVs and singular vectors was introduced. While this, basically noniterative method, provided some noise immunity, it showed inadequate restoration in the presence of strong noise. In Barakat & Newsam [5], in the presence of moderate noise, the problem of extrapolation of bandlimited signals was treated using a filtered SV decomposition. In Mammone & Rothacker [41], while imposing some additional constraints on the object estimate, the Youla's general method of alternating orthogonal projections onto convex set was viewed as a discrete system degradation matrix eigenvalue and eigenvector filtering. In Ref. [39], a linear programming method to recover a diffraction limited image or to restore the Fourier spectra was presented. This method, particularly suitable for sparse images, used the simplex constrained optimization algorithm. In Ref. [14], by limiting the set of reconstructable signals and using a constrained associative memory, a robust one-step inverse filter was obtained.

In this Chapter, a new iterative method of discrete-space signal restoration in the presence of appreciable noise, is proposed. The weighted least-squares (WLS) and best linear unbiased estimate (BLUE) algorithms [44] are considered from a point of view of designing a suitable symmetric weighting matrix W that performs an implicit SV filtering of a system degradation operator without disturbing the system consistency. A new linear system degradation matrix SV filtering scheme, that compensates for ill-conditioning of the system degradation, is incorporated into this new WLS algorithm weighting matrix. Two different signal restoration cases, in the presence of appreciable noise, are considered. First, when both the object signal vector and the noise or measurement error are unknown, the problem is nonstatistical and a minimum norm least-squares estimate is sought. The restoration is performed using the WLS algorithm. Second, in a statistical case, with an assumed noise statistics, the BLUE algorithm that minimizes the noise variance is employed. Here, the new weighting matrix is used in combination with the noise covariance matrix to form a weighted BLUE (WBLUE) algorithm. To enable imposition of a priori known object signal constraints, a recursive computation of the WLS estimate and WBLUE is employed. Since the WBLUE algorithm reduces in form to the WLS algorithm the identical recursive computation of the estimate can be utilized for both of them. This recursive WLS algorithm serves as a kernel of the new constrained iterative method. Also, to eliminate the system inconsistency due to

measurement error or noise, a preprocessing of the system degradation model is introduced.

The Chapter is organized as follows. In section 5.2, the problem of linearly degraded signal restoration is formulated and the form of the discrete system degradation matrix is indicated. Using a SV decomposition, the ill-conditioned nature of this matrix is pointed out. In section 5.3, the relationship between the system degradation matrix SV filtering and the WLS and WBLUE algorithms is established. Based on a desired system degradation matrix SV filtering, the new weighting matrix W is derived. Both the WLS and WBLUE algorithms are presented in the same format, so that the same recursive object estimate computation could be performed. In section 5.4, after presenting details of the recursive algorithm, a new constrained iterative method is presented. In section 5.5, the application of this algorithm for the reconstruction of linearly degraded binary signals in the presence of strong noise is considered. Using noisy degraded object signals and a non-negativity constraint, an object signal estimate is evaluated. The imposition of some other constraints is also discussed. Superresolving restoration with different level of additive noise is demonstrated. In section 5.6, the summary and conclusions are presented.

## 5.2. A LINEAR DISCRETE-SPACE SYSTEM DEGRADATION MODEL

A linear discrete-space system degradation model used here is established by the Eq. (4.1) through (4.4) of chapter 4. An alternative approximative representation of the degradation matrix H can be obtained by evaluating in the frequency domain the inverse discrete Fourier transform (IDFT) of the discrete periodic representation of the ILPF. This IDFT yields a periodic ILPF impulse response sequence which may be used to form a circulant matrix H. It can be shown [53] that the elements of the circulant H are

$$h_{n,m} = (1/N)(\sin(\pi(m-n)(2M+1)/N)/\sin(\pi(m-n)/N)) \qquad (5.1)$$

where N is the number of IR sequence samples, and M is the discrete ILPF cutoff-frequency. If N is sufficiently large, either the truncated or the circulant H matrix can be expected to be a good approximation to $H_{inf}$.

The H matrix SVD defined by Eq. (1.18) through (1.20) can also be formulated as (see Eq. (1.21))

$$H = ULV^T \qquad (5.2)$$

where U and V are unitary matrices with the orthogonal eigenvectors $u_k$ and $v_k$ as their columns, respectively, and L is a diagonal matrix with the H matrix SVs as its elements, i. e.,

$$L = \mathrm{diag}[\theta_1, \theta_2, \ldots, \theta_N] . \qquad (5.3)$$

The SVs are bounded on the open interval $(0,1)$ with a sharp transition between those close to unity and those close to zero. This SV behavior corresponds to the ILPF transfer function bandwidth $W_c = (2M + 1)2\pi/N$ where M defines its discrete cutoff-frequency. The number of SVs close to unity is approximately equal to $2M + 1$. To see this effect, consider a circulant H. The $H^TH$ circulant matrix [25], using a DFT matrix F and its inverse $F^{-1}$, can be diagonalized as

$$D = FH^THF^{-1} \qquad (5.4)$$

where the diagonal matrix D is

$$D = \mathrm{diag}(p_0, \ldots, p_M, q_0, \ldots, q_{N-2M}, p_{M+1}, \ldots, p_{2M}) \qquad (5.5)$$

with $2M + 1$ approximately unity, $p_0, \ldots, p_{2M}$, elements corresponding to the filter pass-band, and $N-(2M+1)$ close to zero, $q_0, \ldots, q_{N-2M}$ elements, corresponding to its stop-band. This behavior of the SVs is not limited to an ILPF. Any low-pass, either circulant or non-circulant, matrix degradation operator

with the transfer function that closely approximates an ILPF transfer function, will show a similar SV behavior.

A system degradation matrix H condition number [20] c(H) is defined as

$$c(H) = \frac{\delta_1(H)}{\delta_N(H)} \qquad (5.6)$$

where $\delta_1$ and $\delta_N$ are the largest and smallest SVs of H, respectively. In general, c(H) is a measure of distance of the H matrix from the space of the singular matrices. A large condition number indicates the degree of ill-conditioning of H. By using an appropriate SV filtering, the condition number can be decreased. This preconditioning step is also desirable for the numerical stabilization of the determination of the $H^{-1}$. In the next section, when designing a weighting matrix, we show how an appropriate SV filter can be incorporated into the WLS and WBLUE signal recovery algorithms.

## 5.3. SYSTEM DEGRADATION MATRIX SINGULAR VALUE FILTERING VIA LEAST-SQUARES ALGORITHM WEIGHTING MATRIX

In the previous section, a model for an ideal noiseless low-pass degradaton system has been established. However, in the presence of additive noise, Eq. (4.4) is

$$\mathbf{g} = \mathbf{H}\mathbf{f} + \mathbf{n} \tag{5.7}$$

where n is an unknown error or noise vector. If both the object f and noise n vectors are unknown, the problem is deterministic, and it can be solved using a WLS method. This method yields the minimum norm estimate of f, among those which minimize the error

$$\|\mathbf{g} - \mathbf{H}\mathbf{f}\|^2. \tag{5.8}$$

The WLS estimate is [44]

$$\mathbf{f}_{wls} = (\mathbf{H}^T\mathbf{W}^2\mathbf{H})^+\mathbf{H}^T\mathbf{W}^2\mathbf{g} \tag{5.9}$$

where $W^2$ is a symmetric positive definite weighting matrix and + stands for the pseudoinverse. In general, there is no specific rule how to form the matrix $W^2$. In the following, it will be shown that a $W^2$ matrix can be formed so as a desired SV filtering is performed that improves the condition number of H. This improvement leads to a numerical stabilization of the inversion process and also to an improved convergence rate of a recursive WLS estimation algorithm.

The SVs of the ill-conditioned H can be separated into p and q sets (see Eq. (5.5)); the former are "close" to unity while the latter are "close" to zero. By an appropriate manipulation of the two sets of the SVs, for example, by decreasing the magnitude of the average difference between the two SV sets, the condition number c(H) can be improved. Furthermore, by decreasing, for example, the stop-band attenuation of the H (increasing the magnitute of the lower-index SVs), and using this modified H in a recursive procedure to estimate the object signal, enhances the high-frequency components of the estimated signal, leading to an improved convergence rate. An appropriate SV filter is a step function that modifies the SVs as

$$\tilde{\sigma}_k = \begin{cases} \alpha\sigma_k, & \text{when } \sigma_k \text{ in the p set} \\ \beta\sigma_k, & \text{when } \sigma_k \text{ in the q set} \end{cases} \quad \text{for } k = 0, 1, \ldots, N-1 \quad (5.10)$$

where $\alpha < \beta$, and $\alpha$ and $\beta$ are heuristically chosen constants. The $\alpha$ parameter decreases the "unity" SVs while the $\beta$ parameter increases the "zero" SVs of H. The effect of this SV filter is to decrease the effective c(H) improving both the stability and convergence rate of a recursive reconstruction algorithm that will be presented in the next section.

In general, to find an appropriate W matrix, first a diagonal matrix X

$$X = \mathrm{diag}[x_0, x_1, \ldots, x_{N-1}] \tag{5.11}$$

is formed such that the new diagonal L' matrix

$$L' = XL \tag{5.12}$$

represents the desired filtered SVs. For a symmetric weighting matrix W, using Eq. (5.2), Eq. (5.9) can be written as

$$f_{wls} = [(WULV^T)^T(WULV^T)]^+(WULV^T)^T W\mathbf{g}. \tag{5.13}$$

If the choice for the weighting matrix W is such that

$$WULV^T = UXLV^T \tag{5.14}$$

than

$$f_{wls} = [(UXLV^T)^T(UXLV^T)]^+(UXLV^T)^T W\mathbf{g}. \tag{5.15}$$

It is clear that the W must satisfy

$$WU = UX \tag{5.16}$$

or

$$W = UXU^T. \tag{5.17}$$

The expression of Eq. (5.17) determines the symmetric weighting matrix W. The WLS estimate can now be written as

$$f_{wls} = (H_f^T H_f)^+ H_f^T W g \tag{5.18}$$

where the filtered system degradation matrix is

$$H_f = UXLV^T \tag{5.19}$$

Here, the X matrix diagonal elements $x_0, x_1, \ldots, x_{2M+1}$ (see Eq. (5.10)), are formed using the $\alpha$ parameter, while the $\beta$ parameter forms the remaining N-(2M+1) elements. Using the identity $(H_f^T H_f)^+ H^T = H_f^+$ and introducing

$$g_f = Wg, \tag{5.20}$$

Eq. (5.18) becomes

$$f_{wls} = H_f^+ g_f. \tag{5.21}$$

In the following section, for the determination of $f_{wls}$, Eq. (5.21) will serve as a model for a recursive constrained algorithm.

In the least-squares estimation theory no statistical assumptions are necessary either about the noise (measurement

error) n or the object vector f. However, when the noise statistics is known, a better choice of estimator is the BLUE algorithm. It is well known [44] that the BLUE is a minimum error variance estimate. When n is a known noise process, based on the given observation (measurement) vector g, the BLUE for the vector f is [44, 1]

$$f_{bl} = (H^T R^{-2} H)^+ H^T R^{-2} g \qquad (5.22)$$

where $R^2$ is a symmetric, positive definite noise covariance matrix and $R^{-2}$ denotes its inverse. It is assumed that the noise n is real and an inverse noise covariance matrix $R^{-2}$ exists. When $W^2 = R^{-2}$, the BLUE corresponds to a WLS estimate. For white noise, $R^2$ is a diagonal matrix

$$R^2 = \mathrm{diag}[r_1, r_2, \ldots, r_N] \qquad (5.23)$$

with elements that are noise variances. For white, zero mean, and identical variance noise,

$$R^2 = rI \qquad (5.24)$$

where I is an identity matrix, the BLUE coincides with an identity weighting matrix WLS estimate.

Since the BLUE algorithm (see Eq. (5.22)) and the WLS (see Eq.(5.9)) are in the same format, a new symmetric weighting matrix $\tilde{W}$ that accounts for both the H matrix SV filtering and a heavier weighting of the more accurate signal measurements (through the covariance matrix $R^2$) can be introduced. Assuming a white noise, the new weighting matrix W is

$$\tilde{W}^2 = WR^{-2}W. \tag{5.25}$$

With this new $\tilde{W}$, using Eq. (5.9), we have

$$f_{wls} = [H^TWR^{-2}WH]^+H^TWR^{-2}W\mathbf{g}, \tag{5.26}$$

or

$$f_{wls} = [(WH)^TR^{-2}WH]^+(WH)^TR^{-2}W\mathbf{g}, \tag{5.27}$$

and finally

$$f_{wls} = [H_f{}^TR^{-2}H_f]^+H_f{}^TR^{-2}\mathbf{g}_f. \tag{5.28}$$

Eq. (5.28) can be recognized as the BLUE of a modified degradation system with the degradation matrix $H_f$ and output $\mathbf{g}_f$. Thus, the WBLUE with filtered degradation matrix $H_f$ is

$$f_{wbl} = [(R^{-1}H_f)^TR^{-1}H_f]^+(R^{-1}H_f)^TR^{-1}\mathbf{g}_f \tag{5.29}$$

or

$$f_{wbl} = [H_{fb}{}^TH_{fb}]^+H_{fb}{}^T\mathbf{g}_{fb} = H_{fb}{}^+\mathbf{g}_{fb} \tag{5.30}$$

where $H_{fb} = R^{-1}WH$ and $\mathbf{g}_{fb} = R^{-1}W\mathbf{g}$. Eq. (5.30) is in the same form as Eq. (5.21), thus for the evaluation of $f_{wbl}$ and $f_{wls}$, an

identical constrained iterative algorithm, presented in the next section, can be applied.

## 5.4. A CONSTRAINED ITERATIVE LEAST-SQUARES METHOD

If the pseudo-inverse $H_f^+$ ($H_{fb}^+$) is available, Eq. (5.21) and (5.30) provide a direct solution of the restoration problem. However, on the one hand, to exploit a priori knowledge about the object signal, which leads to the imposition of constraints on the evolving estimate, a recursive algorithm is desirable. On the other hand, most pseudo-inversion algorithms employ only elements of the matrix being inverted and disregard the measured signal $\mathbf{g}$ as an element of the estimate. Therefore, for the determination of a matrix pseudoinverse, our choice is a recursive least-squares algorithm based on a theorem of Greville [21, 22]. The intention here is not to compute the pseudo-inverse $H_f^+$, but to evaluate the estimate $f_{wls}$ exploiting the recursive matrix pseudo-inverse computation. In this section the recursive computation of a least-squares estimate will be briefly presented while the details of the derivation are left for the Appendix. The proposed constrained iterative method is based on this recursive least squares algorithm.

Let $H_N$ denote an N row system degradation matrix H, with the row vectors $h_1^T$, $h_2^T$, ..., $h_N^T$. The measured sampled vector is $g_N = (g_1, g_2, \ldots, g_N)^T$ where now the subscript N denotes the number of scalar elements of $\mathbf{g}$. Assume that the $(k-1)^{th}$ observation element $g_{k-1}$ (an element of $g_N$) is

$$g_{k-1} = h_{k-1}^T f + n_{k-1} \tag{5.31}$$

where $n_{k-1}$ is a corresponding noise vector n scalar element. The least-squares solution for $f$, based on $k-1$ observations (measurements) $g_{k-1} = (g_1, g_2, \ldots, g_{k-1})^T$, is

$$f^{(k-1)} = H_{k-1}^{+} g_{k-1}. \tag{5.32}$$

If the new $k^{th}$ observed sample is

$$g_k = h_k^T f + n_k, \tag{5.33}$$

then the least-squares estimate for $f$ is

$$f^{(k)} = H_k^{+} g_k. \tag{5.34}$$

From Eq. (5.32) and (5.34), and using Greville's theorem (see Appendix), a relationship between $f^{(k-1)}$ and $f^{(k)}$ is

$$f^{(k)} = \begin{cases} f^{(k-1)} + \dfrac{d_k}{h_k^T d_k} (g_k - h_k^T f^{(k-1)}) & \text{if } \|d_k\|^2 \neq 0 \\ f^{(k-1)} & \text{otherwise} \end{cases} \tag{5.35}$$

where the $d_k$ is the unnormalized component of $h_k$ orthogonal to the subspace spanned by $(h_1, h_2, \ldots, h_{k-1})$ and $\|d_k\|$ is the quadratic vector norm of $d_k$. The recursion starts with either $f^{(0)} = 0$ or $f^{(0)} = g$.

In deriving the recursive least-squares algorithm of Eq. (5.35), it has been assumed that an exact solution to Eq. (4.4) exists (see the Appendix). However, in practice, due to an imperfect degradation model and the noisy measured signal, an exact solution for f may not be feasible. For this case, a simple transformation of the measured, noisy signal $\mathbf{g}$, and system degradation matrix H, generalizes the algorithm. Let the new vector $\tilde{\mathbf{g}}$ and matrix $\tilde{H}$ be defined as

$$\tilde{\mathbf{g}} = H^T\mathbf{g}, \tag{5.36}$$

$$\tilde{H} = H^TH. \tag{5.37}$$

To estimate $\tilde{H}^+\tilde{\mathbf{g}}$ the algorithm of Eq. (5.35) is used. Since (see Ref. [1])

$$\tilde{H}^+\tilde{\mathbf{g}} = (H^TH)^+H^T\mathbf{g} \tag{5.38}$$

and

$$(H^TH)^+H^T = H^+, \tag{5.39}$$

it follows that

$$\mathbf{f} = \tilde{H}^+\tilde{\mathbf{g}} = H^+\mathbf{g}. \tag{5.40}$$

Using the modified $\tilde{H}$ and $\tilde{\mathbf{g}}$ and the Eq. (5.35) an estimate of f is evaluated following iterative method described below.

The unconstrained recursive least squares algorithm of Eq. (5.35), can be considered as the kernel of a constrained iterative algorithm. A number of different object signal

constraints can be introduced. For example, an object signal lower amplitude bound (non-negativity) constraint P (see Eq. (2.31)), or/and the finite spatial extent operator S (see Eq. (2.39)) can be utilized. If f satisfies both the non-negativity and finite spatial extent constraints, than

$$f = PSf. \tag{5.41}$$

To evaluate f, the following constrained iterative algorithm is formed:

1. Form $\tilde{H} = H^T H$ and $\tilde{g} = H^T g$.
2. Determine W or $\tilde{W}$ (Eq. (5.17) or Eq. (5.25)).
3. Form either $H_f, g_f$ pair (Eq. (5.19) and (5.20)) or $H_{fb}, g_{fb}$ pair (Eq. (5.30)).
4. Compute $d_k$ and $h_k^T d_k$ for $k = 1, \ldots, N$ (Eq. (A.10)). Set $f^0 = \tilde{g}$.
5. For k = 1 to N do

$$f^{(k)} = \begin{cases} PSf^{(k-1)} + \dfrac{d_k}{h_k^T d_k} (g_k - h_k^T PSf^{(k-1)}) & \text{if } \|d_k\|^2 \neq 0 \\ PSf^{(k-1)} & \text{otherwise} \end{cases}$$

If $\|f^{(k)} - f^{(k-1)}\| >$ Error, Return to S.

otherwise Exit.

If the magnitude of the difference between two successive estimates is less then a predetermined error, the stopping rule

$$|f^{(k)} - f^{(k-1)}| < \text{Error} \qquad (5.42)$$

terminates the iteration. However, in practice, it is difficult to set in advance the termination error while still maintaining the accuracy of the reconstruction. Another alternative is to preset the maximum number of the iterations to be performed.

## 5.5. EXPERIMENTAL RESULTS

Using simulated test signals, representing different levels of system degradation and in the presence of different level of additive noise, the proposed iterative algorithm was tested using Fortran code on an IBM-3081 computer. The SV decomposition was performed using an IMSL Fortran library routine that is based on a Lawson & Hanson [27] algorithm. For the calculations, single precision arithmethic was used. Both f and g were 128 element vectors, while the degradation operator H was an 128*128 square matrix. Several simulations, exploiting only the non-negativity constraint were performed. For the purpose of a comparison, several examples that exploit simultaneously both the non-negativity and the finite spatial extent constraints were considered.

A number of different combinations of SV filtering parameters ($\alpha$, $\beta$) (see Eq. (5.10)) were tested. The $\alpha$ parameter exercised a much greater influence on the reconstruction quality and the algorithm convergence rate. For all our examples, the SV filtering parameters ($\alpha$, $\beta$) = (0.5, 100) were used. These parameters decrease the condition number by a factor of 200. As a SV filtering example, in Fig. 5.1., the original SVs (circles) of the H matrix with cutoff frequency of $w_c = \pi/8$ and the filtered SVs (squares), are shown. This plot illustrates a typical SV behavior of an ill-conditioned system degradation operator and

the effect of a step-function SV filter. It can be noticed that while the lower-to-higher-index-order SV ratio decreased the general shape of the SV curve is preserved.

In the following examples, various signal reconstruction results are presented. Fig. 5.2 presents the results of the superresolution of two impulses. Fig. 5.2a) shows the 128 samples of (f,g) pair. The f contains two impulses separated by 6 sample units, while the g is a response of an ILPF with cutoff frequency of $w_c = \pi/8$. Fig. 5.2b) presents a noisy g with a signal-to-noise-ratio (SNR) of 4db while in Fig. 5.2c) the result of superresolving reconstruction of f, after 1000 iterations, is presented. It can be observed, that even in the presence of high-level of noise, the restored impulses are well separated. In Fig. 5.3a), a signal containing four impulses located at 46, 54, 66 and 78 sample positions, and the response of an ILPF with cutoff frequency of $w_c = \pi/8$, are presented. Fig. 5.3b), shows output signal g as in Fig. 5.3a) with the additive noise (SNR = 5.31db). Fig. 5.3c) presents the superresolution of four impulses from noisy g after 500 iterations while the Fig. 5.3d) shows the same result obtained after 1000 iterations. As it can be observed, even in the presence of high level of noise, the impulses are correctly restored.

In Fig. 5.4a), an input f containing eight impulses arbitrarily located at 20, 28, 46, 56, 66, 80, 96 and 106 sample

positions and an ILPF ($w_c = 10(\pi/64)$) response, are presented. In Fig. 5.4b) noisy ILPF output of the signal of Fig. 5.4a) with SNR of 9.79db is shown. Fig. 5.4c) presents the restoration result after 500 iteration while Fig. 5.4d) presents the same result after 1000 iterations. Again, all the input impulses are correctly reconstructed. Fig. 5.5a) shows the signal of Fig. 5.4a) heavier degraded, now with an ILPF with cutoff frequency of $w_c = 9(\pi/64)$. Noisy degraded signal of Fig. 5.5a), with SNR of 8.56db, is shown in Fig. 5.5b). The result of restoration after 1000 iterations is presented in Fig. 5.5c). It can be observed that good restoration results, even with heavy degradation and large noise, can be achieved. Next, in Fig. 5.6, using both the non-negativity and finite spatial extent constraints, the four impulse signal of Fig. 5.3a) is reconstructed. As one would expect, an additional improvement over the result of Fig. 5.3c), where only a non-negativity constraint was applied, is achieved.

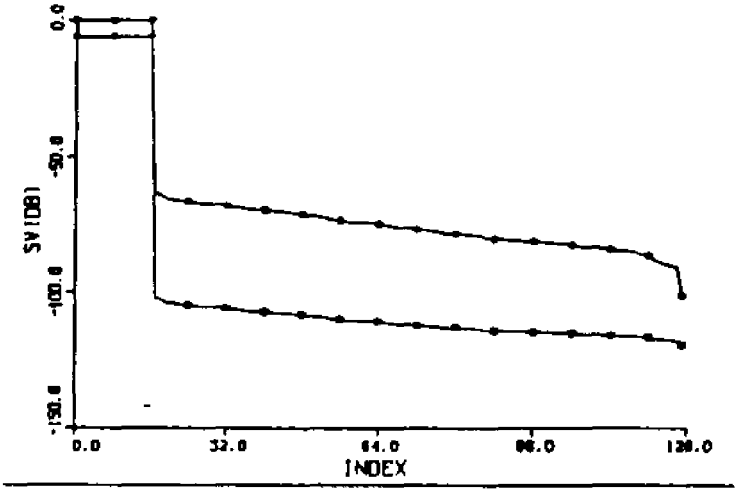


Fig. 5.1 Logarithmic plot of the SVs of the H matrix ($\omega_s = \pi/8$) before and after SV filtering ($\alpha = 0.5$, $\beta = 100$).

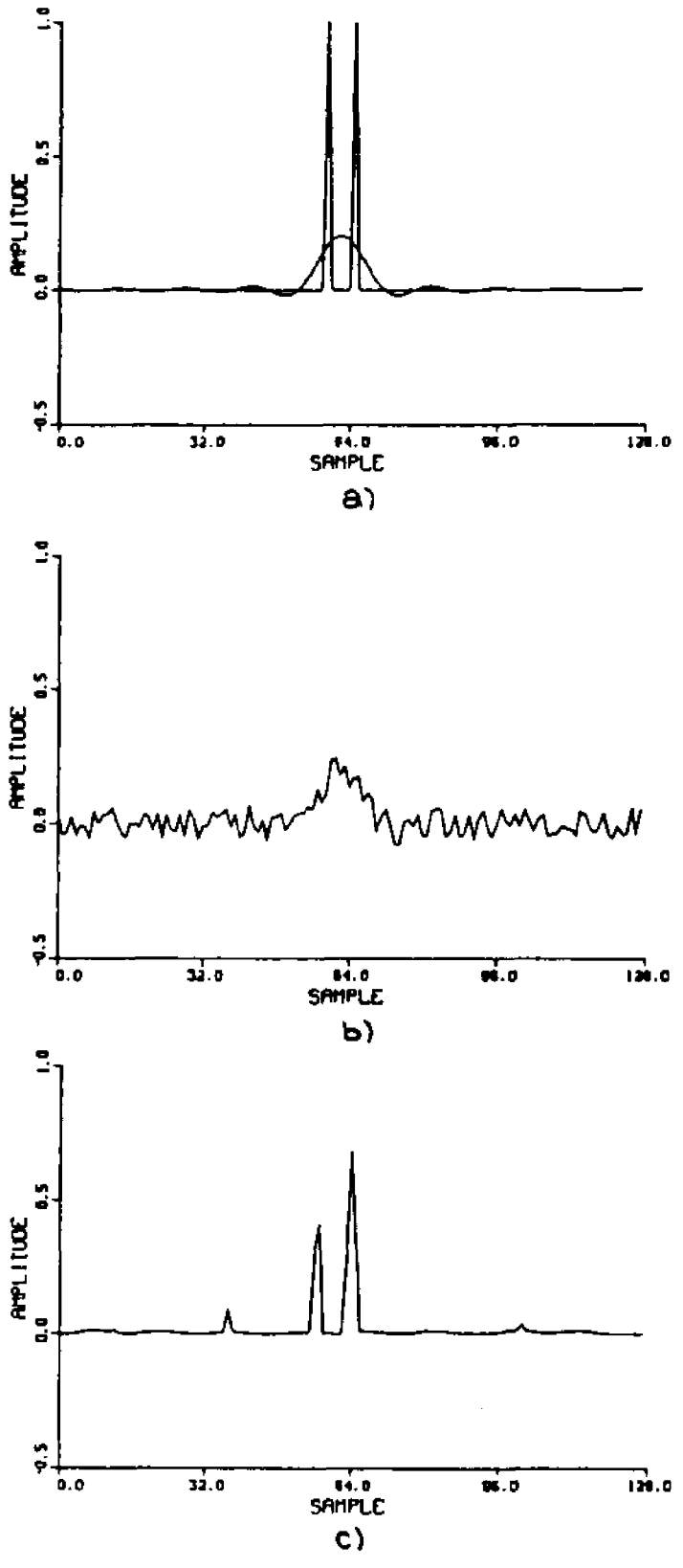


Fig. 5.2a) Input/Output signals of an ILPF with cutoff $\omega_c = \pi/8$. b) Noisy ILPF output (SNR = 4dB). c) The restored signal after 1000 iterations.

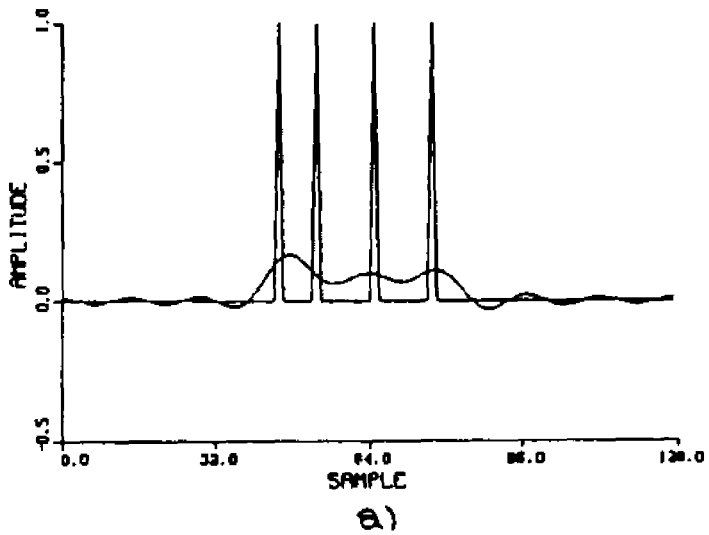


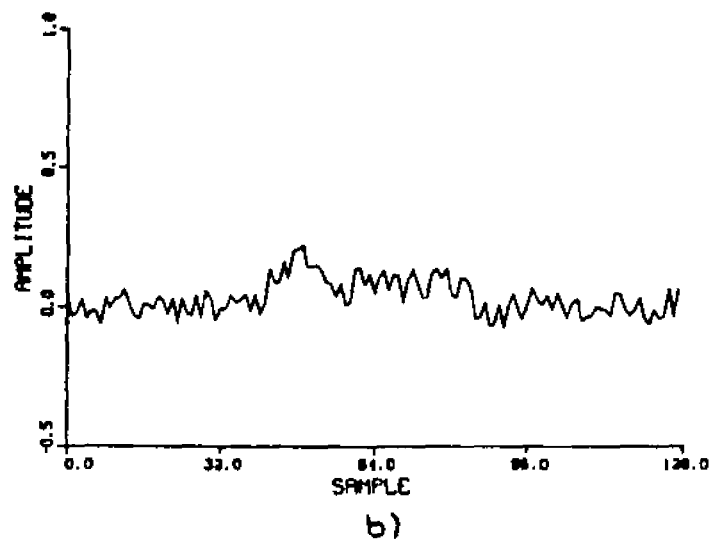


Fig. 5.3a) Input/Output signals of an ILPf with cutoff $\omega_c = \pi/8$. b) Noisy ILPf output (SNR = 5.31db). c) The result of restoration after 500 iterations. d) The result of restoration after 1000 iterations.

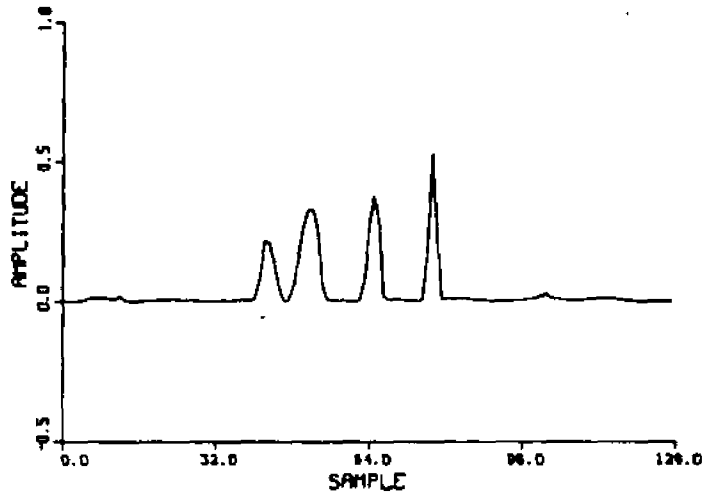


c)

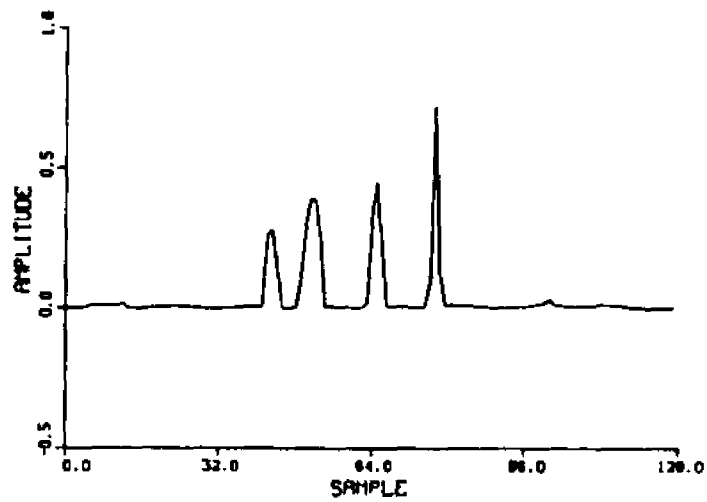


d)

Fig. 5.3Continued.

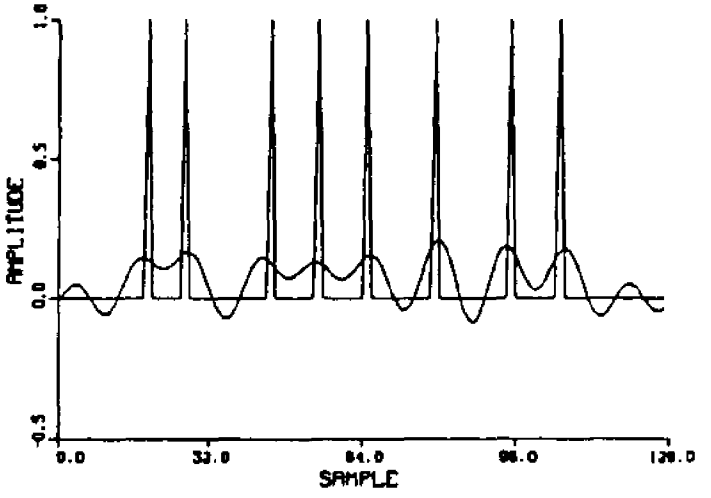


a)

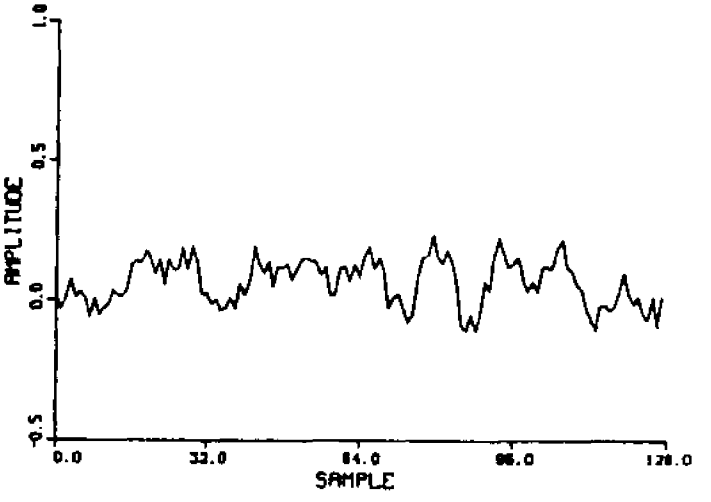


b)

Fig. 5.4a) Input/Output signals of an ILPF with cutoff $\omega_c = 10(\pi/64)$. b) Noisy ILPF output (SNR = 9.79db). c) The result of restoration after 500 iterations. d) The result of restoration after 1000 iterations.

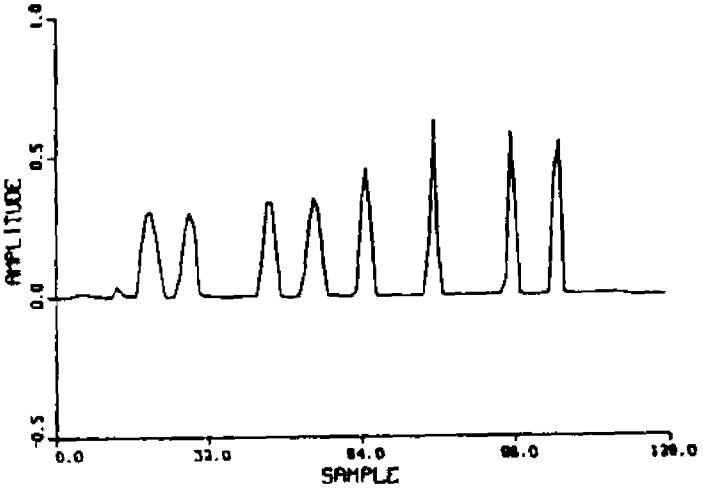


c)

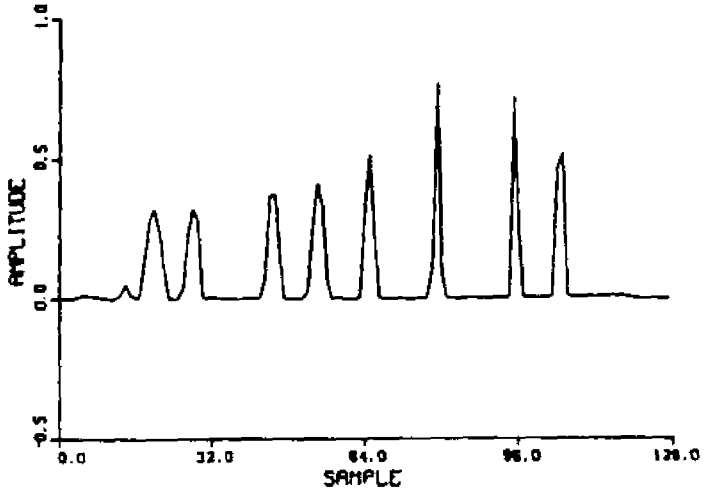


d)

Fig. 5.4 Continued.

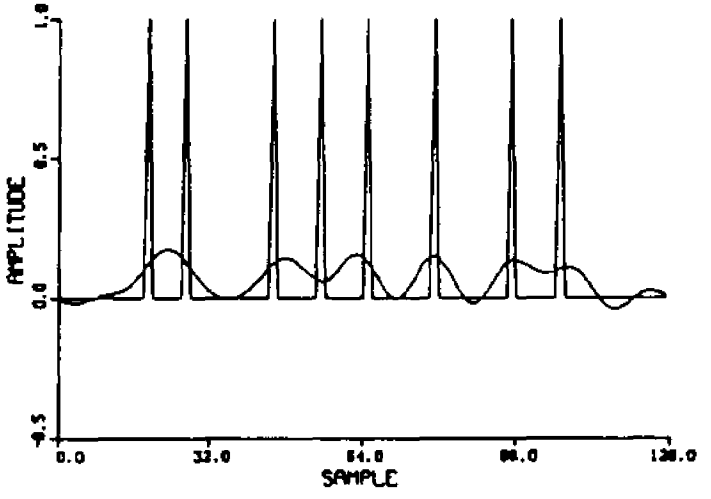


a)

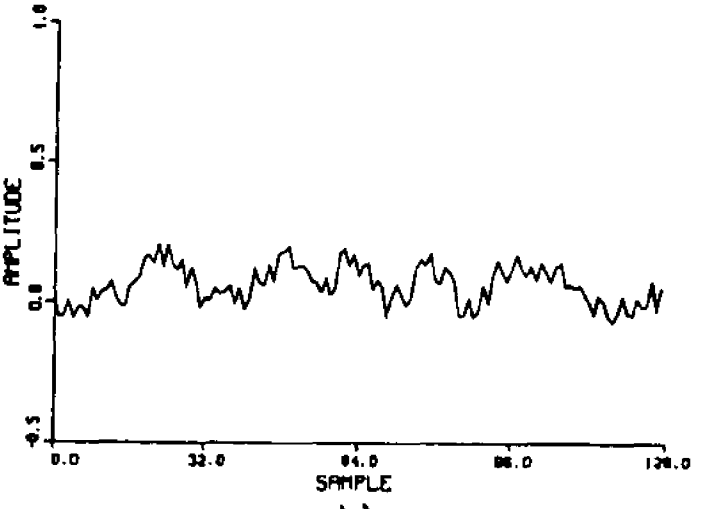


b)

Fig. 5.5a) Input/Output signals of an ILPf with cutoff $\omega_c = 9(\pi/64)$. b) Noisy ILPf output (SNR = 8.56db). c) The result of restoration after 500 iterations. d) The result of restoration after 1000 iterations.

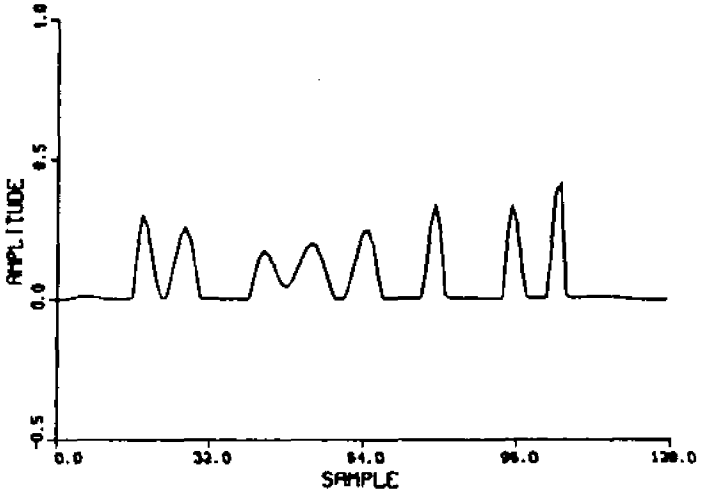


c)

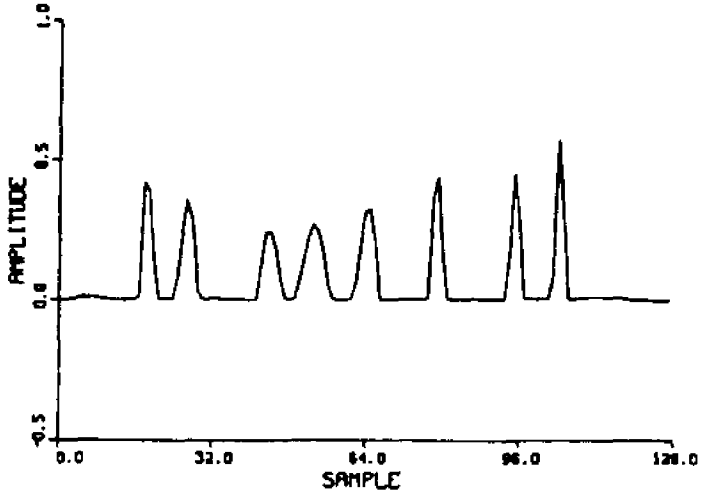


d)

Fig. 5.5 Continued.

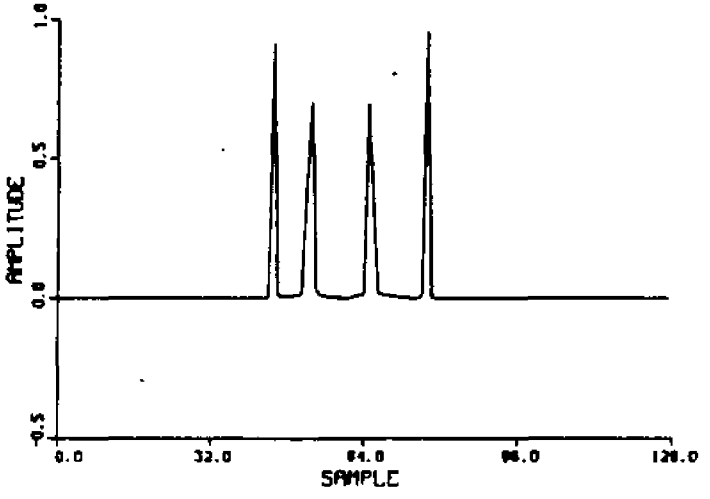


Fig. 5.6 The result of restoration of noisy signal in Fig. 3b) using an additional constraint of finite spatial extent (500 iterations).

## 5.6. SUMMARY AND CONCLUSION

The nonlinear discrete iterative signal restoration methods frequently use regularization techniques that impose constraints on the system degradation operator SVs. By introducing a SV taper, these methods provide a compromise between the noise and the spatial high-frequency content of the estimate. The method proposed in this thesis uses a step-type SV filtering function that deemphasizes the lower-index-order SVs while simultaneously emphasizing the higher-index-order SVs, thus providing their better ratio. This considerably decreases the condition number of the degradation matrix. The SV filtering function is incorporated into a weighting matrix of the WLS and WBLUE algorithms. Hence, the weighting matrix implicitly compensates for the ill-conditioned nature of the system degradation operator, without materially disturbing the consistency of the system degradation model, thus providing a stable estimate.

Both algorithms, the WLS and WBLUE, are in the same format suitable for a recursive object estimate computation. The recursive algorithm, serving as a kernel of the constrained iterative algorithm, allows for the imposition of additional constraints on the estimate. Both the non-negativity and the finite-spatial extent constraints have been incorporated into the algorithm. While the proposed method was tested using an LSI degradation operator, however, the degradation that is linear

space-variant can also be recovered. To demonstrate both superresolving and reconstructing properties of the proposed method, several numerical examples were presented.

# APPENDIX

Applying Greville's theorem [21, 22], the $H_k^+$ can be determined as

$$H_k^+ = [(I - c_k h_k^T) H_{k-1}^+ | c_k] \qquad (A.1)$$

where I is an N*N identity matrix, and column vector

$$c_k = \begin{cases} \dfrac{d_k}{s_k}, & \text{if } s_k \neq 0 \qquad (A.2a) \\ \dfrac{d_k'}{s_k'}, & \text{otherwise} \qquad (A.2b) \end{cases}$$

where

$$d_k = (I - H_{k-1}^+ H_{k-1}) h_k, \qquad (A.3)$$

$$s_k = h_k^T (I - H_{k-1}^+ H_{k-1}) h_k \qquad (A.4)$$

and

$$d_k' = H_{k-1}^+ (H_{k-1}^+)^T h_k, \qquad (A.5)$$

$$s_k' = 1 + h_k^T H_{k-1}^+ (H_{k-1}^+)^T h_k. \qquad (A.6)$$

Thus, using Eq. (A.1), Eq. (5.31) becomes

$$f^{(k)} = f^{(k-1)} + c_k (g_k - h_k^T f^{(k-1)}) \qquad (A.7)$$

If an exact (not necessarily unique) solution to $g = Hf$ exists, the expression for $c_k$ can be simplified. In that case, there are two options: either $h_k^T$ is linearly independent, or it is dependent upon the previous row vectors of $H_k$. In the former case, $d_k$ is a non-zero vector, and Eq. (A.2a) applies. Otherwise, when $h_k^T$ is a linear combination of the previous rows, Eq. (A.2b)

applies. In that case, multiplying both sides of Eq. (A.7) by $h_k^T$ yields

$$g_k = h_k^T f^{(k-1)} + \frac{\|h_k^T H_{k-1}^+\|^2}{1 + \|h_k^T H_{k-1}^+\|^2} (g_k - h_k^T f^{(k-1)}) \quad (A.8)$$

where $\|.\|$ denotes the quadratic vector norm. Since $\|h_k^T H_{k-1}^+\|^2 > 0$, Eq. (A.8) is only satisfied for $(g_k - h_k^T f^{(k-1)}) = 0$. Substituting this result into Eq. (A.7) yields $f^{(k)} = f^{(k-1)}$. Thus, the recursive algorithm to compute a least-squares estimate is

$$f^{(k)} = \begin{cases} f^{(k-1)} + \dfrac{d_k}{h_k^T d_k} (g_k - h_k^T f^{(k-1)}) & \text{if } \|d_k\|^2 \neq 0 \\ f^{(k-1)} & \text{otherwise} \end{cases} \quad (A.9)$$

To determine the $d_k$'s, the Gram-Schmidt orthogonalization procedure (GSO), or equivalently, the modified GSO (MGSO) can be used [20]. Using GSO, the result is

$$d_1 = h_1$$

and

$$d_k = h_k - \sum_{i \in S_k} \frac{(h_k, d_i)}{\|d_i\|^2} d_i \quad (A.10)$$

where $S_k = \{i \mid i < k-1, \text{ and } \|d_i\| \neq 0\}$, and $(.,.)$ denotes a vector inner product.

# 6. LOW SPACE-BANDWIDTH PRODUCT SIGNAL EXTRAPOLATION USING A NEW ROBUST ITERATIVE RANDOM GRAIN ALLOCATION SCHEME

## 6.1. INTRODUCTION

Several authors considered the extrapolation of a low space-bandwidth product (SBP) signal in the space domain, or the estimation of the Fourier spectra in the frequency domain in a frame of a deterministic iterative or one-step extrapolating procedure. Both Rushforth [54] and Gerschberg [19] considered the restoration of optical image details degraded by the diffraction effects of a finite aperture optical system. Papoulis [48] described the extrapolation and spectral estimation problem from a Fourier analysis point of view. Youla [72] described it as an orthogonal projection onto a convex set. This point of view has proved to be a very fruitful area of research [Stark [62]]. While the above iterative methods yield an exact estimate, the inversion of the degradation process using noisy sampled data is highly unstable. Furthermore, because a finite set of samples does not uniquely specify a sequence outside of its observation interval [59], in general, discrete signal extrapolation is very sensitive to noise.

Sabri and Steenaart [57] proposed a one-step matrix formulation of the extrapolation problem. A similar approach has been taken by Cadzow [9]. Although a one-step method [57,9] is appealing, it is also sensitive to noise. On the other hand, algorithms that employ a finite discrete Fourier transform (DFT) are limited in their frequency resolution both because of the limited number of samples and by implicit windowing of the data. In Ref. [11], using a deterministic estimation theory, a minimum energy solution was presented. On the other hand, in Ref. [29], using a minimum least squares norm criterion, some of the existing bandlimited signal extrapolation algorithms were unified. This criterion also corresponds to a minimum energy solution. Schafer [59] has shown that a space-limiting distortion can be modeled by a general functional equation, an equation that is also applicable to many other signal reconstruction problems. In Ref. [39, 40] a method to recover a difraction limited image or restore the Fourier spectra using linear programming is presented. In Ref. [14] by limiting the set of reconstructable signal to a linear degradation system input-output training set of signals, a robust inverse filter was obtained using a linear associative memory.

In this Chapter, for the low SPB signal extrapolation in the presence of noise, using an approach similar to a Monte-Carlo method [31, 6], a new iterative algorithm is proposed. The Monte-Carlo method has been used as a tool in solving comple-

optimization problems. For example, Metropolis [45] applied it for the calculation of the properties of substances composed of interacting individual molecules. Frieden [16, 15] used it to restore linearly-degraded binary images. Kirkpatrick [33] adapted it as a building block for a new optimization scheme, termed as Simulated Annealing, for finding the location of the extrema for a function of a large number of independent variables. In Ref. [10], to recognize various binary noisy image patterns, the method of Simulated Annealing was applied. In a similar approach, Frieden [18] considered the restoration of binary images degraded by a point-spread operator using some a priori information. Here, the new algorithm constructs an unknown sequence from a variable size elementary grain D. The desired estimate is based on the number of samples acquired on a given measurement interval and the prior knowledge of the signal frequency bandlimit. While scanning through the unknown sequence sample locations, D is used to update a sample value. The grain is initially comparatively large but is miniscule as compared to the amplitude of the reconstructed signal. As the estimate approaches its final form the value of D decreases. The procedure consists of iteratively adding a given grain D, with randomly-chosen sign, to the previous value of each signal sample position. If an error criterion is satisfied, the newly assigned grain, i. e., the corresponding updated signal sample, is accepted, otherwise it is rejected (i. e., its previous value is restored). Here, the error criterion, equivalent to the change in system energy used in the method of Simulated Annealing, is the first vector norm ($l_1$-norm)

of a cumulative error. This is the difference of the measured space truncated vector and the current bandlimited estimate of the entire object vector. While in Simulated Annealing an increase in system energy is occasionally allowed, with our method, with each newly accepted grain, the error function must be monotonically nonincreasing. A preprocessing step, that compensates for both the inconsistency of the linear degradation model and for the presence of noise, of both the degradation operator and the measured sequence, is also introduced. The addition of other constraints, such as the upper bound of a signal, is also considered.

In section 6.2., a general space-truncation-degradation model of a bandlimited sequence is introduced. In section 6.3., the details of the new iterative algorithm are presented. In section 6.4., computer simulation examples for the extrapolation of both sinusoidal as well as other bandlimited signals are presented. Extrapolation results using different length observation segments, and in the presence of different levels of additive noise, are presented. In section 6.5., the summary and conclusions are given.

## 6.2. PROBLEM FORMULATION

A discrete bandlimited signal $f(n)$, $n = 0, \pm 1, \pm 2, \ldots$, sampled at a higher rate than the Nyquist rate, is bandlimited to the radian frequency $w_c < \pi/T$ (where $T$ is the sampling period) if its Fourier transform $F(w)$ satisfies the relation

$$F(w) = 0 \text{ for } |w| > w_c \tag{6.1}$$

and

$$F(w) = \sum_{n=-\infty}^{\infty} f(n)\exp(-jwn), \quad |w| < w_c \tag{6.2}$$

where $|.|$ denotes the absolute value and $j = \sqrt{-1}$. In this chapter, the extrapolation of a sequence $g(n)$ that is identical to $f(n)$ in the observation interval of length $2L + 1$, and zero elsewhere, is considered. This problem is equivalent to the restoration of the Fourier spectra of $f(n)$ from the Fourier spectra of the spatially-truncated sequence $g(n)$.

The linear spatial truncation operator $S$

$$S[f(n)] = g(n) = \begin{cases} f(n), & |n| < L \\ 0, & \text{otherwise} \end{cases} \tag{6.3}$$

extracts from the sequence f(n) the observation segment and extrapolates the remaining sequence by zeros. Let the discrete bandlimiting operator B be

$$B[f(n)] = \sum_{k=-\infty}^{\infty} f(k) \frac{\sin[w_c(n-k)]}{\pi(n-k)} \tag{6.4}$$

where $w_c$ is its radian cutoff frequency. The infinite bandlimiting matrix $B_{inf}$ corresponding to the bandlimiting operator B is

$$B_{inf} = (b_{nk}), \quad n,k = 0, \pm 1, \ldots \tag{6.5}$$

where the matrix elements are

$$b_{nk} = \frac{\sin[w_c(n-k)]}{\pi(n-k)} \tag{6.6}$$

The space truncation operator S can also be expressed as an infinite matrix

$$S_{inf} = (s_{nk}), \quad n,k = 0, \pm 1, \ldots \tag{6.7}$$

where the matrix elements are

$$s_{nk} = \begin{cases} 1, & n=k \text{ and } |n| < L \\ 0, & \text{otherwise} \end{cases} \tag{6.8}$$

For an infinite vector $f_{inf}$, with the elements corresponding to the bandlimited sequence f(n), the $B_{inf}$ operator is an identity operator, i. e.,

$$f_{inf} = B_{inf} f_{inf} \tag{6.9}$$

The samples of the observed sequence g(n), as in Eq. (6.3), form an infinite vector $g_{inf}$, such that

$$g_{inf} = S_{inf} f_{inf}. \tag{6.10}$$

Next, using the identity of Eq. (6.9), Eq. (6.10) becomes

$$g_{inf} = S_{inf} B_{inf} f_{inf}. \tag{6.11}$$

Introducing the $H_{inf}$ operator as

$$H_{inf} = S_{inf} B_{inf}, \tag{6.12}$$

yields, as the discrete model for this problem,

$$g_{inf} = H_{inf} f_{inf}. \tag{6.13}$$

In order to obtain a tractable finite model, in practice, the infinite vectors $g_{inf}$, $f_{inf}$ and matrix $H_{inf}$ are truncated [29] to a finite matrix system

$$g = Hf \qquad (6.14)$$

where g and f are M- and N-element observation and object vectors, respectively, and H is an M*N element truncated version of the $H_{inf}$ matrix. We can now formally state the finite segment bandlimited signal extrapolation problem as the determination of f from the knowledge of g and H. Eq. (6.14) implies that, using one of the available methods for determining the inverse of H, a solution for f may be generated. However, the rank of the H matrix, corresponding to the number of samples of the observed segment, is deficient. Furthermore, a singular value decomposition (SVD) [20] of H clearly shows its ill-conditioned nature, i. e. its singular values (SV) fall abruptly off from approximately unity to nearly zero as a function of the SBP. The SVs of H follow the trend of the eigenvalues of the Digital Prolate Spheroidal Sequences [60]. Therefore, H is either a singular or nearly-singular matrix. This nature of H introduces numerical instability in constructing its pseudoinverse using, for instance, some of the direct methods described in Ref. [1]. On the other hand, while using an SVD and a truncated set of SVs [67] the pseudoinverse numerical problem can be stabilized, due to imprecise model of H, it also increases the inconsistency of Eq. (6.14) causing a loss of its fidelity. This is so because by discarding the higher order SVs of H most of the signal's high-frequency content is eliminated. In addition, the computationally quite expensive SVD signal extrapolation is basically an one-step

method, that does not allow for an easy application of additional constraints or prior knowledge about the signal.

## 6.3. A RANDOM GRAIN ALLOCATION ITERATIVE EXTRAPOLATION ALGORITHM

The new iterative algorithm while exploiting the frequency bandlimit as a constraint allows for a gradual reconstruction of the missing parts of a partially observed sequence. The entire sequence is constructed from elementary grains. The iterative algorithm scans, in either a random or sequential order, the extrapolated sequence sample positions. At each iteration step, a grain D is potentially added (subtracted) to (from) the old sample value. However, the new grain (an incremental sample change) is not accepted until it is verified that it reduces, or at least it does not change an error estimate in comparison to its previous value. In each iteration step, the error is estimated using an error vector $l_1$-norm defined as

$$e = \|g - Hf\|_1 \tag{6.15}$$

where $\|.\|_1$ denotes the vector $l_1$-norm [20]. In order to evaluate the error in Eq. (6.15), as it will be shown later, it is not necessary to perform a matrix-vector multiplication in each iteration step. A simple multiplication of a column of H by the current value of the elementary grain will be sufficient. In order to allow for sample fluctuations, the sign of the grain D is set at each iteration step using a random number generator (RNG). The sequence sample positions are scanned several times, each time adding to the old sample value the grain D with

randomly chosen sign, subject to the constraint that the error of Eq. (6.15) is not allowed to increase. The details of this procedure will be described next.

To start the algorithm it is necessary to set the initial grain size $D_0$ and object vector $f_0$. Also, a heuristic schedule for the grain size change should be established. In general, $D_0$ should be much smaller then the extrapolated signal maximum amplitude. The initial object vector $f_0$ can be the null vector, i. e. a vector with zeros as its elements. Using Eq. (6.14), the initial error vector $e_0$ is

$$e_0 = g - Hf_0 \tag{6.16}$$

If, for example, the initial $f_0$ is the null vector, the $l_1$-norm of the error vector $e_0$ equals the $l_1$-norm of the degraded $g$ vector, i. e.

$$||e_0||_1 = \sum_{i=1}^{N} |g_i| \tag{6.17}$$

where the $g_i$'s, $i = 1, \ldots, N$, are the elements of the space truncated vector sequence $g$. Let the degradation matrix $H$, in Eq. (6.14), be represented by its column vectors $h_i$, $i = 1, \ldots, N$,

$$H = [h_1, h_2, \ldots, h_N]. \tag{6.18}$$

The algorithm starts by assigning either a value +D or -D, depending on the random number drawn from the RNG, to a chosen element position of f, say $f_n$. Following Eq. (6.15), the resulting error vector $e_1$ is

$$e_1 = e_0 - h_n D \tag{6.19}$$

To keep track of changes of the error vector e $l_1$-norm, at each iteration step, two auxilliary error parameters, $r_{old}$ and $r_{new}$, are introduced. For example, after the first iteration step

$$r_{old} = \|e_0\|_1 \tag{6.20}$$

$$r_{new} = \|e_1\|_1. \tag{6.21}$$

The error difference r, describing the effect of the added grain D to the value of the $n^{th}$ element position of f, is

$$r = r_{new} - r_{old} \tag{6.22}$$

Next, using this r, the following decision rule is adopted: if $r < 0$ the assigned grain D is accepted, i. e., the $n^{th}$ sample of f is $f_n = D$. Otherwise, because the assigned grain leads to an increase of $\|e_1\|_1$ as compared to the previous value of $\|e_0\|_1$, the grain is discarded. If a grain is accepted, before the start of the next iteration step, the $r_{old}$ is replaced by $r_{new}$, i. e.,

$$r_{old} <= r_{new} \tag{6.23}$$

Now, the algorithm is ready to proceed to the next iteration step.

In the second iteration step, a new, say $f_m$, sample position of the object vector f is chosen. Again, depending upon the random number drawn from the RNG, the sample position $f_m$ is assigned either a +D or -D grain. The error vector $e_2$ is formed as

$$e_2 = e_1 - h_m D. \tag{6.24}$$

Forming $r_{new}$

$$r_{new} = ||e_2||_1 \tag{6.25}$$

and the error difference r and applying the previous decision rule, the acceptance of the sample update is tested. Note that now the $r_{old}$ and $r_{new}$ contain the $l_1$-norms of the error vectors $e_1$ and $e_2$, respectively. If $r < 0$, the grain assigned to the $m^{th}$ element of the f vector is accepted, otherwise it is rejected.

In the $k^{th}$ iteration step a $j^{th}$ element position, $f_j$, of the object vector f is considered. Following the previous two examples, the grain +D is assigned to $f_j$, and the error vector is formed as

$$e_k = e_{k-1} - h_j D \tag{6.26}$$

Again, $r_{new} = \|e_k\|_1$ and $r_{old} = \|e_{k-1}\|_1$. Forming the difference $r = r_{new} - r_{old}$ and applying the previous decision rule it is then decided whether the assigned grain will be accepted or not. If the new grain is accepted, then $r_{old}$ is replaced with the present error norm $r_{new}$.

Suppose now that all the N sample positions of f have been sequentially chosen so that none of the positions are repeated. Then, after N (where N is the number of elements of f) iteration steps, the error vector $e_N$ would be

$$\begin{aligned} e_N &= e_{N-1} - h_N D \\ &= g - h_1(\pm D \text{ or } 0) - h_2(\pm D \text{ or } 0) - \ldots - h_N(\pm D \text{ or } 0) \end{aligned} \tag{6.27}$$

or in a matrix form

$$e_N = g - [h_1, h_2, \ldots, h_N] \begin{bmatrix} \pm D \text{ or } 0 \\ \vdots \\ \pm D \text{ or } 0 \end{bmatrix} \tag{6.28}$$

where the grain vector $(\pm D \text{ or } 0, \ldots, \pm D \text{ or } 0)^T$, with zero elements at the positions where a grain has not been accepted, represents the current estimate of the bandlimited sequence f. It should be noted that, if each sample position is chosen using a

uniform distribution RNG, after every N sample position drawings, it completes on the average one scan through the entire set of f sample positions. If the sample positions are sequentially chosen, then after N iteration steps exactly one scan through the sequence sample positions is completed. Therefore, with a fixed grain, the same procedure of N sample position choosing and estimate updating should be repeated several times. This step constitutes one of the inner loops of the iterative algorithm. In an outer loop, according to a prearranged heuristic schedule, the grain size is changed. The entire procedure is repeated until either a preset error is reached or a preset maximum number of iterations is exceeded.

The algorithm presented above can be summarized as follows:

**Initialization:**

$f = 0$, $e_0 = g$; Set the Error

$r_{old} = \|e_0\|_1 = \|g\|_1$

**Loop1:** Do for $i = 1$ to OUTER

Set the size of grain D

**Loop2:** Do for $k = 1$ to INNER

Choose sample position p

If RN $> 0$: $D = +D$

Otherwise: $D = -D$

$e_k = e_{k-1} - h_p D$

$r_{new} = \|e_k\|_1$

$r = r_{new} - r_{old}$

If $r < 0$: $f_p <= f_p + D$, $r_{old} <= r_{new}$

Otherwise: $e_k = e_k + h_p D$

Return to Loop2

If $r_{new} <$ Error Go to EXIT

Otherwise: $e_0 = e_{inner}$

Return to Loop1

EXIT: Bandlimit f.

As it can be observed, this algorithm requires INNER*M (where M is the H matrix column dimension) inner loop (Loop2) multiplications. The number of inner loops (Loop2) depends, in general, on the extrapolated signal amplitude and the initial grain size $D_0$. The number of outer loop (Loop1) passes depends on the grain-size-change schedule. For example, for a fixed grain size of $D = 0.01$ and an unity signal amplitude (i. e., peak-to-peak signal amplitude of 2), a sequence sample should be scanned for a minimum of $(2/0.01) = 200$ times. However, at each sample position, there will be many grains that will cause an error increase leading to their rejection. Therefore, for this case, a sequence sample should be scanned approximately 300 times. Hence the number of multiplications per sample is 300M. Assuming N extrapolated sequence samples, the total number of

multiplications is 300MN. This estimate of the number of multiplications is comparable to an estimate of the number of multiplications of the existing iterative bandlimited signal extrapolation algorithms.

The new algorithm also allows for an easy introduction of additional constraints. For example, to introduce a signal amplitude upper bound constraint, after each sample update, an amplitude test should be performed. If it exceeds a limit, the corresponding sample update (grain) is rejected.

In the last step of the algorithm, corresponding to the EXIT line, the estimate is bandlimited, by either multiplying it by the H matrix, or perhaps using an FFT algorithm. This step smooths the estimate and eliminates the noise introduced by the finite grain size.

In the presence of measurement error or noise, Eq. (6.14) is amended as

$$g = Hf + n \tag{6.29}$$

where n is a noise or measurement error vector. Due to the noise and/or imperfect model of the degradation H, the linear system of

Eq. (6.29) may represent an inconsistent system, i. e. the exact solution for $\mathbf{f}$ is not feasible. To obtain a consistent model (see Eq. (6.14)), the following preprocessing of Eq. (6.14) is introduced. Multiplying Eq. (6.14) by $H^T$

$$H^T\mathbf{g} = H^TH\mathbf{f} \tag{6.30}$$

and introducing the notation $H^T\mathbf{g} = \tilde{\mathbf{g}}$ and $H^TH = \tilde{H}$, we have

$$\tilde{\mathbf{g}} = \tilde{H}\mathbf{f}. \tag{6.31}$$

Clearly $\tilde{\mathbf{g}} \in R(H)$, where $R(.)$ denotes range of the H matrix [1]. Starting the iterative algorithm with the modified $\tilde{\mathbf{g}}$ and $\tilde{H}$, ensures the existence of a solution for $\mathbf{f}$. Furthermore, this preprocessing step eliminates the noisy high frequency components of the measured degraded signal $\mathbf{g}$, causing it to be highly resistant to noise.

## 6.4. EXPERIMENTAL RESULTS

In this section, computer simulation results will be presented. To test the new algorithm, several experiments have been performed. Three different extrapolation examples with different SBPs, and different signal-to-noise ratios (SNR) are presented. In all the examples, the discrete Fourier spectrum is computed using a 128 point FFT algorithm. The degradation operator H, constructed as described in Sect. 2., is a 128*128 element square matrix. Both the truncated sequence g and the degradation matrix H are preprocessed as described by Eq. (6.30).

As a first example, consider the extrapolation of a 128 sample sinusoid of frequency $w = \pi/64$, from a short observation segment of 9 samples ($L = 4$). For fine grain size changes, the outer loop (Loop1) has been partitioned into five, equal number of passes, subloops. The initial grain size is $D_0 = 0.01$, while the decremental step size is $DD = 0.0015$. The iterative process stops when either all the five steps of the outer-most loop have been exhausted, or when an error falls below the limit of 0.02. The number of Loop2 passes, corresponding to the number of samples of the extrapolated sequence, is 128. For the sinusoidal sequence example this error limit was reached at the third pass of the outer-most loop. Fig. 6.1a) presents a 128 sample sinusoid

sequence with its 9 sample observation interval. In Fig. 6.1b), the circles show the extrapolation from the 9 sample observation interval while the squares denote the original sequence. In Fig. 6.1c) the Fourier spectra of both the observed and restored spectrum are presented. The restoration in both the space domain, and consequently in the frequency domain, are almost perfect. In Fig. 6.2a), a noisy observed segment, with a SNR of 5.21 db, of Fig. 6.1a) is presented. In Fig. 6.2b) the extrapolation result in the space domain (circles), and the original sequence (squares) are shown. It is clear, that even in the presence of substantial noise, the extrapolation result is very good. In Fig. 6.2c) the Fourier spectrum of the noisy observed segment, from Fig. 6.2a), and the Fourier spectrum of the extrapolated sequence, from Fig. 6.2b), are compared. The estimated spectrum is faithful to its original form.

As a second example, consider the combination of two sinusoidal sequences

$$f(n) = \cos[(\pi/64)n] + \cos[(5\pi/64)n], \qquad (6.32)$$

In Fig. 6.3a), the sequence f(n) and the 33-sample-observation-segment (L = 16) are presented. The original sequence is again denoted by squares while the observed segment g(n), with its zero samples outside of the observation interval, is denoted by circles. The H matrix, (see Eq. (6.14)) has been formed with a

bandlimiting operator (see Eq. (6.7)) where the $w_c = 5\pi/64$. The parameters of the algorithm of Sect. 6.3. are the same as the parameters used in the previous example. In Fig. 6.3b), the circles represent the extrapolated sequence while the squares represent the original sequence. As it can be observed the extrapolated sequence follows very well the original sequence. In Fig. 6.3c), the Fourier spectra of both the observed and the extrapolated sequence are presented. It shows a wide separation of the two frequencies. In Figs. 6.4 and 6.5, the same parameters as shown in Fig. 6.3, but for the addition of noise such that SNR is 11.47db and 5.45db, respectively, are presented. It can be observed that this algorithm shows excellent resistance to noise.

In Figs. 6.6 and 6.7, by bandlimiting a set of uniformly-distributed random numbers to a frequency $w_c = \pi/16$, a bandlimited sequence was generated. Fig. 6.6a) presents both the bandlimited sequence (squares) and its 29 sample observed segment ($L = 14$) (circles). In all the following examples, for the extrapolation of the entire sequence, a 29-sample-observation-segment was used. The H matrix cutoff frequency (see Eq. (6.14)) was set to $w_c = \pi/16$. In this example, to decrease the grain size D, the outer loop (Loop1) was partitioned into three loops with equal number of passes. The initial grain size was $D_0 = 0.03$ and it was decremented in $DD = 0.009$ steps. The process stops either when all the iteration steps of the outer loop have been completed, or when the error bound of 0.02 is reached. In all

these examples, the error bound was reached before the full number of iteration steps was completed. The number of Loop2 passes was arbitrarily set to 128. In Fig. 6.6b), the result of extrapolation of the sequence shown in Fig. 6.6a) is presented. The extrapolation follows the original sequence. In the next example an additional constraint is introduced. The maximum positive amplitude value of the extrapolated signal is constrained to be less then 0.8, i. e. $f(n) < 0.8$. Now a signal sample update that produces a positive sequence amplitude greater then 0.8 is rejected. In Fig. 6.6c), the result of extrapolation of the sequence of Fig. 6.6a) with this additional constraint is presented. It is clear, that with this constraint an added improvement can be achieved.

In Figs. 6.7a) and b), the results of extrapolation of the sequence of Fig. 6.6a) in the presence of additive noise, are presented. The additional constraint $f(n) < 0.8$ is also used. In Fig. 6.7a), the original sequence is denoted by squares, while the noisy observed segment, with a SNR of 3.89db, is denoted by circles. In Fig. 6.7b), the extrapolated sequence (circles), and the original sequence (squares) are shown. In Fig. 6.7c), a larger noise, such that SNR is -8.157db, is imposed on the observed sequence segment of Fig. 6.6a). Again, the original sequence is denoted by squares while the noisy observed sequence is denoted by circles. In Fig. 6.7d), the extrapolated sequence is represented by circles, while the original sequence is

represented by squares. As these Figures show, a very good extrapolation result can be obtained.

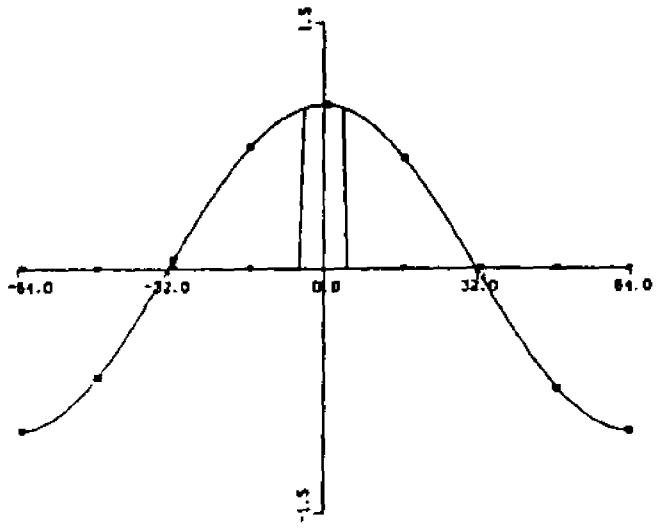


Fig. 6.1a) The 128 samples of the $\cos(\omega_c n)$ sequence (squares) and the observed segment of 9 samples (circles).

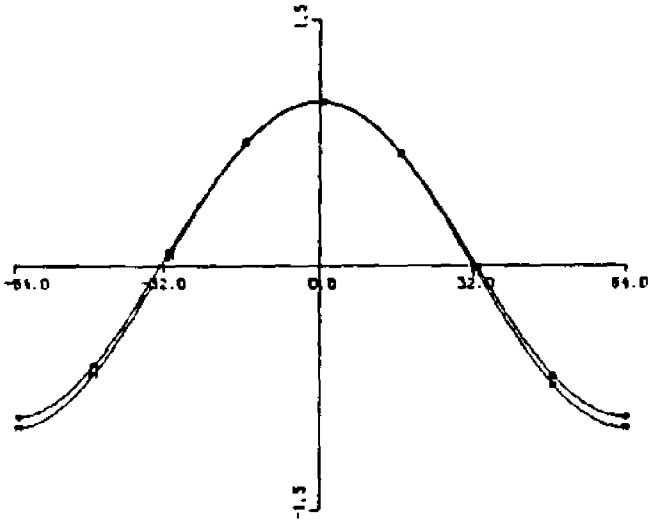


Fig. 6.1b) The space domain extrapolation from the 9 samples (circles), and the original sequence (squares).

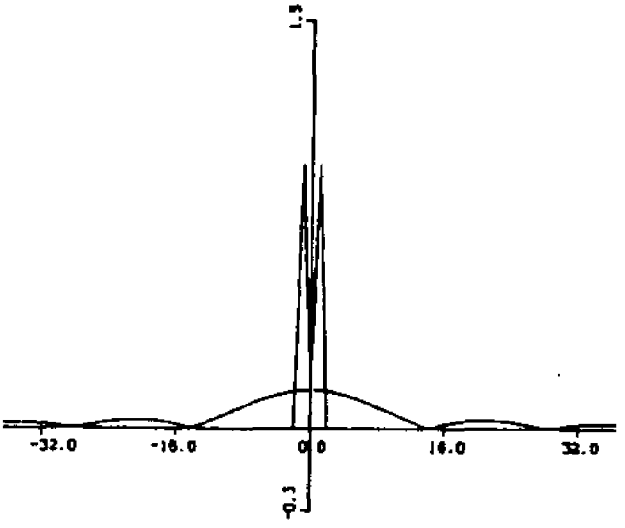


Fig. 6.1c) The Fourier spectrum of the 9 sample observed segment in Fig. 6.1a), and the restored spectrum.

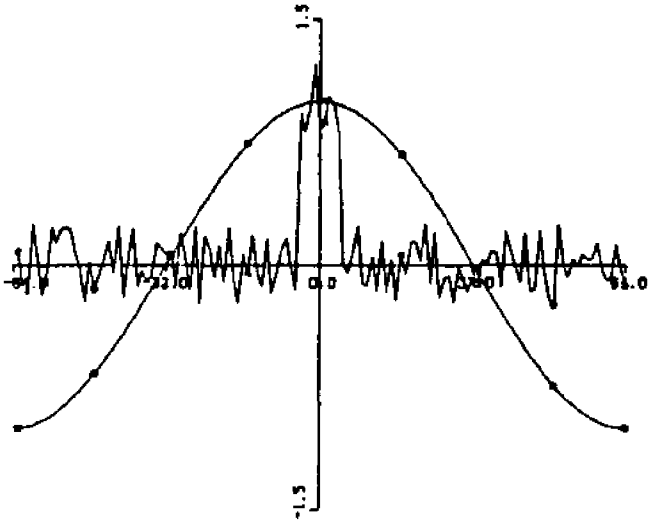


Fig. 6.2a) Sequence of Fig. 6.1a) with noisy observed segment, SNR = 5.21db.

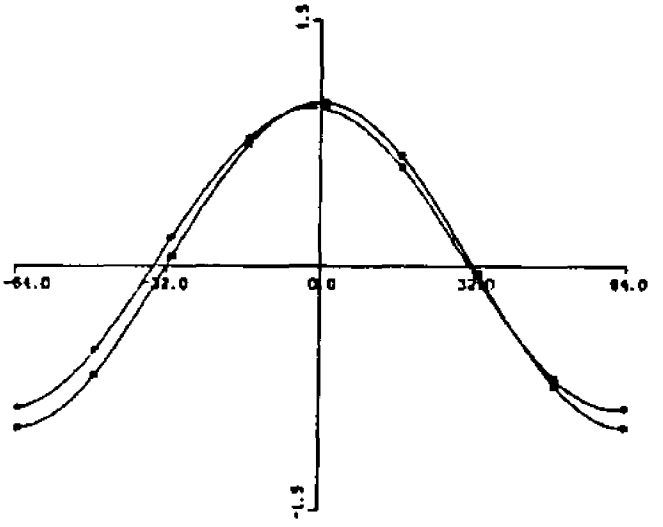


Fig. 6.2b) The space domain extrapolation of the noisy 9 samples observed segment (circles), and the original sequence (squares).

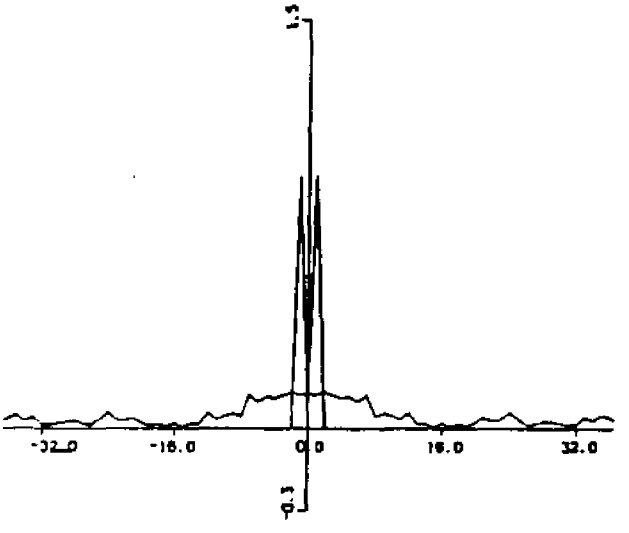


Fig. 6.2c) The Fourier spectrum of the 9 samples observed noisy segment, and the restored Fourier spectrum.

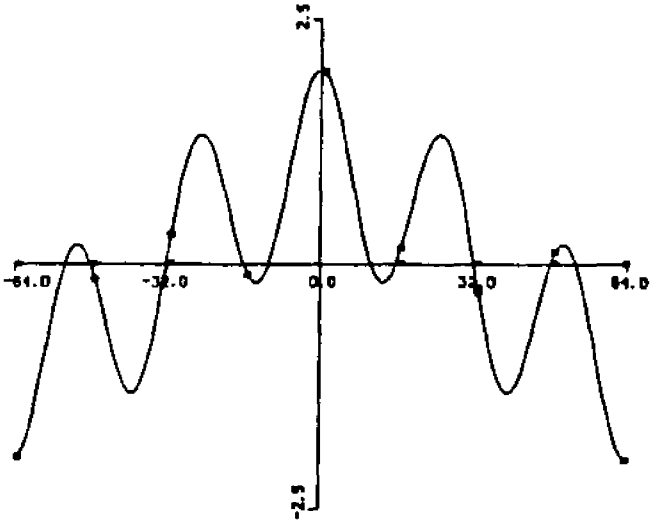


Fig. 6.3a) The 128 samples of the $\cos(\omega_o n) \cdot \cos(5\omega_o n)$ sequence (squares), and the 33 samples observed segment (circles).

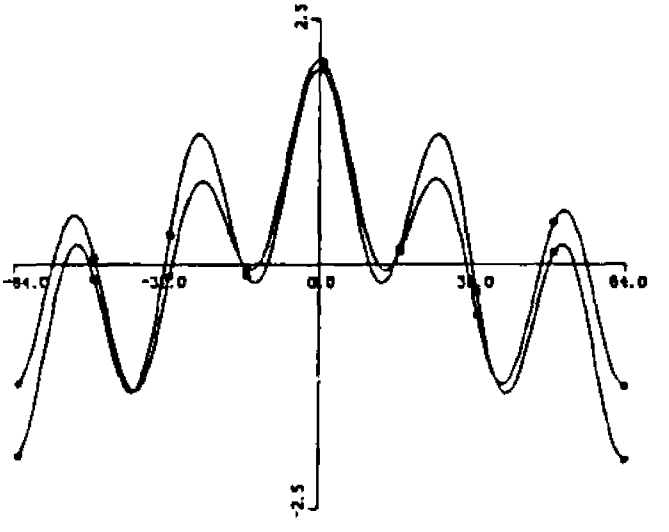


Fig. 6.3b) The original sequence (squares), and the space domain extrapolation (circles)

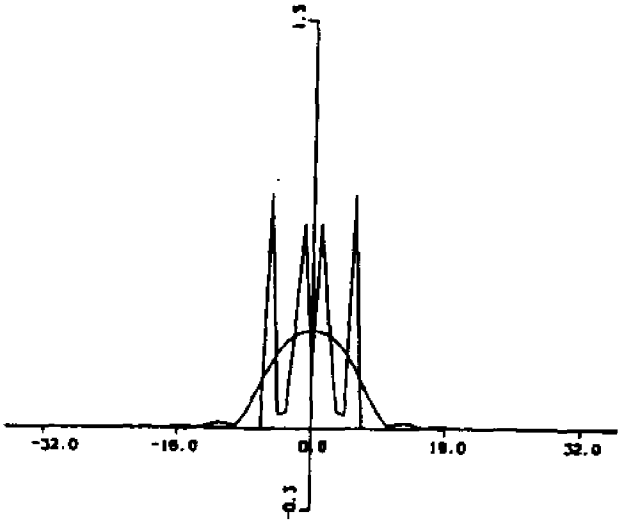


Fig. 6.3a) The Fourier spectrum of the 33 samples observed segment, and the restored Fourier spectrum.

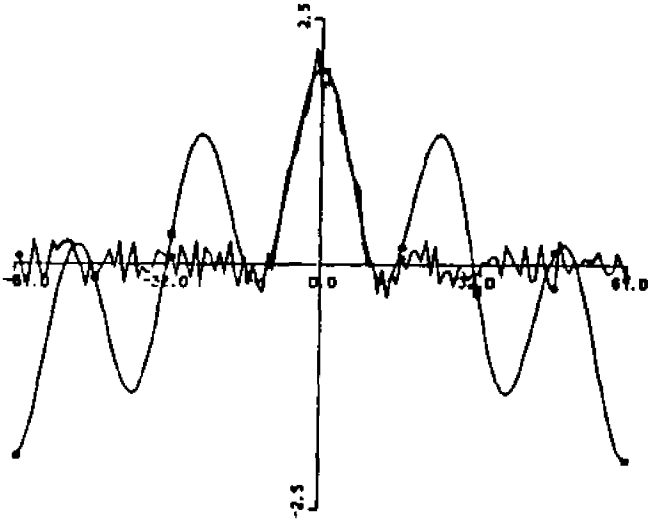


Fig. 6.4a) The noisy observed segment of Fig. 6.3a), SNR = 11.47db.

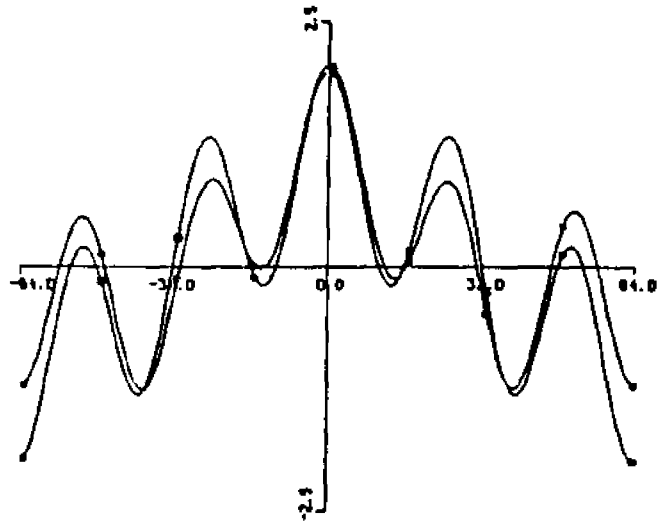

Fig. 6.4b) The noiseless original sequence of Fig. 6.3a) (squares), and the space domain extrapolation of Fig. 6.4a) (circles).

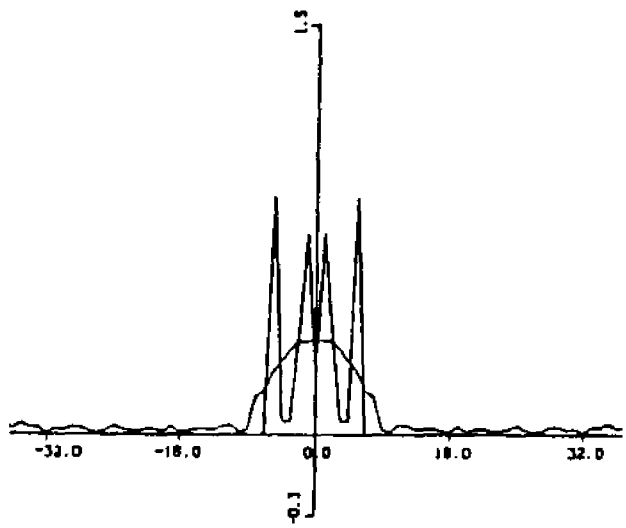


Fig. 6.4c) The Fourier spectrum of the observed segment of Fig. 6.4a), and the restored Fourier spectrum.

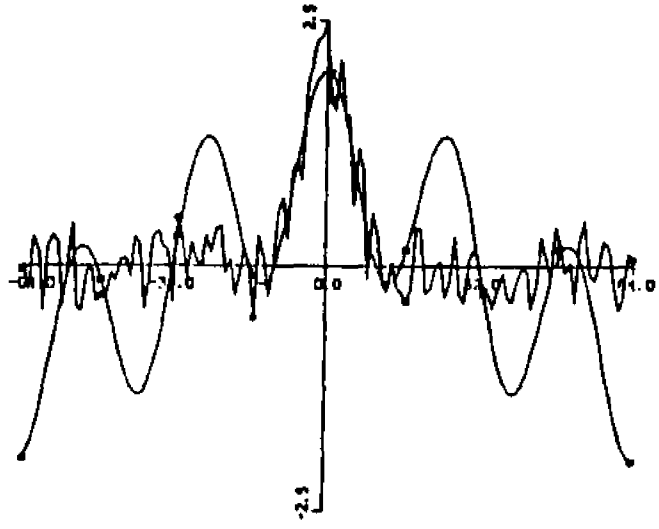

Fig. 6.5a) Noisy observed segment of Fig. 6.3a), SNR = 5.45db.

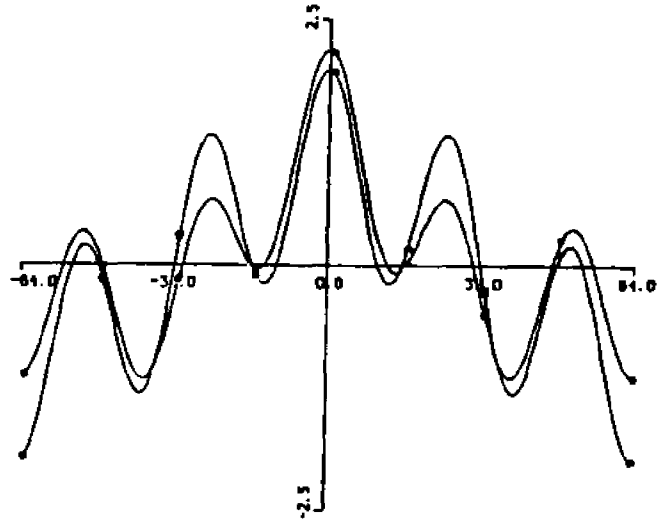

fig. 6.5b) The noiseless sequence of fig. 6.3a) (squares), and the space domain extrapolation of fig. 6.5a) (circles).

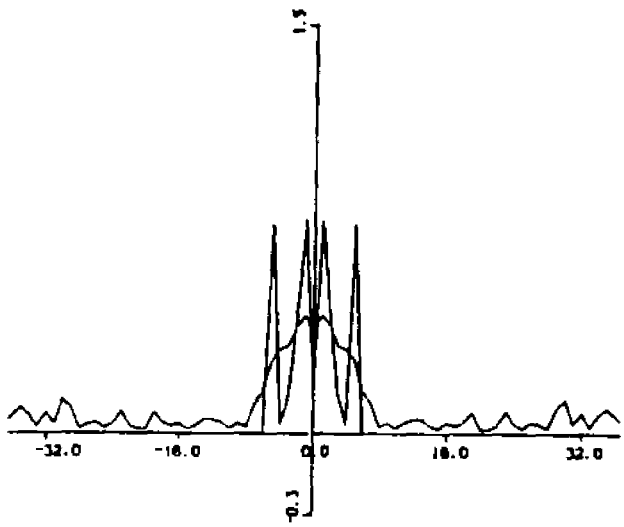


Fig. 6.5c) The Fourier spectrum of the observed noisy segment of Fig. 6.5a), and the restored Fourier spectrum.

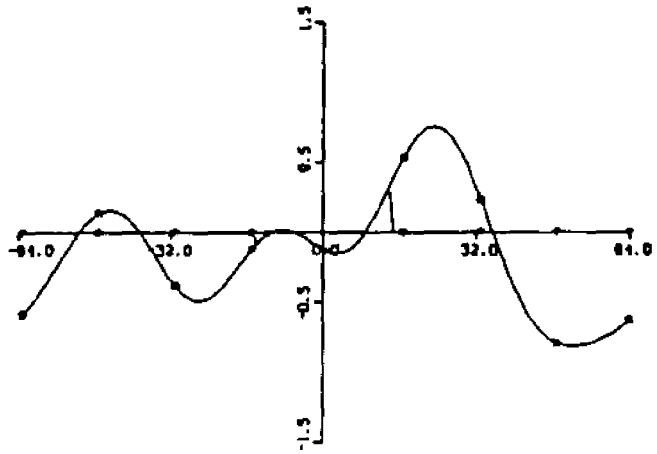


Fig. 6.6a) A noiseless bandlimited sequence (squares), and the observed segment of 29 samples (circles).

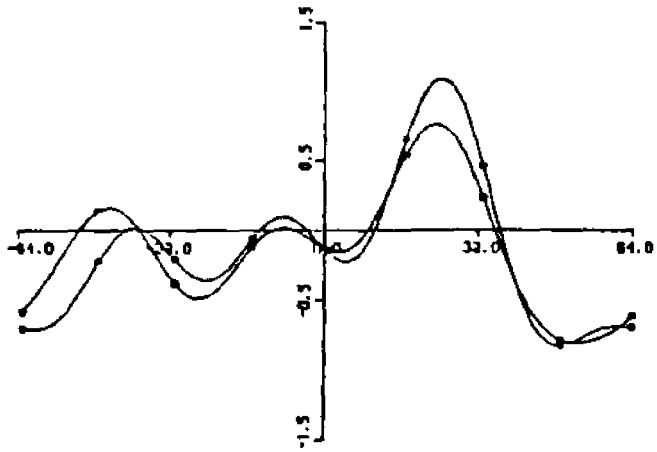


Fig. 6.6b) The original sequence of Fig. 6.6a) (squares), and the extrapolation from the observed segment of 29 samples (circles).

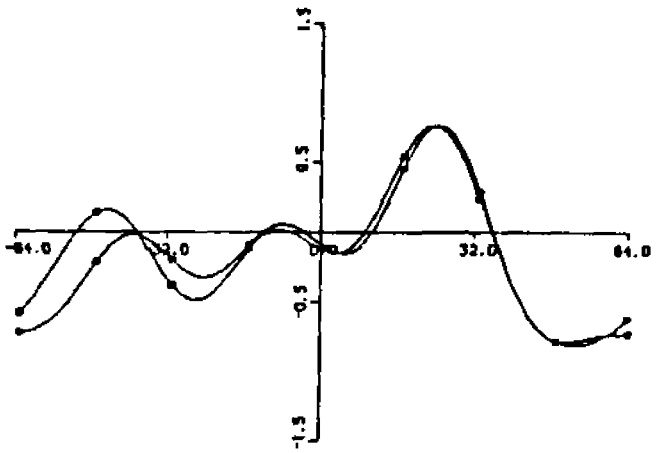


Fig. 6.6c) As in Fig. 6.6b) with additional constraint that the maximum positive amplitude of the bandlimited sequence is no greater then 0.8.

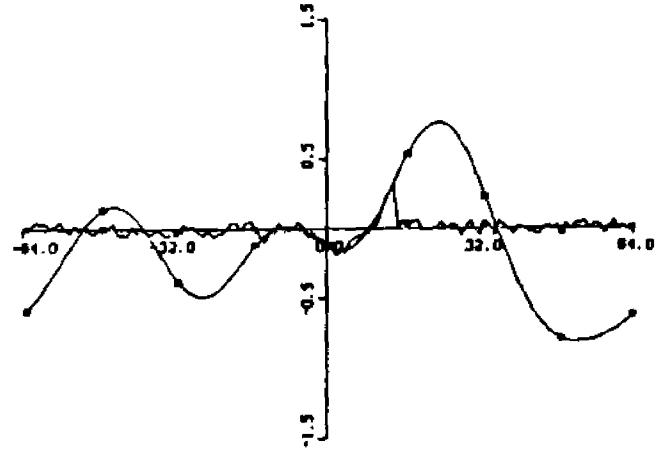


Fig. 6.7a) The noisy bandlimited sequence of Fig. 6.6a) (squares), and the noisy observed segment of 29 samples, SNR = 3.89db (circles).

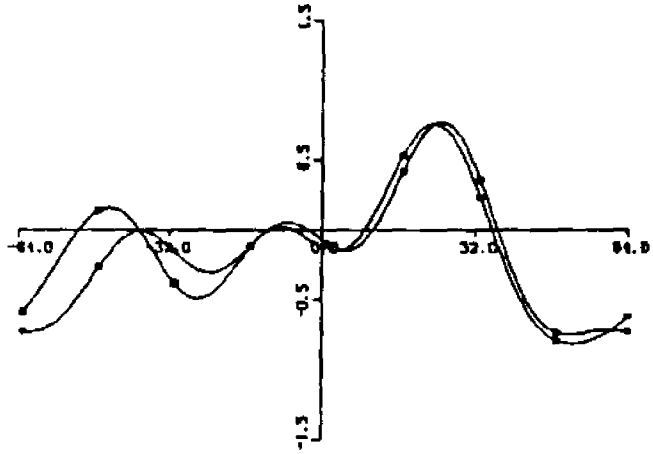


Fig. 6.7b) The original bandlimited sequence of Fig. 6.6a) (squares), and the space domain extrapolation from the noisy observed segment as in Fig. 6.7a) (circles). The additional constraint that the maximum positive amplitude of the sequence is no greater then 0.8 is used.

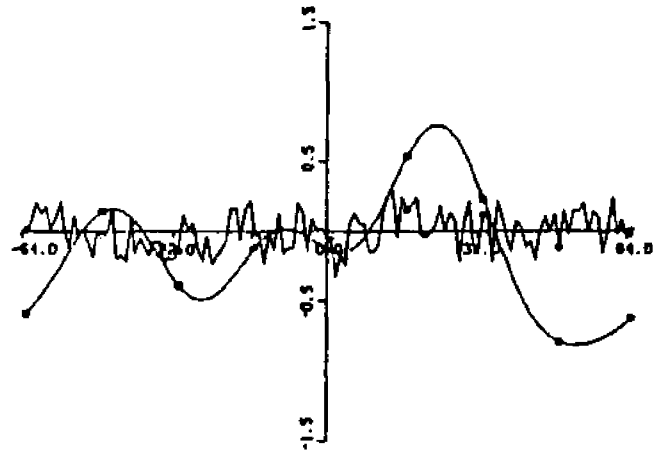


Fig. 6.7c) As in Fig. 6.7a) with SNR = -8.157db.

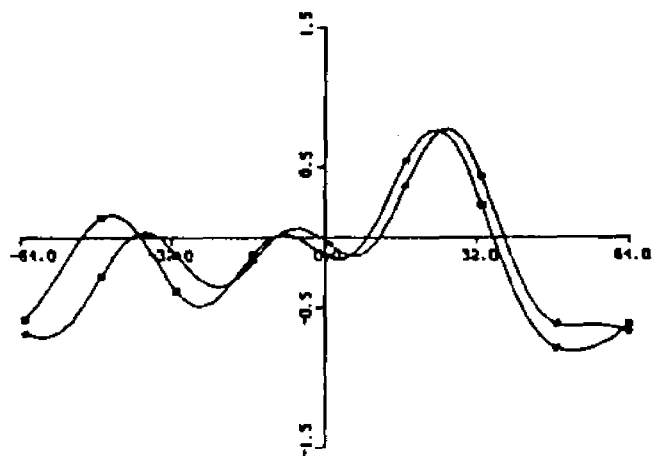


Fig. 6.7d) The bandlimited sequence of Fig. 6.7a) (squares), and the space domain extrapolation from the noisy observed segment as in Fig. 6.7c) (circles). The additional constraint that the maximum positive amplitude is no greater then 0.8 is used.

## 6.5. SUMMARY AND CONCLUSION

A new iterative algorithm for the extrapolation of a space-truncated bandlimited signal in the presence of considerable noise has been presented. The new algorithm is based on the constructing of the samples of an unknown bandlimited sequence from variable size elementary grains. The criterion for an acceptable sample-update (grain) is the $l_1$-norm of the error. To avoid unnecessary quadratic terms and to speed-up the algorithm, the $l_1$-norm, instead of the usual quadratic $l_2$-norm, has been used. A decision rule, for acceptable sample-update (grain) in each iteration step, forces a nonincreasing error criterion. To determine both the new sample location and the sign of the elementary grain D being added (subtracted) to (from) the current value of the sample position, a RNG is used. The number of multiplications of the kernel loop (Loop2) of the algorithm is approximately INNER*M (where M is the column dimension of the H matrix, and INNER depends on a number of elements such as the number of samples of the sequence being extrapolated, the signal amplitude, the initial grain $D_0$ size, and on the schedule of decreasing $D_0$, (i. e., a "cooling" schedule). The number of passes of the outer loop (Loop1) depends on the "cooling" schedule. Either the maximum number of Loop1 passes or the maximum $l_1$-norm error defines a stopping criteria. Thus, the required estimate can be obtained prior to completion of the prescribed number of Loop1 passes. To eliminate the inconsistency

of the linear system that is due to noise and/or to the imprecise model of the degradation operator H, a preprocessing step has been introduced. This step allows the achievement of the correct signal estimate even in the presence of strong noise.

To test the algorithm for different SBP signal extrapolation and in the presence of different noise levels, several examples have been considered. The resulting estimates yield good results both in the space and frequency domains. In all the examples tested, the total number of multiplications for an N*N H matrix and N-sample sequence, varies between approximately $300N^2$ to $600N^2$. It has also been indicated that with this approach it is easy to introduce the additional constraints. Furthermore, in the example where an upper signal bound constraint is introduced, dramatic signal estimate improvement can be expected.

# 7. SUMMARY AND ALTERNATE APPLICATIONS

Three new methods of solving ill-conditioned problems, appropriate for a variety of applications which pertain to increasing the resolution of a measured signal, are presented. The first method is a stabilized direct inversion of the system degradation operator based on the modified LAM algorithm. The second method is an iterative constrained WLS (BLUE) algorithm which incorporates a singular value filtering mechanism through a specific design of the algorithm weighting matrix. The third method is a new algorithm for bandlimited signal extrapolation, or equivalently the resolution of the Fourier spectra, using a Monte-Carlo method approach. These methods are shown to increase the resolution of a measured signal beyond the limit imposed by the uncertainty principle of signal processing.

The first chapter contains material of an introductory nature. In Chapter 2, the contemporary methods of increasing resolution or equivalently extrapolating the spectrum of a signal, are given. In general, these methods are found to be computationally expensive and highly sensitive to noise. In Chapter 3, based on a modified linear associative memory algorithm for the least-squares optimal pattern (vector) maching, a new method, suitable for determining of inverse of an ill-conditioned system degradation operator, is developed. In Chapter

4, using this new CAM method, superresolving reconstruction of an arbitrary binary object from its degraded image, in the presence of appriciable noise, is demonstrated. It is shown that using an appropriate training set of signals, related idealy by a perfect degradation operator inverse, the CAM method yields a general one step inverse filter in a form of a two dimensional array of coefficients. For both LSI and LSV discrete degradation systems, a CAM inverse degradation system matrix has been computed. The performance and superresolving properties of these inverse degradation matrices were tested on several 1D and 2D numerical examples. Since the CAM linearly degraded signal recovery requires only a single matrix-vector multiplication, this method is suitable for an optical or electronics real-time hardware implementation.

The nonlinear discrete iterative signal restoration methods frequently use regularization techniques that impose constraints on the system degradation operator SVs. By introducing a SV taper, these methods provide a compromise between the noise and the spatial high-frequency content of the estimate. The new iterative method, presented in Chapter 5, uses a step-type SV filtering function that deemphasizes the lower-index-order SVs while simultaneously emphasizing the higher-index-order SVs, thus providing their better ratio. This considerably decreases the condition number of the degradation matrix. The SV filtering function is incorporated into a weighting matrix of the WLS and

WBLUE algorithms. Hence, the weighting matrix implicitly compensates for the ill-conditioned nature of the system degradation operator, without materially disturbing the consistency of the system degradation model, thus providing a stable estimate. Both the non-negativity and the finite-spatial extent constraints have been incorporated into the algorithm. As it has been demonstrated on several numerical examples, the new iterative method shows superresolving properties and excellent resistance to noise. When the off-line signal restoration is affordable, this method permits the recovery of heavily degraded signals, contaminated by a high level noise, which hitherto were considered lost for all the existing signal recovery methods. In Chapter 6, a partialy observed bandlimited sequence extrapolation in the space domain, or equivalently resolution of the Fourier spectra in the frequency domain, in the presence of considerable noise, is investigated. A new method is developed that reconstructs the unknown portion of a bandlimited sequence using the grains of variable size as the elementary building blocks of each sequence sample. While exploiting the extrapolated sequence frequency bandlimit as a constraint the new algorithm employs a decision rule, based on a nonincreasing l1-norm of a cumulative error vector, to update the sequence samples. As the extrapolated sequence approaches its final form, to allow for subtle sample updates, the elementary grain size is decreased using a schedule for gradual change of the elementary grain size which is similar to the temperature schedule of the Simulated Annealing method. A preprocessing, that compensates for the degradation system model

inconsistency, due to either presence of noise, and/or lack of precision of the linear degradation operator, is employed. It is also shown that an additional constraint, such as a given signal upper-bound, can easily be incorporated into the algorithm to improve the quality of reconstruction. Several extrapolation results for low SBP sinusoidal and random bandlimited sequences, in the presence of high level of noise, are presented. Thus, superresolving spectral estimation is demonstrated. This algorithm is particularly suited for the bandlimited signal extrapolation applications when the observation interval is short and the level of noise is high, as it is the case, for example, in radar signal processing.

Further research efforts should addres the variety of possible applications. The extension of presented methods can be made to a wide diversity of disciplines. The list of possible applications include: Geophysics (signal restoration from seismographs), Neurophysics (EEG signals), Speech Communication, i. e. given a particular speech signal, it is of interest to determine the general type of sound it is. In addition one is interested in the identity of the sound which can be obtained from the spectrum. Further investigation should be pursued of the superresolving capabilities of these methods for image enhancement of electron-microscope images, video images received from onboard space and aircraft and for image enhancement of medical diagnostic images, such as CAT-scans, ultrasound images,

coventional X-rays and Neutron Magnetic Resonance images. The methods presented could also be utilized to increase the resolution of existing sonar and radar systems.

## 8. REFERENCES

1. A. Albert, Regression And The Moore-Penrose Pseudoinverse, Academic Press, New York, 1972.

2. H. C. Andrews and B. R. Hunt, Digital Image Restoration, Prentice-Hall, Englewood Cliffs, N. J., 1977.

3. H. C. Andrews and C. L. Patterson, "Singular Value Decomposition And Digital Image Processing", IEEE Trans. on ASSP, ASSP-24, 1, 26-53 (1976).

4. C. T. Baker, L. Fox, D. F. Muyers, and K. Wright, "Numerical Solution of Fredholm Integral Equations of The First Kind", Comp. J., 7, 141-152 (1964).

5. R. Barakat and G. Newsam, "Algorithms for Reconstruction of Partialy Known, Band-Limited Fourier-Transform Pairs From Noisy Data", J. Opt. Soc. Am., 2, 2027-2038 (1985).

6. K. Binder, Ed., Monte Carlo Methods, Springer-Verlag, Berlin, 1986.

7. G. E. P. Box and G. M. Jenkins, Time Series Analysis: Forecasting and Control, Holden-Day, San Francisco, CA, 1970.

8. J. P. Burg, "Maximum Entropy Spectral Analysis", in Proc. 37th Meeting Society of Exploration Geophysicists, Oklahoma City, OK, Oct. 1967.

9. J. A. Cadzow, "An Extrapolation Procedure for Bandlimited Signals", IEEE Trans. ASSP-27, 4-12 (1979).

10. P. Carnevalli, L. Coletti, S. Patarnello, "Image Processing by Simulated Annealing", IBM J. Res. and Develop., 29, 569-579 (1985).

11. D. P. Colba, "Optimal Estimaton for Bandlimited Signals Including Time Domain Consideration", IEEE Trans. ASSP, 31, 113-122 (1983).

12. S. D. Conte and C. de Boor, Elementary Numerical Analysis, An Algorithmic Approach, McGraw-Hill, New York, 1980.

13. J. Durbin, "The Fitting of Time Series Models", Rev. Inst. Int. de Stat., 28, 233-244 (1960).

14. G. Eichmann and M. Stojancic, "Superresolving Signal and Image Restoration Using a Linear Associative Memory", Appl. Opt., 10, 1911-1918 (1987).

15. B. R. Frieden, "Image Enhancement and Restoration", in "Picture Processing And Digital Filtering," T. S. Huang, Ed., Springer Verlag, New York, 1975.

16. B. R. Frieden, "Image Restoration by Decision-Rule Allocation of Pseudo-Grains", Presented at Spring Meeting of the Optical Society of America, Washington, D. C., 1974.

17. B. R. Frieden , "Maximum-Information Data Processing: Application to Optical Signals", J. Opt. Soc. Am., 71, 294-303 (1981).

18. B. R. Frieden, C. K. Zoltani, "Monte Carlo Restoration of Binary Objects", J. Opt. Soc. Am. A, 3, 731-734 (1986).

19. R. Gerschberg, "Super-resolution Through Error Energy Reduction", Opt. Acta, 21, 709-720 (1974).

20. G. H. Golub and C. F. Van Loan, Matrix Computations, John Hopkins Press, Baltimore, Maryland, 1983.

21. T. N. E. Greville, "Some Applications of the Pseudoinverse of a Matrix," SIAM Rev., 2, 15-22 (1960).

22. T. N. E. Greville, "The Pseudo Inverse of a Rectangular Matrix and its Applications to the Solution of Systems of Linear Equations," SIAM Rev., 1, 38-43 (1959).

23. C. W. Groetsch, The Theory of Tikhonov Regularization for Fredholm Equations of the First Kinde, Pitman Publishing Limited, London, 1984.

24. C. W. Helstrom, "Image Restoration by the Method of Least Squares", J. Opt. Soc. Am., 3, 57, 297-303 (1967).

25. R. A. Horn and C. A. Johnson, Matrix Analysis, Cambridge University Press, New York, 1985.

26. S. J. Howard , "Method for Continuing Fourier Spectra Given by The Fast Fourier Transform", J. Opt. Soc. Am., 71, 95-98 (1981).

27. S. J. Howard, "Continuation of Discrete Fourier Spectra Using a Minimum Negativity Constraint", J. Opt. Soc. Am., 71, 819-824 (1981).

28. V. Hutson and J. S. Pym, Applications of Functional Analysis and Operator Theory, Academic Press, New York, 1980.

29. A. K. Jain and S. Ranganath, "Extrapolation Algorithms for Discrete Signals with Application in Spectral Estimation", IEEE Tran. ASSP, ASSP-29, 4, 830-845 (1981).

30. P. A. Jansson, Ed., Deconvolution With Applications In Spectroscopy, Academic Press, Orlando, 1984.

31. M. H. Kalos and P. A. Whitlock, Monte Carlo Methods, Volume 1: Basics, John Wiley, New York, 1986.

32. T. Kohonen, Self-Organization And Associative Memory, Springer Verlag, Berlin, 1984.

33. S. Kirkpatrick, C. D. Gellat, and M. P. Vecchi, "Optimization by Simulated Annealing", Science, 220, 671-680 (1983).

34. S. M. Kay and S. L. Marple, Jr., "Spectrum Analysis - A Modern Perspective", Proc. IEEE, 69, 1380-1419 (1981).

35. H. Landau, "On the Recovery of a Band-Limited Signal after Instantenious Companding and Subsequent Band Limiting", Bell Sys. Tech. J., 39, 351-364 (1960).

36. H. Landau and W. L. Miranker, "The Recovery of Distorted Band-Limited Signals", J. Math. Anal., 2, 97-104 (1961).

37. C. L. Lawson and R. J. Hanson, Solving Least Squares Problems, Prentice-Hall, Englewood Cliffs, New Jersey, 1974.

38. N. Levinson, "The Wiener (Root Mean Square) Error Criterion in Filter Design and Prediction", J. Math. Phis., 25,261-278 (1947).

39. R. Mammone and G. Eichmann, "Superresolving Image Restoration Using Linear Programming", Appl. Opt., 21, 496-501 (1982).

40. R. Mammone and G. Eichmann, "Restoration of Discrete Fourier Spectra Using Linear Programming", J. Opt. Soc. Am., 8, 987-992 (1982).

41. R. Mammone and R. J. Rothacker, "General Iterative Method of Restoring Linearly Degraded Images", J. Opt. Soc. Am., 4, 208-215 (1987).

42. S. L. Marple, Jr., Digital Spectral Analysis with Applications, Prentice-Hall, Englewood Cliffs, New Jersey, 1987.

43. J. Meada and K. Murata, "Restoration of Band-Limited Images by an Iterative Regularized Pseudoinverse Method", J. Opt. Soc. Am., 1, 28-34 (1984).

44. J. M. Mendel, Lessons in Digital Estimation Theory, Prentice-Hall, Englewood Cliffs, New Jersey, 1987.

45. N. Metropolis, A. W. Rosenbluth, M. N. Rosenbluth, A. H. Teller and E. Teller, "Equation of State Calculations by Fast Computing Machines", J. Chem. Physics, 21, 1087-1092 (1953).

46. A. Oppenhaim and R. Schafer, Digital Signal Processing, Prentice-Hall, Englewood Cliffs, New Jersey, 1975.

47. S. J. Orfanidis, "Optimum Signal Processing: An Introduction", Macmillan Publishing Company, New York, 1985.

48. A. Papoulis, "A New Algorithm in Spectral Analysis and Bandlimited Extrapolation", IEEE Trans. Circuits Syst., CAS-22, 735-742 (1975).

49. A. Papoulis, Signal Analysis, McGraw-Hill, N. Y., 1977.

50. W. K. Pratt, Digital Image Processing, Jhon Wiley & Sons, New York, 1978.

51. L. D. Pyle, "Generalized Inverse Computation Using the Gradient Projection Method", J. Assoc. Comput. Mach., 11, 422-429 (1964).

52. C. K. Rushforth and R. L. Frost, "Comparison of Some Algorithms for Reconstructing Space-Limited Images", J. Opt. Soc. Am., 70, 1539-1544 (1980).

53. C. K. Rushforth, A. E. Crawford and Y. Zhou, "Least-Squares Reconstruction of Objects with Missing High-Frequence Components", J. Opt. Soc. Am., 72, 204-211 (1982).

54. C. K. Rushforth and R. Harris, "Restoration, Resolution, and Noise", J. Opt. Soc. Am., 58, 539-545 (1968).

55. C. K. Rushforth and R. Harris, "Restoration, Resolution, and Noise", J. Opt. Soc. Am., 58, 539-545 (1968).

56. B. Rust, W. R. Burrus and C. Schneeberger, "A Simple Algorithm for Computing the Generalized Inverse of a Matrix", Comm. ACM, 9, 381-387 (1966).

57. M. S. Sabri and W. Steenart, "An Approach to Bandlimited Extrapolation: The Extrapolation Matrix", IEEE Trans. Circuits Syst., CAS-25, 74-78 (1978).

58. J. L. C. Sanz and T. S. Huang, "Unified Hilbert Space Approache to Least-Squares Linear Signal Restoration", J. Opt. Soc. Am., 73, 1455-1465 (1983).

59. R. W. Schafer, R. M. Mersereau, and M. A. Richards, "Constrained Iterative Restoration Algorithms", Proc. IEEE, Vol. 69, 432-450 (1981).

60. D. Slepian, "Prolate Spheroidal Wave Functions, Fourier Analysis and Uncertainty-V : The Discrete Case", Bell Syst. Tech. J., 57, 1371-1430 (1978).

61. D. Slepian and H. O. Pollak, "Prolate Spheroidal Wave Functions, Fourier Analysis and Uncertainty I", Bell Syst. Tech. J., 40, 43-64 (1961).

62. H. Stark, V. Cahana and H. Webb, "Restoration of Arbitrary Finite-Energy Optical Objects from Limited Spatial and Spectral Information", J. Opt. Soc. Am., 17, 635-642 (1981).

63. H. Stark, Ed., Image Recovery: Theory and Application, Academic Press, New York, 1987.

64. H. Stark, S. Cruze, and G. Habelter, "Restoration of Optical Objects Subject to Nonnegative Spatial or Spectral Constraints", J. Opt. Soc. Am., 72, 993-1000 (1982).

65. G. S. Stiles and Dong-Lih Deng, "On the Effect of Noise on the Moore-Penrose Generalized Inverse Associative Memory," IEEE Trans. on PAMI, 3, 358-360 (1985).

66. M. Stojancic and G. Eichmann, "Superresolving Signal and Image Restoration Using Associative Memory", Presented at 1985 Annual Meeting of the Opt. Soc. Am., Washington D. C., October 1985.

67. B. J. Sullivan and B. Liu, "On the Use of Singular Value Decomposition in Discrete-Time Band-Limited Signal Extrapolation", IEEE Trans. ASSP, 32, 1201-1212 (1984).

68. A. N. Tikhonov and V. Y. Arsenin, Solutions of Ill-Posed Problems, Winston and Sons, Washington D. C., 1977.

69. P. H. Van Cittert, "Resolution Enhancement of Spectra", Z. Physik, 69, 298-301 (1931).

70. G. Walker, "On Periodicity in Series of related terms", Proc. Roy. Soc. London, Series A, 131, 518-532 (1931).

71. G. Y. Yule, "On a Method of Investigating Periodicities in Disturbed Series, with Special Reference to Wolfer's Sunspot Numbers", Philosophical Trans. Royal Soc. London, Series A, 226, 267-298 (1927).

72. D. C. Youla, "Generalized Image Restoration by the Method of Alternating Orthogonal Projections", IEEE Trans. Circuits Syst., CAS-25, 695-702 (1978).

73. Y. Zhou and C. K. Rushforth, "Least Squares Reconstruction of Spatially Limited Objects Using Smoothness and Non-negativity Constraints", Apl. Opt., 21, 1249-1252 (1982).